UNIVERSITÀ
DEGLI STUDI
DI PADOVA

Sede Amministrativa: Università degli Studi di Padova
Dipartimento di Scienze Chimiche

SCUOLA DI DOTTORATO DI RICERCA IN SCIENZE MOLECOLARI
INDIRIZZO: SCIENZE FARMACEUTICHE
CICLO XXVIII

Development of oral and topical sucrose esters-based formulations for the delivery of lipophilic molecules

Direttore della scuola: Ch.mo Prof. Antonino Polimeno
Coordinatore d'indirizzo: Ch.mo Prof. Alessandro Dolmella
Supervisore: Dott.ssa Erica Franceschinis
Co-supervisore: Ch.mo Prof. Nicola Realdon

Dottorando: Carlo Codemo

Anno accademico: 2015/2016

Abstract

The present study is the result of a collaboration with a private company that operates in the food supplements field (Labomar Srl, Istrana - Italy) within a particular doctorate category called "Apprendistato di alta formazione e ricerca". The main purpose of the research project has been the design and characterization of a formulation platform able to deliver lipophilic active molecules both by oral and topical administration. Dealing with a company mainly operating in the food supplements market, food grade excipients have been the first to be chosen: glycerin, medium chain fatty acids (MCFA) and sucrose esters (SEs).

In the first part of the study the design of experiments has been used as a mathematical approach for the development of a set of formulations. Subsequently formulations have been characterized through dynamic light scattering, rheology measurements (including sweep test), differential scanning calorimetry (DSC) analysis and transmission electron microscopy (TEM). The developed formulations have been able to form emulsions with a droplet size up to 280 nm after dispersion in water and a direct relation between sucrose monopalmitate (SMP) concentration and viscosity has been found. It has been observed that the combination of SEs, water, glycerine and MCFA in specific ratios is able to form both classical emulsions and transparent gel-emulsion, also referred as high internal phase ratio emulsions (HIPREs), exhibiting a liquid crystalline molecular organization. On the basis of results, two formulations named F01 and F03 have been selected in order to develop oral and topic dosage forms.

Formulation F03 is a HIPREs containing the 75% of oil phase, it is characterized by high viscosity and small droplet size. It has been selected for the development of two oral dosage forms: a water-soluble powder and a medicated jelly. In order to evaluate the ability of these formulations to increase the water solubility of lipophilic molecules resveratrol and coenzime Q_{10} have been loaded as model molecules. The dissolution performances of the oral formulations have been assessed. Release profiles show an increase in actives solubility: compared to bulk powder, resveratrol release has been increased two times by the jelly formulation, and three times by the powder formulation (adsorbed-HIPREs), reaching a rapid onset. Coenzime Q_{10} is practically water-insoluble while the jelly formulation is able to release 20% of the total CoQ_{10}, as long as the adsorbed-HIPREs reach 40%.

The last part of the study deals with the development and the characterization of topical dosage forms. First of all, two of the initial formulations has been selected (F01 and F03) and appropriate excipients have been added to improve spreadability and release of actives: ethoxy diglycol and polyethylene glycol 400 have been used as solubilizers,

while glyceryl stearate and xanthan gum have been used as thickeners. Secondly, formulations have been characterized through optical and TEM microscope analysis, DSC and rheology measurements. Finally, the formulations have been loaded with resveratrol as model molecule and release and in-vitro absorption tests have been carried out. Results have been shown that the majority of the formulations follow a first-order kinetic release. Resveratrol release and absorption could be modified by modulating rheology of the formulations and the physical state of the active molecule; in particular, the maximum resveratrol absorption has been registered with formulation labelled as AF201, containing ethoxy diglycol as solubilizer and glyceryl stearate as thickener.

In conclusion, the information and the results obtained from this study should facilitate the rational design and fabrication of lipid-based delivery systems for lipophilic food and cosmetic actives. The initial aim to produce a formulation platform capable to delivery lipophilic active molecules by oral and topical administration has been achieved. Once the administration route and the active molecule have been chosen, an affordable and effective formulation could be provided and adapted to nutraceutical, cosmetic and pharmaceutical industry as well.

Riassunto

Il presente studio è il risultato della collaborazione con un'azienda produttrice di integratori alimentari (Labomar srl, Istrana) e si inserisce in un particolare tipo di dottorato definito "Apprendistato di alta formazione e ricerca". Lo scopo principale del progetto è lo sviluppo e la caratterizzazione di una piattaforma formulativa capace di veicolare principi attivi lipofili sia per via orale che topica. Trattandosi di un'azienda operante principalmente nel mercato degli integratori alimentari gli eccipienti scelti nella fase iniziale sono di grado alimentare: glicerina, acidi grassi a media catena (MCFA) e esteri del saccarosio.

La prima parte dello studio riguarda lo sviluppo di una serie di formulazioni mediante l'utilizzo del *design of experiment* e la loro caratterizzazione mediante l'uso di tecniche quali *dynamic light scattering*, misure reologiche, scansione calorimetrica differenziale (DSC) e microscopia a trasmissione elettronica (TEM). Le formulazioni iniziali una volta disperse in acqua sono in grado di creare emulsioni fini; la fase interna arriva ad avere un diametro di 280 nm ed è stata verificata una relazione diretta fra viscosità e concentrazione di saccarosio monopalmitato (SMP) nella formulazione. Si è scoperto inoltre che la combinazione di SMP, acqua, glicerina e MCFA in specifici rapporti può dare luogo alla formazione sia di classiche emulsioni che di emulsioni-gel, spesso chiamate *high internal phase ratio emulsions (HIPREs)* caratterizzate da una struttura interna a cristalli liquidi.

La formulazione F03 è un HIPREs contenente il 75% di fase oleosa ed è caratterizzata da elevata viscosità. É stata scelta come base per lo sviluppo di due forme orali: una polvere idrosolubile e una gelatina medicata. Per valutare la capacità di queste formulazioni di aumentare la solubilità in ambiente acquoso di molecole lipofile entrambe sono state caricate con due molecole modello (resveratrolo e coenzima Q_{10}). In seguito è stato valutato il rilascio in-vitro delle due molecole modello. I profili di rilascio dalle formulazioni orali indicano un sostaziale aumento della solubilità degli attivi: la gelatina raddoppia la solubilità del resveratrolo (rispetto alla sostanza tal quale) mentre la formulazione in polvere (HIPREs-adsorbito) riesce a triplicarla in circa dieci minuti. Il coenzima Q_{10} tal quale è praticamente insolubile in acqua, la gelatina riesce a rilasciarne in soluzione circa il 20% (sul totale caricato), mentre l'HIPREs-adsorbito arriva al 40%.

L'ultima parte dello studio riguarda lo sviluppo e la caratterizzazione di formulazioni topiche. Sono state selezionate due tra le formulazioni iniziali (F01 e F03) e vi sono stati aggiunti eccipienti per migliorare la spalmabilità e il rilascio degli attivi: etossi diglicole e polietilene glicole 400 sono stati usati come solventi mentre gliceril stearato e gomma di xantano come viscosizzanti. Dopo caratterizzazione mediante microscopia ottica e

TEM, DSC e misure reologiche le formulazioni sono state caricate con resveratrolo come molecola modello per verificarne il rilascio e l'assorbimento mediante test in-vitro. É stato verificato che il rilascio dalla maggior parte delle formulazioni testate segue una cinetica di primo ordine. Il rilascio e l'assorbimento di resveratrolo può essere modificato modulando le caratteristiche reologiche della formulazione e lo stato fisico dell'attivo; in particolare il massimo valore di assorbimento è stato registrato con la formulazione AF201, contenente etossi diglicole e gliceril stearato.
In conclusione, le informazioni e i risultati ottenuti con questo studio possono facilitare lo sviluppo e la produzione di formulazioni per la veicolazione di attivi lipofili alimentari e cosmetici. L'obiettivo iniziale di sviluppare una piattaforma formulativa capace di veicolare molecole lipofile sia per via orale che topica è stato raggiunto. Una volta scelta la via di somministrazione e la molecola di interesse sarà possibile sviluppare una formulazione efficiente e dai costi contenuti, utilizzabile dall'industria alimentare, cosmetica e farmaceutica.

Contents

List of Figures

List of Tables

Abbreviations

DLS	**D**ynamic **L**ight **S**cattering
DoE	**D**esing of **E**xperiments
DSC	**D**ifferential **S**canning **C**alorimetry
HIPREs	**H**igh **I**nternal **P**hase **R**atio **E**mulsions
HLB	**H**ydrophilic **L**ipophilic **B**alance
LCS	**L**iquid **C**ristalline **S**ystem
MCFA	**M**edium **C**hain **F**atty **A**cid
SEDDS	**S**elf **E**mulsifying **D**rug **D**elivery **S**ystem
SEs	**S**ucrose **Es**ters
SMP	**S**ucrose **M**ono **P**almitate
TEM	**T**ransmission **E**lectron **M**icroscopy

Chapter 1

Introduction

1.1 Aim and general premises

The whole doctorate course was funded by a private company: Labomar Srl (Istrana, TV - Italy) within a particular doctorate category called "Apprendistato di alta formazione e ricerca". Labomar is a research, development and manufacturing enterprise, devoted to innovation in food supplements, medical devices and cosmetics. Hence, the research project was oriented on the design and characterization of a formulation platform able to satisfy the company targets. Since Labomar is mainly a food supplements enterprise it was peremptory to use only food grade raw materials and to realize samples with a good taste, at least for what concerns oral dosage forms. The economic aspect was also essential, both regarding raw materials and production processes, in order to contain costs and to be competitive on the market. Prior and during the development of the formulation platform, aim of this work, the major terms and restrictions which were taken into account are:

- using food grade excipients (at least for what concern oral dosage forms)
- maintain low cost of raw materials and of production processes
- achieve easy scale-up of the production process
- obtain formulation flexibility, in order to deliver different active molecules in different dosage forms and route of administration

Table 1.1: Recommended HLB values for different pharmaceutical applications.

Application	**HLB**
Emulsification	Low to high (3-15)
Solubilization	High (10-15)
Controlled/sustained release	Low to high (3-15)
Absorption/penetration enhancement	High (especially with C12-C14 fatty acids)
Lubrication	Low to medium (3-8)
Disintegration	High (10-15)

1.2 Sucrose Esters

1.2.1 Structure and Properties

Sucrose esters (SEs) are non-ionic surface active agents consisting of sucrose as hydrophilic group and a maximum of eight fatty acids per molecule as lipophilic groups. The most common fatty acids used in SEs are lauric, myristic, palmitic, stearic, oleic, behenic and erucic acids. Changing the nature or the number of the fatty acid groups, a wide range of hydrophilic-lipophilic balance (HLB) values can be obtained [1]. Most of the SEs are manufactured in different grades, allowing their use in food, cosmetics and pharmaceuticals. The commercial SEs are mixtures with various esterification degrees. SEs with high monoesters contents are more hydrophilic, whereas a high esterification degree results in liphophilic SEs. SEs with different hydrophilicities can be used in different fields of pharmaceutical technology, *e.g.* for emulsification, solubilization, dissolution modification, absorption enhancement or lubrication as reported in Table 1.1. Depending on the composition, SEs exist as solids, waxy materials or liquids. SEs, and especially those with higher HLB values, can form gels in an aqueous environment. Depending upon their degree of esterification, SEs melt at low temperatures, usually between 45 and 65 ℃. The lipophilic SEs have characteristic melting points, while SEs with higher HLB values merely soften during heating. They can be heaten up to 180℃ without harmful effects on their properties [2].

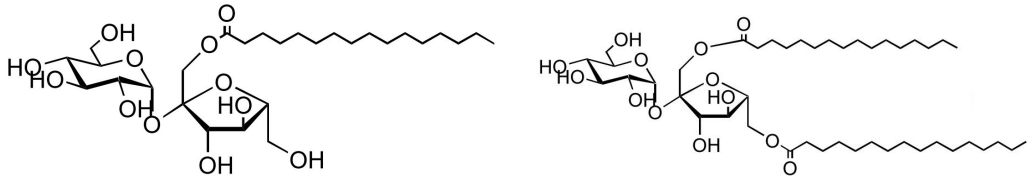

(a) *Sucrose mono-palmitate and regioisomers.* (b) *Sucrose di-palmitate and regioisomers.*

Figure 1.1: Sucrose mono-palmitate *(a)* and di-palmitate *(b)* structure.

Table 1.2: Applicability of SEs as emulsifiers in various formulation systems.

Formulation	**Reference**
Emulsions, suspensions	Akoh (1992), Yokoi et al. (2005)
Microemulsions	Thevenin et al. (1996), Bolzinger et al. (1999), Garti et al. (1999), Fanun (2008)
Vescicles	Mollee et al (2000), Honeywell-Nguyen et al. (2003)
Microspheres, microparticles	Miyazaki et al. (2006), Youan et al. (2004)
Nanoparticles, nanosuspensions	Zimmermann and Müller (2003), Lippacher et al. (2004)

1.2.2 Pharmaceutical and food applications of SEs

1.2.2.1 Emulsification and stabilization

SEs are widely used as food additives (E473) [3], and have also been noted as good emulsifying and stabilizing agents in the pharmaceutical field, for example Klang et al. [4] developed sucrose stearate based nanoemulsions. Table 1.2 summarizes the possible applicability of SEs as emulsifiers and stabilizers in conventional and advanced drug delivery systems.

1.2.2.2 Bioavailability modification

SEs are usually used to increase the release of poorly water-soluble drugs, for example sucrose distearate was used to improve solubility of canrenone [5], but was also used to achieve sustained and/or controlled release [6]. Besides the modification of drug dissolution, other properties of SEs result in interactions with biological barriers, and their effects on absorption and penetration are therefore widely investigated.

Oral absorption enhancement

Studies have demonstrated that sucrose laurate is able to enhance the absorption of cyclosporine A in an ex vivo experiment involving the use of normal gut epithelial tissue and Peyer's patch tissue of guinea pigs and in particular drug absorption is higher than those obtained with the commercial oral solution. In this study four hydrophilic SEs were compared with other enhancers, such as ethanol, oleic acid and ethoxy diglycol. Among the SEs tested, only sucrose laurate (L-1695 - 1,5%) was able to increase the passage of the drug through the buccal and palatal mucosae [6].

The effects of SEs are also investigated in cell culture models. The effect of some food emulsifiers, including SEs, on P-glycoprotein drug efflux pump was studied using human

intestinal Caco-2 cells. Results have shown that the accumulation of daunomycin, a P-glycoprotein substrate, was markedly enhanced by SEs. Authors concluded that this effect was not due to P-glycoprotein inhibition but rather to the increased daunomcin permeability of the cell membranes that was induced by the emulsifiers. In the evaluation of the potential use of SEs as oral absorption enhancers [1], water-soluble SEs (L-1695 sucrose laurate, M-1695 sucrose myristate and P-1695 sucrose palmitate) were tested for toxicity and paracellular permeability with the Caco-2 cell line model. In agreement with other previous findings, L-1695 at a concentration of 200 μg/ml significantly reduced the transepithelial electrical resistance and increased the paracellular transport of the marker molecule fluorescein in Caco-2 cell layers without changing the immunostaining of thight junctions, indicating its possible use as oral absorption enhancer.

Skin permeability enhancement

The skin permeation behaviour of SEs is evaluated mostly in solution dosage forms, microemulsion systems and recently in transdermal therapeutic systems (TTS patches). For example, Lerk and Sucker [7] reported that sucrose laurate has intermediate skin permeability-enhancing properties and proposed that this SE is a suitable, non-irritating excipient for the dermal formulation of poorly water soluble drugs such as cyclosporine A. An enhancement in rabbit percutaneous absorption of estradiol was also observed using a sucrose laurate hydrogel [8].

The effects of SEs on the permeability of the human stratum corneum and on the percutaneous penetration of various active principles were investigated by Ayala-Bravo et al. [9]. They compared the effect of two hydrophilic SEs on the stratum corneum properties: sucrose oleate O-1570 (HLB 15) and sucrose laurate L-1695 (HLB 16) dispersed in water or in ethoxydiglycol. Results have been show that the combination of SEs and ethoxydiglycol can temporarily alter the stratum corneum barrier properties, promoting the permeation. Okamoto et al. [10] examined the effects of different SEs on the transdermal permeation of lidocaine and ketoprofen. They found that sucrose laurate with a HLB value of 16 increased the permeation of ionized lidocaine from an aqueous vehicle. On the other hand, sucrose laurate with an HLB value of 5, which was not reported earlier as an absorption enhancer, increased the permeation of lidocaine and ketoprofen from propylene glycol. Transdermal therapeutical systems containing metoprolol and different SEs (S-370, S-970, S-1670, M-1695, and L-1695) were prepared and investigated by Csòka et al. [11]; the results revealed that all SEs tested enhance drug release. In particular SEs with shorter fatty acid chain and higher HLB value increased ten fold the amount of drug released.

Csizmazia et al. have compared the effect of sucrose laurate (S-1670) and ethoxydiglycol

on ibuprofen penetration [12]. They concluded that SEs can increase the skin penetration and permeation of ibuprofen efficiently, and ethoxydiglycol leads to ibuprofen accumulation in the stratum corneum, thereby ensuring sustained drug release. These authors have also investigated the effect of sucrose laurate on ibuprofen permeation. Hydrogel with and without sucrose laurate have been tested using a special bilayer stratum corneum structure. Results have shown that sucrose laurate based gel did not cause greater alterations in the stratum corneum structure than the ibuprofen gel without sucrose laurate. It has been proven that SEs act as an effective hydratation enhancer and increases the penetration of ibuprofen through the skin.

1.2.3 Regulatory and toxicological status of sucrose esters

SEs are approved as food additives (E473) and are widely used in the food industry. In 1992, the Scientific Committee for Food estabilished an acceptable daily intake (ADI) of 0-20 mg/kg bw/day for SEs of fatty acids and sucroglycerides derived from palm oil, lard and tallow fatty acids. In 2004, in the light of new studies the European Food Safety Authority (EFSA) re-examined the safety of these food additives and established an ADI of 40 mg/kg bw/day for SEs of fatty acids.

Since SEs are often used in various food products, their absorption, distribution and metabolism have been thoroughly evaluated [13–15], the results showed that the SEs are hydrolysed to sucrose and fatty acids prior to intestinal absorption and the extent of the hydrolysis depending on the degree of esterification of the SEs. SEs having the higher fatty acids, such as the octa- and hepta-esters, are not absorbed by humans and are excreted unchanged, while those having the lower fatty acids are partially hydrolysed and absorbed as sucrose and individual fatty acids.

The tolerability of SEs has been confirmed in animal tests. The oral toxicity and carcinogenicity of sucrose stearate (S-570) were evaluated by Takeda and Flood [16]. Results have demonstrated that there are no SEs-related effects on survival, tumor incidence and other findings.

SEs based on palmitic, stearic or lauric acids are registered in the Japanese Standards of Cosmetics Ingredients, most of the SEs are also registered in Cosmetics Directive of the European Union, and they can therefore be used in cosmetics and personal care products marketed in Europe. In the pharmaceutical field, SEs are employed as emulsifiers, solubilizers, bioavailability/permeation enhancers and SEs with medium/low HLB values can be also used as lubricant.

1.3 Supramolecular aggreagates structures

The supramolecular aggregation of molecules resulting in a 3-D structure formation can be described as an aggregation phenomenon, in particular it can be associated to a micellization process. In the micellisation process, molecular geometry plays an important role because it affects the packing ability of the amphiphiles molecules. The main structures are spherical micelles, vesicles, bilayers, or inverted micelles (see Fig. 1.3). Two opposing forces control the self-association process: hydrocarbon-water interactions that promote aggregation (pulling surfactant molecules out of the aqueous environment), and head group interactions that work in the opposite sense. These two contributions can be considered as an attractive interfacial tension term due to hydrocarbon tails and a repulsion term depending on the nature of the hydrophilic group (see Fig. 1.2) More recently, this basic idea was reviewed and quantified by Mitchell and Ninham [17] and Israelachvili [18], resulting in the concept that aggregation of surfactants is controlled by a balanced molecular geometry. In brief, the geometric treatment separates the overall free energy of association into three critical geometric terms:

- the minimum interfacial area occupied by the head group, a_o;
- the volume of the hydrophobic tail(s), v;
- the maximum extended chain length of the tail in the micelle core, l_c.

Formation of a spherical micelle requires that l_c is equal or less than the micelle core radius, R_{mic}. For spherical micelles, the aggregation number, N, can be expressed either as the ratio of micellar core volume (V_{mic}) and the volume of the hydrophobic tail (v):

$$N = \frac{V_{mic}}{v} = \frac{\frac{4}{3}\pi R_{mic}^3}{v}$$

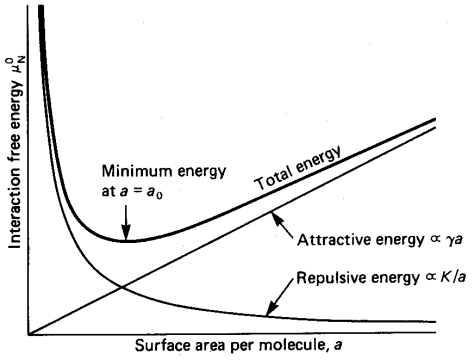

Figure 1.2: Relation between interaction free energy μ_N^0 and surface head area a.

Table 1.3: Expected aggregate characteristics in relation to surfactant critical packing parameter.

P_p	**Surfactant type**	**Expected aggregate structure**
<0,33	Single-chain surfactants with large head groups	Spherical or ellipsoidal micelles
0,33 - 0,5	Single-chain surfactants with small head groups, or ionics in the presence of large amounts of electrolyte	Large cylindrical or rod-shaped micelles
0,5 - 1,0	Double-chain surfactants with large head groups and flexible chains	Vesicles and flexible bilayers structures
1,0	Double-chain surfactants with small head groups or rigid, immobile chains	Planar extended bilayers
>1,0	Double-chain surfactants with small head groups, very large and bulky hydrophobic groups	Reversed or inverted micelles

or as the ratio between the micellar area, A_{mic}, and the cross-sectional area, a_o

$$N = \frac{A_{mic}}{a_o} = \frac{4\pi R_{mic}^2}{a_o}$$

Equating the two previous:

$$\frac{v}{a_o R_{mic}} = \frac{1}{3}$$

Since l_c cannot exceed R_{mic} for a spherical micelle:

$$\frac{v}{a_o l_c} \leq \frac{1}{3}$$

More generally, this defines a critical packing parameter, P_p, as the ratio of volume to surface area:

$$P_p = \frac{v}{a_o l_c}$$

The parameter v varies with the number of hydrophobic groups, chain unsaturation, chain branching and chain penetration by other compatible hydrophobic groups, while a_o is mainly governed by electrostatic interactions and head group hydration. P_p is a useful parameter since it allows the prediction of aggregate shape and size. The predicted aggregation characteristics of surfactants cover a wide range of geometric possibilities, and the main types are presented in Table 1.3.

1.4 Emulsion and microemulsion formation and stability

A simple way for describing emulsion and microemulsion formation is to consider a subdivision of the dispersed phase into very small droplets. Then the configurational entropy change, ΔS_{conf}, can be approximately expressed as [19]:

$$\Delta S_{conf} = -nk_b[\ln \phi + \frac{(1-\phi)}{\phi} \ln (1-\phi)] \tag{1.1}$$

where n is the number of the droplet of dispersed phase, k_b is the Boltzmann constant and ϕ is the dispersed phase volume fraction. The associated free energy change can be expressed as a sum of the free energy for creating new area of interface, $\Delta A\gamma_{12}$, and the configurational entropy in the form [20]:

$$\Delta G_{form} = \Delta A\gamma_{12} - T\Delta S_{conf} \tag{1.2}$$

where ΔA is the change in interfacial area A (equal to $4\pi r^2$ per droplet of radius r) and γ_{12} is the interfacial tension between phases 1 and 2 (e.g., oil and water) at temperature T (Kelvin).

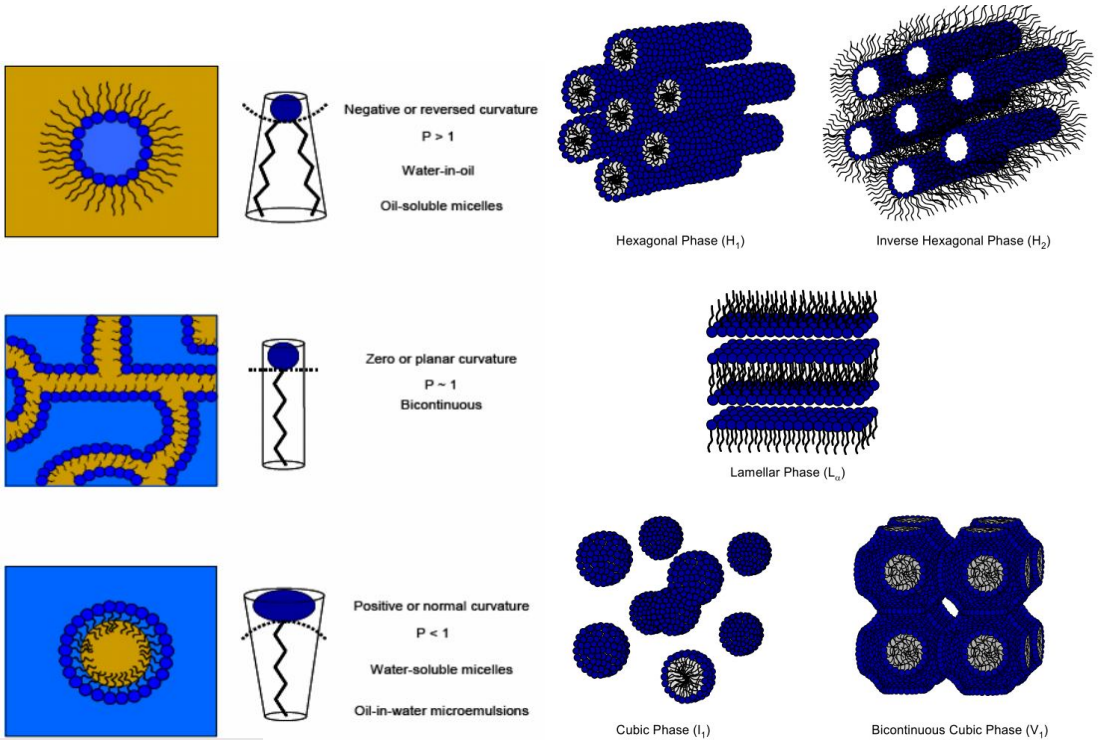

Figure 1.3: Changes in the critical packing parameters (P_p) of amphiphilic molecules give rise to different aggregation structures.

The combination of Eq.(1.1) and (1.2) gives an expression for obtaining the maximum interfacial tension between phases 1 and 2. During emulsification, the droplet number increases and ΔS_{conf} is positive. If the surfactant reduces the interfacial tension to a sufficiently low value, the energy term in (1.2) ($\Delta A\gamma_{12}$) will be relatively small and positive, allowing a negative (and hence favourable) free energy change, and thus resulting in spontaneous emulsification.

In surfactant-free oil-water systems, $\gamma_{o/w}$ is of the order of 50 mN/m, and during emulsion and microemulsion formation the increase in interfacial area, ΔA, is very large, typically a factor of 10^4 to 10^5. Therefore in the absence of surfactant, the second term in Eq.(1.2) becomes very high, and in order to fulfill the condition $\Delta A_{12} \leq T\Delta Sconf$, the interfacial tension should be very low (approximately 0,01 mN/m). Some surfactants (double chain ionics [21] and some non-ionics [22]) can produce extremely low interfacial tensions (typically 10^{-2} to 10^{-4} mN/m) but in most cases, such low values cannot be achieved by a single surfactant since the CMC is reached before a low value of $\gamma_{o/w}$ is attained. An effective way to further decrease $\gamma_{w/o}$ is to include a second surface-active species (either a surfactant or medium-chain alcohol), acting as a co-surfactant. This can be explained in terms of the Gibbs equation extended to multicomponent systems. It relates the interfacial tension to the surfactant film composition and the chemical potential, μ, of each component of the system, as:

$$d\gamma_{o/w} = -\sum_i (\Gamma_i d\,\mu_i) \approx -\sum_i (\Gamma_i RTd\,\ln C_i) \tag{1.3}$$

where C_i is the molar concentration of component i in the mixture, and Γ_i the surface excess. Assuming that surfactants and co-surfactants, with concentration C_s and C_{co} respectively, are the only adsorbed components (i.e.,$\Gamma_{water} = \Gamma_{oil} = 0$), the previous equation becomes:

$$d\gamma_{o/w} = -\Gamma_s RTd\,\ln C_S - \Gamma_{co} RTd\,\ln Cco \tag{1.4}$$

and its integration gives:

$$\gamma_{o/w} = \gamma^o_{o/w} - \int_0^{C_s} \Gamma_s RTd\,\ln C_s - \int_0^{C_{co}} \Gamma_{co} RTd\,\ln C_{co} \tag{1.5}$$

The equation above shows that $\gamma^o_{o/w}$ is lowered by two terms, both from the surfactant and co-surfactant so their effects are additive. It should be mentioned, however, that the two molecules should be adsorbed simultaneously and should not interact with each

other (otherwise they lower their respective activities), i.e., have completely different chemical nature, so that mixed micellization does not occur.

Predicting emulsion and microemulsion type

A well-known classification of emulsion and microemulsions was proposed by Winsor [23] who identified four general types of phase equilibria:

- **Winsor I:** the surfactant is preferentially soluble in water and an oil-in-water (o/w) emulsion and microemulsions is formed. The surfactant-rich water phase coexists with the oil phase where surfactant is only present as monomers at low concentration
- **Winsor II:** the surfactant is mainly in the oil phase and a water-in-oil (w/o) emulsion or microemulsions is formed. The surfactant-rich oil phase coexists with the surfactant-poor aqueous phase
- **Winsor III:** three-phase system, where a surfactant-rich middle-phase coexists with both an excess water and oil surfactant-poor phases (middle-phase emulsion and microemulsion)
- **Winsor IV:** a single-phase (isotropic) micellar solution, that forms upon addition of a sufficient amount of amphiphile (surfactant plus alcohol).

Depending on surfactant type and sample environment, type I, II, III or IV winsor phase equilibria is formed, the dominant type being related to the molecular arrangement at the interface (see below). Phase transitions are brought about by increasing either electrolyte concentration (in the case of ionic surfactants) or temperature (for non-ionics). Various investigators have focused on interactions in an adsorbed interfacial film to explain the direction and extent of interfacial curvature. The first theory was proposed by Bancroft [24] and Clowes [25] who considered the adsorbed film in emulsion systems to be duplex in nature, with an inner and an outer interfacial tension acting independently. The interface would then curve such that the inner surface was one of higher tension. Bancroft's rule was stated as "that phase will be external in which the emulsifier is most soluble"; i.e., oil-soluble emulsifiers will form w/o emulsions and water-soluble emulsifiers will form o/w emulsions.

In order to take into account the influence of amphiphiles and solvents at the interfacial curvature, Winsor [23] had proposed the R-ratio parameter. The primary concept is to relate the energies of interaction between the amphiphile layer and the oil and water

regions. Therefore, this R-ratio compares the tendency for an amphiphile to disperse into oil, to its tendency to dissolve in water. If one phase is favoured, the interfacial region tends to take on a definite curvature. In micellar or microemulsion solutions, three distinct (single or multicomponent) regions can be recognized: an aqueous region, W, an oil or organic region, O, and an amphiphilic region, C. As shown in figure 1.4 , it is useful to consider the interfacial zone as having a definite composition, separating essentially bulk-phase water from bulk-phase oil.

Cohesive interaction energies therefore exist within the surfactant (C) layer, and these determine interfacial film stability. They are depicted schematically in Fig. 1.4: the cohesive energy between molecules x and y is defined as A_{xy} , and is positive whenever interaction between molecules is attractive. A_{xy} is depicted as the cohesive energy per unit area between surfactant, oil and water molecules residing in the anisotropic interfacial C layer. For surfactant-oil and surfactant-water interactions A_{xy} can be considered to be composed of two additive contributions:

$$A_{xy} = A_{Lxy} + A_{Hxy} \tag{1.6}$$

where A_{Lxy} quantifies interaction between non-polar portions of the two molecules (typically London dispersion forces) and A_{Hxy} represents polar interactions, especially hydrogen bonding or Coulombic interactions. Thus, for surfactant-oil and surfactant-water interactions, cohesive energies to be considered are:

$$A_{co} = A_{Lco} + A_{Hco} \tag{1.7}$$

$$A_{cw} = A_{Lcw} + A_{Hcw} \tag{1.8}$$

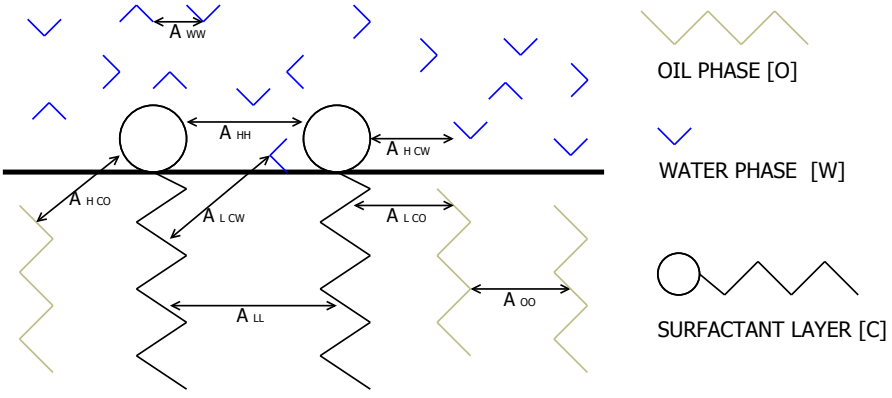

Figure 1.4: Interaction energies in the interfacial region of an oil-surfactant-water system. Adapted from [26]

A_{Hco} and A_{Lcw} are generally very small values and can be ignored.
Other cohesive energies are those arising from the following interactions:

- water-water, A_{ww}
- oil-oil, A_{oo}
- hydrophobic-hydrophobic chains (L) of surfactant molecules, A_{LL}
- hydrophilic-hydrophilic chains (H) of surfactant molecules, A_{HH}

The cohesive energy A_{co} evidently promotes miscibility of the surfactant molecules with the oil region, and A_{cw} with water. On the other hand, A_{oo} and A_{LL} oppose miscibility with oil, while A_{ww} and A_{HH} oppose miscibility with water. Therefore, interfacial stability is ensured if the difference in solvent interactions in C with oil and water bulk phases is sufficiently small. Too large a difference, thus, too strong affinity of C for one phase or the other, would drive to a phase separation. Winsor expressed qualitatively this variation in dispersing tendency by:

$$R = \frac{A_{co}}{A_{cw}} \tag{1.9}$$

To account for the structure of the oil, and the interactions between surfactant molecules, an extended version of the original R-ratio was proposed [27]:

$$R = \frac{A_{co} - A_{oo} - A_{LL}}{A_{cw} - A_{ww} - A_{HH}} \tag{1.10}$$

In brief, Winsor's primary concept is that this R-ratio of cohesive energies, stemming from interaction of the interfacial layer with oil, divided by energies resulting from interactions with water, determines the preferred interfacial curvature. Thus, if R >1, the interface tends to increase its area of contact with oil while decreasing its area of contact with water. Thus oil tends to become the continuous phase and the corresponding characteristic system is type II (Winsor II). Similarly, a balanced interfacial layer is represented by R=1.

1.5 High internal phase ratio emulsions (HIPREs)

Highly concentrated emulsions are an interesting class of emulsions characterized by an internal phase volume fraction (Φ) exceeding 0,74, the critical value of the most

compact arrangement of uniform, undistorted spherical droplets [28, 29]. Consequently, their structure consists of deformed polyhedral and/or polydisperse droplets separated by a thin film of continuous phase, a structure resembling gas-liquid foams. They are high-internal-phase emulsions (HIPREs) which are also referred to in the literature as gel emulsions [30–32], hydrocarbon gels, biliquid foams, etc. The internal or dispersed phase of highly concentrated emulsions can be either polar or non-polar and, as ordinary emulsions, they are classified in two categories: water-in-oil (W/O) and oil-in-water (O/W). However, they can be classified according to other criteria such as the microstructure of the continuous phase or the interaction forces between droplets. Phase behavior studies have shown [30, 33, 34] that highly concentrated emulsions separate into two phases: one phase is a submicellar surfactant solution in water (or a surfactant solution in oil) and the other phase can be either a microemulsion [30, 34] or a cubic liquid crystalline phase [31]. The stability of highly concentrated emulsions is greatly affected, as in conventional emulsions, by the nature of the components, the volume fraction of the dispersed phase, the oil surfactant weight ratio, presence of additives, and temperature [35]. The time taken for phase separation, which may vary from minutes to years, can be significantly retarded by appropriate selection of the different composition variables and temperature. One characteristic property of highly concentrated emulsions is their high viscosity as compared to that of the constituent phases. They are non-Newtonian fluids characterized by a yield stress below which they show a solid-like behavior [29, 36, 37]. Determination of the rheological properties by means of dynamic (oscillatory) measurements showed that they have a viscoelastic response that can be fitted to a Maxwell liquid element: an elastic modulus produced by interfacial area increase and a viscous modulus produced by the loss caused by slippage of droplets against droplets. The values of relaxation time were found to be proportional to the continuous phase viscosity and inversely proportional to the continuous phase volume fraction [38]. The characteristic properties of highly concentrated emulsions are of particular interest for theoretical studies and for applications. They are widely used as formulations in cosmetics, foods, and pharmaceuticals.

1.5.1 Stability

HIPREs are kinetically stable systems, which break into two liquid phases with time. The time taken for separation which may vary from minutes to years and it can be significantly retarded by the appropriate selection of composition variables and temperature. The changes in structure of the continuous phase strongly affect the gel emulsion stability. As described above, a change in microemulsion structure from bicontinuous to W/O type was observed with an increase in the oil/surfactant ratio [32].

1.5.2 Oil in water (O/W) gel emulsion formation

The mechanism of O/W gel emulsion (HIPREs) formation was determined by Ozawa and colleagues [39] by studying the phase behavior of HIPREs as function of temperature and following the emulsification process conductimetrically. It was found that during the emulsification process liquid crystal structures and microemulsion often coexist and it was observed that the faster the cooling rate of the gel emulsion, the smaller the droplets and narrower the size distribution. This was attributed to the fact that at a temperature lower than the single-phase microemulsion, there is an extremely unstable emulsion region. If the cooling rate is fast, the system passes this region in a short time and the coalescence of oil droplets is very slow.

1.6 Liquid crystalline systems (LCS)

The liquid crystalline state combines properties of both liquid and solid states. The liquid state is associated with the ability to flow, whereas solids have an ordered, crystalline structure. Crystalline solids exhibit short as well as long-range order in context of both position and orientation of the molecules. Liquids are amorphous in general but may show short-range order in context of position and/or orientation. Liquid crystals show at least orientational long-range order and may show short-range order where the positional long-range order has disappeared. Accordingly, liquid crystalline phases represent intermediate states, also called mesophases. A prerequisite for the formation of liquid crystalline phases is an anisometric molecular shape which is generally associated with a marked anisotropy of the polarizability. Molecules that can form mesophases are called mesogens. Depending on the molecular shape, rod-like mesogens form calamitic mesophases, whereas disk-like mesogens form discotic mesophases. Rod-shaped molecules are often drug excipients (e.g., surfactants). Even drug compounds, such as salts of organic acids or bases, with anisometric molecular shape fulfill the requirements for the formation of calamitic mesophases.

1.6.1 Formation

Starting with the crystalline state, the mesophase is reached by increasing the temperature or by adding a solvent. Accordingly, a differentiation can be made between thermotropic and lyotropic liquid crystals, respectively.
Thermotropic Liquid Crystals are formed by the action of heat on certain solids and occur as a phase of matter between a solid and a liquid, they are of no interest for our purposes so their argumentation is not reported here.

Lyotropic liquid crystals differ from thermotropic liquid crystals. They are formed by mesogens which are not the molecules themselves but their hydrates or solvates as well as associates of hydrated or solvated molecules. In the presence of water or a mixture of water and an organic solvent as the most important solvents for drug molecules, the degree of hydration or solvation, respectively, depends on the amphiphilic properties of a drug molecule. Hydration of the mostly rod-shaped molecule -and the same holds for solvation- results in different geometries, cone or cylinder (see Sec. 1.3). Cylinders arrange in layers, resulting in a lamellar phase with alternating polar and non-polar layers. Water and aqueous solutions can be included in the polar layers, resulting in an increase of the layer thickness. Analogously, lipophilic molecules can be included in the non-polar layers. In addition to the increased layer thickness of the lamellar phase, lateral inclusion between molecules is also possible, this produces an increase in the solvent concentration, and thus a change from a rod shape to a cone shape of the solvated molecules, leading to a phase change. A range of lyotropic mesophases are possible, depending on the mesogen concentration, the lipophilic or hydrophilic characteristics of the solvent, and the molecule itself [40]. Polar amphiphilic lipids that possess a very low aqueous solubility often self-assemble into lyotropic LCS in the presence of an excess of water [41]. Depending upon the nature of the lipid, the presence of additives, and solution conditions the structures formed often include the lamellar, reversed hexagonal and reverse bicontinuous cubic phase. The two or three-dimensional liquid crystalline structure consists of discrete lipidic hydrophobic and aqueous hydrophilic domains and imparts a high viscosity to these materials. Sustained release of amphiphilic, hydrophilic and lipophilic drugs under diffusion control can be achieved from the liquid crystalline matrix [42–44].

It is known that the LCS can provide appropriated response for prolonged time, improving drug efficacy and reducing side effects. These systems can be administered by different routes including ocular, oral, intraperitoneal, intramuscular, subcutaneous and cutaneous. The development of new drug carrier systems based in the LCS structure has been a promising approach to increase and control the drug skin penetration [45]. Liquid crystalline phases are mixtures having the mechanical properties of a liquid (often very viscous) and optical characteristics of a crystal (optical anisotropy). Liquid crystalline systems are thermodynamically stable, thermotropic and lyotropic systems that can be stored for long periods without alterations [46, 47]. Lyotropic liquid crystalline phases can be used as topical drug delivery systems because the high ability of drug solubilization, thermodynamic stability and high similarity with the intercellular lipid membranes of the skin and they also present a wide range of rheological properties. Swarbrick and Siverly investigated the topical application of vehicles containing LCS and established

Table 1.4: Application of lipid formulations in various BCS category drugs

BCS class	**Issues**
Class I	Enzymatic degradation, gut wall efflux
Class II	Solubilization and bioavailability
Class III	Enzymatic degradation, gut wall efflux and bioavailability
Class IV	Solubilization, enzymatic degradation, gut wall efflux and bioavailability

that the percutaneous absorption of lipophilic drug model decreases significantly when the proportion of liquid crystalline phases increases above 5–10% [48].

1.7 Lipid formulations

Lipid formulations for oral administration of drugs generally consist of a drug dissolved in a blend of two or more excipients, which may be triglyceride oils, partial glycerides, surfactants or co-surfactants. The primary mechanism of action which leads to improved bioavailability is usually avoidance, or partial avoidance, of the slow dissolution process which limits the bioavailability of hydrophobic drugs from solid dosage forms. Ideally the formulation allows the drug to remain in a dissolved state throughout its transit through the gastrointestinal tract. The availability of the drug for absorption can be enhanced by presentation of the drug as a solubilizate within a colloidal dispersion. This objective can be achieved by formulation of the drug in a self-emulsifying system or alternatively by taking advantage of the natural process of triglyceride digestion. In practice lipid formulations range from pure oils, at one extreme, to blends which contain a substantial proportion of hydrophilic surfactants or cosolvents. Active molecules that may find advantage in being vehicled within lipid formulations can be identified by the Lipinski's rule of five [49]. In the discovery setting, the rule of five predicts that poor absorption or poor permeation is more likely when in the active molecule there are more than five H-bond donors, more than ten H-bond acceptors, the molecular weight is higher than 500 Da and the calculated logP is lower than 5. Use of lipid formulations can be extended to all four categories of biopharmaceutical classification system (BCS) class drugs [50]. These systems can help in solving the under-mentioned problems of all the categories of BCS class drugs, as depicted in Table 1.4.

The Lipid Formulation Classification System was introduced as a working model in 2000 [51], and an extra type of formulation was added in 2006. The main purpose of the Lipid Formulation Classification System is to enable in-vivo studies to be interpreted more readily and, subsequently, to facilitate the identification of the most appropriate

Table 1.5: The Lipid Formulation Classification System: characteristic features, pros and cons of the four essential types of lipid formulations

Type	Excipients	Properties	Pros	Cons
I	Oils without surfactants (*e.g.* tri- di- and monoglycerides)	Nondispersing, requires digestion	GRAS status; simple	poor solvent capacity unless drug is highly lipophilic
II	Oils and water-insoluble surfactants	SEDDS formed without water soluble components	Unlikely to lose solvent capacity on dispersion	Turbid o/w dispersion (particle size 0,25-2 μm)
III	Oils, surfactants and cosolvents (both water-insoluble and water-soluble excipients)	SEDDS/SMEDDS formed with water-soluble components	Clear or almost clear dispersion; drug absorption without digestion	Possible loss of solvent capacity on dispersion; less easily digested
IV	Water-soluble surfactants and cosolvents (no oils)	Formulation disperses typically to form a micellar solution	Formulation has good solvent capacity for many drugs	Likely loss of solvent capacity on dispersion; might not be digestible

formulations for specific drugs (*i.e.* with reference to their physicochemical properties) [52] . Table 1.5[1] indicates the fundamental differences between types I, II, III and IV formulations [54].

1.7.1 Self-emulsifying drug delivery systems (SEDDS)

Among the different lipid formulations, in recent years much attention has been focused on self-emulsifying drug delivery systems (SEDDS). The clinical usefulness of the SEDDS is evident from the commercially available formulations containing cyclosporin A, ritonavir and saquinavir. SEDDS are mixtures of drug, oils, surfactants and/or co-solvents which form fine oil-in-water emulsions upon dilution with aqueous medium or in vivo administration. The digestive motility of the stomach and intestine provides the agitation necessary for the self-emulsification process. The small oil droplets produced by self-emulsification provide a large interfacial area for pancreatic lipase and promote rapid

[1] adapted from [53]

release of the drug. The surfactants are also able to improve drug bioavailability by various mechanisms including improved drug dissolution, increased intestinal epithelial permeability, increased tight junction permeability and decreased P-glycoprotein-mediated efflux.

1.8 Sucrose esters and complex aggregate systems

In view of the fact that most basic studies on microemulsions, emulsion gels (HIPREs) and liquid crystalline systems have been conducted with standard surfactants, such as polyoxyethylene-type nonionic surfactants, alkyl sulfates, quaternary ammonium salts and dialkyl sulfosuccinate that are not permitted in food systems for health restrictions it is important to search for new surfactants to prepare such aggregate systems. Food-grade surfactants are limited in their number and structure. Among the hydrophobic surfactants one can find mono- and diglycerides of fatty acids; sorbitan esters, polyglycerol esters, such as polyglycerol polyricinoleate (PGPR) and sucrose ester (sucrose polystearate). Among the hydrophilic surfactants, the selection is somewhat larger, and emulsifiers such as ethoxylated sorbitan esters, polyglycerol esters, sodium stearoyl lactylate and sucrose esters, are food-grade compounds. Sucrose esters are manufactured and used mostly in Japan and only recently other countries registered sucrose esters as food-grade permitted emulsifiers. Sucrose esters exists in a large variety of HLB values, the monosubstituted (sucrose monostearate, monooleate, monolaurate, etc.) have high HLB values and will dissolve in water, while the sucrose poly-fatty acid esters are hydrophobic, with low HLB values and will mostly be oil soluble. It is therefore expected of the surfactant monolayer curvature at the oil-water interfaces that the sucrose polyesters will form W/O emulsions while the sucrose monoesters will form the O/W emulsions. It is quite surprising that the use of sucrose esters, for the formation of complex aggregate systems, is very limited, and practically no systematic studies have been carried out. The main reason for this, is that commercial sucrose esters are complex mixtures of different fatty acids with very complicated isomeric compounds (the fatty acid react in different positions), and the final product can be mono-, di-, or polyesterified and their mixtures.

Several authors [55–57] reported that sucrose esters are not able to form microemulsions without co-surfactants. Co-surfactants used in microemulsion studies are very often represented by short chain alcohols [58], their main functions are to reduce interfacial tension positioning at the oil-water interface and act also as co-solubilizers. Unfortunately the only alcohol admitted in high quantity by food regulations is ethyl alcohol. Ethyl alcohol does not suit our formulative expectations, because of its toxicity it is not well accepted by the market, also, alcoholic products represents only a very little part

of the nutraceutical market, then the use of alcohol was not taken into account.

1.9 Dissolution and release modeling fundamentals

Regardless the administration route, key factor for the success and reliability of a whatever formulation is drug bioavailability, defined as the rate and extent to which the active drug is absorbed from a pharmaceutical form and becomes available at the site of drug action. Although metabolism and physiological factors highly affect drug absorption by living tissues, bioavailability strongly depends on drug permeability through cell membranes and drug solubilization in physiological fluids. Indeed, especially for what concerns oral formulations, if solubilization is the first absorption step, permeation is the second one as drug must dissolve in the physiological fluids and then it must cross cellular membranes. Drugs with improved water solubility can be administered in a lower concentrated dose, with a reduction of local and systemic side-effects; this is crucial for drugs with important side-effect such as antibiotics, antifungals, or antivirals. Moreover, improved dissolution means higher onset of action that is particularly valuable for drugs intended to work immediately as required in pain, antianxiety, or antiemetic management.

Because qualitative and quantitative changes in a formulation may alter drug release and in vivo performance, developing tools that facilitate product development by reducing the necessity of bio-studies is always desirable. In this regard, the use of *in-vitro* drug dissolution data to predict *in-vivo* bio-performance can be considered as the rational development of controlled release formulations. Model dependent methods are based on different mathematical functions, which describe the dissolution profile. Once a suitable function has been selected, the dissolution profiles are evaluated depending on the derived model parameters. The fundamental principle for evaluation of the kinetics of drug release was offered by Noyes and Whitney [59] in 1897 as the equation:

$$\frac{d_M}{d_t} = KS(C_s - C_t) \tag{1.11}$$

where M, is the mass transferred with respect to time, t, by dissolution from the solid particle of instantaneous surface, S, under the effect of the prevailing concentration driving force $(C_s - C_t)$, where C_t is the concentration at time t and C_s is the equilibrium solubility of the solute at the experimental temperature. The rate of dissolution d_M/d_t is the amount dissolved per unit area per unit time and for most solids can be expressed in units of $g \cdot cm^{-2} \cdot s^{-1}$. When C_t is less than 15% of the saturated solubility C_s, C_t has a negligible influence on the dissolution rate of the solid. Under such circumstances,

the dissolution of the solid is said to be occurring under "sink" conditions. In general, the surface area, S is not constant except when the quantity of material present exceeds the saturation solubility, or initially, when only small quantities of drug have dissolved. There are number of kinetic models, which described the overall release of drug from the dosage forms. Because qualitative and quantitative changes in a formulation may alter drug release and in-vivo performance, developing tools that facilitate product development by reducing the necessity of bio-studies is always desirable. In this regard, the use of in-vitro drug dissolution data to predict in-vivo bio-performance can be considered as the rational development of controlled release formulations.

1.10 Model molecules

1.10.1 Ubidecarenon

Coenzyme Q_{10} (Co Q_{10}; ubidecarenon; ubiquinol-10 and/or ubiquinone-10) plays the essential role of electron carrier and proton translocator during cellular respiration and ATP production and protects numerous cellular membranes and plasma lipoproteins against free radical-induced damage. CoQ_{10} is primarily obtained from meat, poultry, fish, and rapeseed oil [60, 61]. In recent years, the use of CoQ_{10} as a nutritional supplement has attracted much attention. Numerous CoQ_{10} products are available on the market, including tablets (chewable and non-chewable), powder-filled capsules, and soft gels containing an oil suspension [62]. CoQ_{10}, a yellow colored crystalline powder with a melting point of 48 °C is practically insoluble in water and poorly absorbed from the gastrointestinal tract. The slow absorption of CoQ_{10} (T_{max} 5-10 h) and the very low oral bioavailability of CoQ_{10} in these products is due of its high molecular weight and poor water solubility (see Fig. 1.5). In the past few years, there has been an extensive effort to improve the oral bioavailability of CoQ_{10} in nutritional supplements. Various formulations for improvement of the oral bioavailability of CoQ_{10} have been investigated, including molecular complexes [63, 64], emulsions [65, 66], and liposomal systems [67].

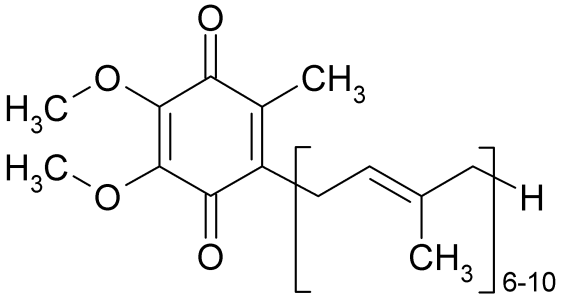

Figure 1.5: Structure of CoQ_{10}

1.10.2 Resveratrol

Resveratrol (3,5,4'-trihydroxystilbene) is a non-flavonoid polyphenolic compound abundant in grapes, peanuts and other foods that are commonly consumed as part of human diet. The compound was first isolated from the root of Polygonum cuspidatum, a plant used in traditional Chinese and Japanese medicine [68]. Starting in the 1990's and continuing to date, scientific studies have reported that resveratrol has a broad range of desirable biological actions, including cardioprotection [69, 70], cancer prevention [71] and prolongation of lifespan in several species [72, 73]. The biological properties of resveratrol are attributed to its ability to inhibit the oxidation of human low-density lipoprotein, while its suppression of cyclooxygenase- 2 and inducible nitric oxide synthase activities also contribute to its anti-inflammatory and antioxidant effects [74, 75]. Furthermore, the chemopreventive effect of resveratrol is thought to be due to inhibition of quinone reductase-2 activity, which in turn up-regulates the expression of cellular antioxidant and detoxification enzymes to improve cellular resistance to oxidative stress [76]. Resveratrol also increases the activity of SIRT (a member of the sirtuin family of nicotinamide adenine dinucleotide-dependent deacetylases), resulting in improved cellular stress resistance and longevity [77]. Resveratrol can also regulate the expression of hormone dependent genes such as the onco-suppressor BRCA1 in breast cells, due to its structural similarity to diethylstilbestrol [78].

Topical application of resveratrol to SKH-1 hairless mice prior to UV-B irradiation significantly inhibited UV-B-induced skin edema and caused a significant decrease in UV-B mediated generation of hydrogen peroxide and infiltration of leukocytes [79]. In another study, pretreatment of normal human epidermal keratinocytes (NHEK) with resveratrol inhibited UV-B-mediated activation of NF-JB pathway. Studies have demonstrated that resveratrol imparts its protective effect against multiple UV-B exposure via modulations in the cki-cyclin-cdk network and MAPK pathway [80]. In long-term studies, topical application of resveratrol (both pre- and post-exposure to UVB) has been shown to result in a significant inhibition in tumor incidence and delay in the onset of tumorigenesis [81]. Other studies demonstrates that topical application of resveratrol protects human skin from the effects of sun damage by decreasing the formation of sunburn cells [82, 83]. There was improvement in the moisture of the skin and its elasticity, an amelioration of skin roughness and depth of wrinkles, combined with a reduction of age-spots color intensity [84]. The presence of specific resveratrol receptor sites in human skin suggests that this polyphenolic compound may be useful to prevent skin disorders associated with aging [85]. The anti-acneic property of resveratrol in volunteers with acne vulgaris has also been reported [86].

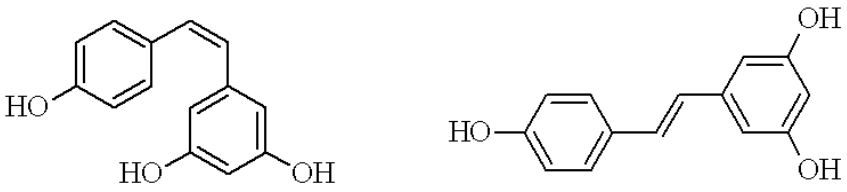

Figure 1.6: Chemical structures of trans-3,4',5-trihydroxystilbene: cis-(Z)-resveratrol, (left) and trans-(E)-resveratrol, (right).

Chapter 2

Development of the Formulation Platform

The aim of the work described in this chapter is the development of a platform formulation based on sucrose esters, medium chain fatty acids, water and glycerin. To rationalize and reduce the number of the tests the Design of Experiments technique is initially used.

2.1 Introduction to Design of Experiments

A process can be represented as a combination of operations which transform inputs (*e.g.* raw materials) in outputs (*e.g.* finished product). It may be influenced by controllable and measurable factors (*e.g.* temperature, concentration and pH), and non-controllable factors (*e.g.* impurities), both able to affect the characteristics of the experimental response. Thus, the knowledge of these factors permits to control the process and the final product characteristics.
In order to determine the amount of oil, surfactant and aqueous phase producing stable emulsions, Design of Experiments (DoE) was used. The DoE considers the experiment as a system composed of independent variables (experimental factors) and dependent variables (experimental responses). DoE measures and analyzes the effects of the changes in the parameters affecting the system properties (experimental responses). The term "experimental factor" identifies a parameter supposed to influence the phenomenon considered and whose variation causes a more or less intense variation of the experimental responses, *i.e.* data obtained experimentally. The experimental factors can be qualitative or quantitative and the alternatives in which they occur are defined levels that

identify the experimental domain, or the area of interest of the study. In the development of the DoE it is necessary to:

- recognize and state the contest
- select the variables and their levels
- choose the experimental responses
- choose the experimental plan (DoE)
- perform the experiments
- point out data statistical analysis

In order to obtain an equation expressing the influence of the experimental factors on the response, it is necessary to postulate a mathematical model suitable for the description of the studied phenomenon. The main model used for the study of many systems is a polynomial model of the first, second, or third degree [87]. The number of the model coefficients increases by increasing the degree of the polynomial and, after the third degree, the number of experiments to be carried out becomes extremely high. However, a polynomial of second or third degree generally are sufficient to represent a phenomenon [88]. Once chosen the mathematical model, it is necessary to define the experiments to be performed in order to calculate the model coefficients and to evaluate the effect of the variables on the experimental response. A set of experiments can be represented by means of the experimental matrices, or "tables" constituted by N lines, corresponding to N experiments, and k columns, corresponding to k variables studied. The variables are the parameters that will potentially affect the characteristics of the system and they may be qualitative (e.g. the type of excipient) or quantitative (e.g. the pH value). In order to assess the interaction between the variables and the responses, variables must be made comparable to each other by transforming them into codified or normalized variables, according to the equation:

$$x_i = \frac{U_i - U_i^0}{\Delta U_i} \tag{2.1}$$

where x_i is the value of the normalized variable, U_i is the value of the natural variable, U_i^0 is the value of the natural variable in the middle of the experimental domain, ΔU_i is the range of the natural variable. Experimental matrices are constructed in terms of normalized values and their choice depends on the postulated model. The experimental plan, which describes the experiments to be performed, is obtained by transforming the normalized values in experimental values. Once performed the experiments and obtained the experimental responses, it is possible to calculate the coefficients of the postulated

model [88].

Study of mixtures

In many product development areas, the application of experiments involving mixtures or blends is quite common. Generally, in mixture studies the interest is in developing better or innovative formulations with optimum characteristics (responses) able to satisfy determined requirements [89]. In the case of mixtures, the variables are quantitative and continuous and they show two important properties:

- they are dependent and their sum equal to 1 or 100% of the mixture composition
- they are dimensionless

Shape and size of the experimental domain depend on the number of formulation variables considered in the study. For k variables, a $k-1$ dimensions domain will be obtained. When $k=3$ the experimental domain is represented by an equilateral triangle, whose vertices correspond to the pure components, the sides to the binary mixtures and the interior points to the ternary mixtures (Fig. 2.1). It is also possible to limit the experimental domain by introducing quantitative constraints and relational limits between variables. Once defined the experimental domain, a mathematical model, able to describe the system, must be postulated and a matrix suitable to calculate the model coefficients must be chosen.
The ability of the model to describe the system and to predict the experimental response is assessed by calculating R^2 and R^2_A coefficients and by performing some additional experiments (test points). The choice of the test points is fundamental in order to have correct information about the quality of the predictive capacity of the model [90]. These

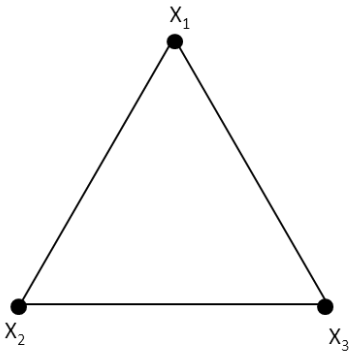

Figure 2.1: Representation of experimental domain for 3 factors mixtures without constraint.

points should be placed where the variance of the measured value is higher. If at the test points the experimental values are very similar to those estimated by using the model, it can be concluded that the mathematical model is appropriate to describe the system and to predict the experimental responses. Otherwise, if the difference between experimental and calculated values is too high, this means that probably coefficients have not been estimated with sufficient accuracy and the model does not fit well the system. In this case a model of higher degree must be chosen to describe the complexity of the system and a higher number of experiments must be performed in order to have a more accurate measure of the coefficients.
If the model provides a good fitting of data it will be possible to create the isoresponse surfaces describing the variation of the response as a function of the mixture composition (Fig. 2.2). The isoresponse surface could be used to choose the mixture having the desired response. For systems including several experimental responses, the overlap of the isoresponse surfaces, allows to identify an area of "optimum", which contains the mixture composition able to give the best experimental responses [89].

2.2 Materials

All materials used were of food grade: medium chain triglycerides (Basf S.p.a. - Ludwigshafen, Germany); sucrose mono-palmitate (Mitsubishi Kagaku Co. - Tokyo, Japan); ubidecarenone (LCM S.p.a. - Milan, Italy); resveratrol (Giellepi S.p.a. - Milan, Italy).

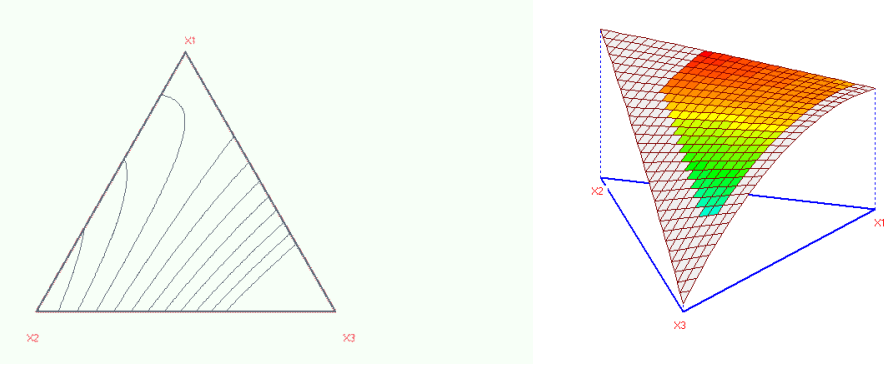

(a) (b)

Figure 2.2: Examples of two-dimensional (a) and three-dimensional (b) isoresponse surfaces.

2.3 Methods

2.3.1 Emulsification procedure

Since one of the main purposes of the study was to easily transfer the laboratory production process to an industrial scale it was essential to minimize the number of steps and to avoid unnecessary procedures. For example in a laboratory scale heating a water solution to 50 or 60 °C is not such an important issue, but if referred to an industrial mixer (*e.g.* 1000 L) an increase of 10 °C will cause the consuming of $1,16 \times 10^4$ W/h[1] as well as time consuming (depending on the heating and cooling system). Consequently the emulsification procedure has been set up on the basis of some preliminary trials and in particular it consists in two main steps:

1. mix and dispersion of sucrose esters in a water/glycerin solution, at 50 °C under gentle stirring ($\approx$ 200 rpm)
2. pouring the oil phase (previously heated to 50 °C) into the dispersion of sucrose esters under mild stirring ($\approx$ 400 rpm)

Once the emulsion was created, the resulting system was then cooled to room temperature.

2.3.2 Droplet size and electrokinetic potential determination

The effect of the components ratio on the particle size and particle size distribution was tested. Particle sizes were determined by dynamic laser light scattering instrument (Nano-ZS, Malvern Instruments, Worcestershire, UK) equipped with a 4 mW helium/-neon laser at a wavelength output of 633 nm. The particle size data is reported as the average mean diameter. To avoid multiple scattering effects, samples were diluted from 3× to 50× in water obtaining a viscosity and a turbidity that permits an optimal reading. Samples were placed in a capillary test tube that was loaded into the instrument operating with predefined parameters. Samples were equilibrated for 1 min at 25 °C inside the instrument before dynamic light backscattering (detection angle = 173°) data were collected. The average particle diameter was calculated by the instrument using the Stokes-Einstein equation, assuming the emulsion droplets to be spherical.
Zeta potential was calculated by determining the Electrophoretic Mobility and then applying the Henry equation. The electrophoretic mobility is obtained by performing

[1]Indicative calculation according to $\Delta E = m \cdot c_s \cdot \Delta T$ where m is the mass, c_s is water specific heat, and ΔT is the temperature variation.

an electrophoresis experiment on the sample and measuring the velocity of the particles using Laser Doppler Velocimetry (LDV). The measurements were done at least in triplicate.

2.3.3 Rheology measurements

Rheology is the study of deformation and flow of materials under external forces. Some equations and the units of these parameters are:

$$\tau = \frac{F}{A} \tag{2.2}$$

where: τ is shear stress ($Pa = kg \cdot m^{-1} \cdot s^{-2}$) and A is area (m^2). The viscosity can be defined as the ratio between shear stress and shear rate:

$$\eta = \frac{\tau}{\gamma} \tag{2.3}$$

where: η is viscosity and γ is shear rate (s^{-1}). Since the unit of shear stress is Pa and the unit of deformation is s^{-1}, the unit of viscosity is $Pa \cdot s$.
Rheology measurements were performed with a thermostated rotational rheometer (Thermo Scientific - HAAKE 550, Palo Alto, USA) composed by:

- thermocontroller HAAKE F3
- heat exchanger HAAKE CH
- Rotovisco RV20
- Rheocontroller RC20
- Stator M5
- Rotor SV-II

Because only Newtonian fluids have a measurable viscosity, which is independent of shear rate, semisolid pharmaceutical dosage forms that are non-Newtonian products exhibit an apparent viscosity. For semi-solids that show thixotropic properties and/or irreversible changes in viscosity after shearing, as in this case, specific attention was given to sample preparation procedures to minimize variability in the measurement of apparent viscosity caused by variable shear stress (e.g. mixing speed and temperature, filling operation, and sample handling). The removable sample holder of the Haake viscometer was filled with the sample, and then inserted into a thermostated water jacket mounted on the viscometer. A small sample adapter (SV-2P spindle), was used to measure the viscosity

of the preparations. The temperature of the sample was kept at 25 ℃ and then repeated measures were taken at 55 ℃. The sample was allowed to settle for 5 min prior to starting measurement. To permit a comparison between different formulations all the tests were performed varying shear rate (γ) from 0 to 50.000 s^{-1} in 2,5 min and from 50.000 to 0 s^{-1} in 2,5 min) and registering shear stress (τ) and viscosity (η). To obtain an easy comparison of data, maximum shear stress value of every formulation was taken into account.
Dynamic frequency sweep tests were carried out at 37 ℃, at 1,0 Pa in the limit of the linear viscoelastic region with a reomether Haake Rheo-Stress RS150 equipped with a parallel plates device (HPP20 profiled with diameter 35 mm). From these measurements, storage modulus (G') and loss modulus (G") were determined for frequencies between 0,01 and 100 Hz and a constant shear stress of 5 Pa. Rheology is able to determine the crystallographic structure of the lipid crystalline phases and dynamic processes occurring during relaxation of liquid crystalline phases, which are directly affecting diffusion properties in heterogeneous phases [91].

2.3.4 Differential scanning calorimetry (DSC)

The thermal behavior of the formulations and their components was determined through DSC investigation using Mettler Toledo DSC 1, STAR^e System (Mettler Toledo GmbH Analytical, Giessen,Germany), weighing 8-13 mg of samples on a microbalance, in standard 40 μl aluminum pans, immediately sealed by a press. An empty pan was used as a reference. Samples were scanned starting from 25 to 55 ℃ at a heating rate of 5 ℃/min. The fusion temperatures of the components and the total heat transferred in any of the observed thermal processes was determined. The DSC results are also useful to identify the liquid crystalline phases and the possible transitions occurring during the storage [92].

2.3.5 Electron microscopy analysis

Morphological and structural examination of selected formulations was carried out using transmission electron microscopy (TEM) Tecnai 12, FEI. After sample dilution with distilled water (1:200) and mixing by slightly shaking, one drop of sample was deposited on copper grids covered with a layer of Formvar standing for 4 min. After, the excess was removed by absorbing on a filter paper. The grids were later stained with one drop of 2% uranyl acetate solution and allowed to dry for 5 min before examination under the electron microscope.

2.3.6 Stability tests

Long term stability
Stability were examined according to ICH guidelines. The formulations were stored under ambient conditions for 12 months, and the system was examined periodically after 1, 3, and 6 months by visual inspection, centrifuge test and rheological evaluation.
Centrifugation stress testing
Stability studies is time consuming process, so accelerated stability test is preferred. Previously thermally tested formulations are placed in centrifuge test tubes and then in the centrifuge basket at a well-balanced equilibrium position at ambient temperature conditions. Formulations were centrifuged at 5.000 and 10.000 rpm for 30 min were applied in order to assess the physical instabilities like phase separation, phase inversion, aggregation, creaming and cracking.
Freeze-thaw cycles
To assess any change in stability, formulations were subjected to three freeze-thaw cycles consisting into storage at 25 ℃ for 24 h and followed by 24 h at -5 ℃ the cycle is repeated three times and change is noted.

2.4 Results

2.4.1 Design of Experiments

Lipophilic molecules generally present poor oral bioavailability due to their low water solubility. A formulation strategy to increase their solubility and thus their availability is represented by the lipid formulations. Lipid formulations are mixtures of the active and oil which may contain also surfactants, co-surfactants and solvents consequently emulsions belong to lipid formulations. The aim of this research project is to produce an oil-in-water emulsion able to delivery lipophilic molecules that can be use as platform to develop both oral and topic formulations.
The development of the platform formulation involves three main steps:

1. selection of the excipients
2. design and development of the formulation
3. characterization of the formulation

During the selection of the excipients it is necessary to take into account different parameters, in particular:

Table 2.1: Solubility of the active molecules in MCFA

Active	**Solubility (mg/ml)**
Ubidecarenon	$52,5 \pm 0,81$
Resveratrol	$0,82 \pm 0,10$

- they must be food grade
- they must have low costs
- they must have good taste

The company has also required the use of medium chain fatty acid (C8-C10) as oil phase. In order to meet all the parameters in this research it was evaluated the possibility to develop a platform employing medium chain fatty acid (MCFA) as oil phase and sucrose esters as surfactant using two lipophilic antioxidants as model active molecules (ubidecarenon and resveratrol). Among the different sucrose esters it was selected the sucrose monopalmitate because it presents the best dispersion in water and because it has the best organoleptic features.
Solubility of the active molecules in the selected oil phase was evaluated and results are reported in Table 2.1.

A mixture composed of water and glycerin (1:2, w/w) was chosen as aqueous phase because it provides the best dispersion of the sucrose esters. Preliminary trials have highlighted the presence of quantitative and relational constraints resumed in Tables 2.2 and 2.3. In order to describe the system a synergic polynomial mathematical model for three variables (Eq. 2.4) was postulated and two experimental responses, median diameter and zeta potential, were chosen:

$$Yi = b_0 + b_1x_1 + b_2x_2 + b_3x_3 + b_{(1-2)}x_1x_2 + b_{(1-3)}x_1x_3 + b_{(2-3)}x_2x_3 \qquad (2.4)$$

Experiments useful to estimate the mathematical coefficients were designed by the Nemrodw software (Nemwrod®, Marseille, France). In order to reduce the number of experiments the exchange algorithm was used and a matrix consisting of 18 experiments (Table 2.4 and Fig. 2.3) was selected.

2.4.2 Pseudo-ternary phase diagrams

The phase behavior of the four-components (sucrose ester:triglyceride:water:glycerin) systems is described on a pseudo-ternary phase diagram in which the weight ratio of two components (water and glycerin) was fixed. Considering the quantitative constraints and

Table 2.2: Applied constraints during the design of the experimental domain.

Component	Lower limit (%)	Upper limit (%)
Sucrose ester	2	15
Water phase	15	1
Oil phase	40	80

Table 2.3: Fixed ratios between components.

Components	Ratio
Water/glycerin	0,5
Water phase/SEs	>1,5
Oil phase/SEs	>5; <30

the relation limits reported above (Sec. 2.4.1) it is possible to define the experimental domain reported in Fig.2.3.

Sucrose monopalmitate (SMP) alone is not able to form microemulsions that cover most of the possible oil, water and surfactant compositions. It has a fairly high critical packing parameter around 0,2-0,45 [93, 94] and this value is further increased if the oil phase penetrates into the alkyl chains of the SMP molecule. In order to produce microemulsions over a wide range of compositions, it is necessary to reduce this parameter by the use of cosurfactants, generally short chain alcohols [21], but, as seen in Sec. 1.8 alcohols are not suitable for food industry purposes. The molecule with more chemical affinity with short chain alcohols and also admitted by food regulations and well tolerated by

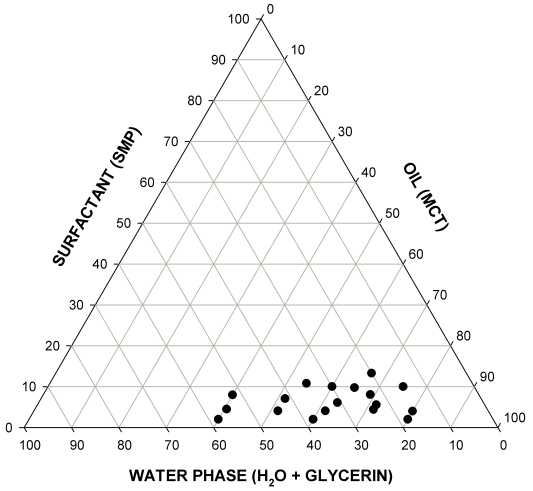

Figure 2.3: Pseudo-ternary diagram of the experimental domain, every dot represents a formulation which composition was derived from the matrix resulting from the DoE.

the market is glycerin. Glycerin acts reducing the packing parameter of the SMP either by making the aqueous phase less hydrophilic, and/or by incorporating itself into the interfacial film. In addition, a cosurfactant can also act increasing the fluidity of the surfactant film, conferring a sufficient flexibility to take up the different curvatures required to form microemulsions. In general an elastic or flexible surfactant film promotes the formation of microemulsion, whereas a lamellar phase is formed with a more rigid film [95].

There was a clear separation between transparent formulations, hereafter referred to as "emulsion-gel" (Eg) and milky formulations, defined as "emulsions" (E). The three formulations that lead to isotropic transparent lamellar phases are highlighted in Table 2.4 and the two separated domains are depicted in Fig. 2.4. Out of the two domains (Eg and E) formulations are unstable, oil and water phases separate under accelerate stability tests (see Sec. 2.3.6).

At the beginning of the study it was thought that the isotropic transparent formulations were microemulsions because of their aspect and the little energy required for the emulsification process and because of the great stability showed. Through further study it was clear that it was not formed any microemulsion, primarily because of the non-Newtonian behavior. It was impossible to obtain a flexible surfactant film to ensure the formation of microemulsion, it was instead obtained concentrated gel-emulsions (see Sec. 1.5) containing 60-75% of oil phase, with a transparent aspect and a very good stability, composed of densely packed oil droplets and lamellar liquid crystalline zones.

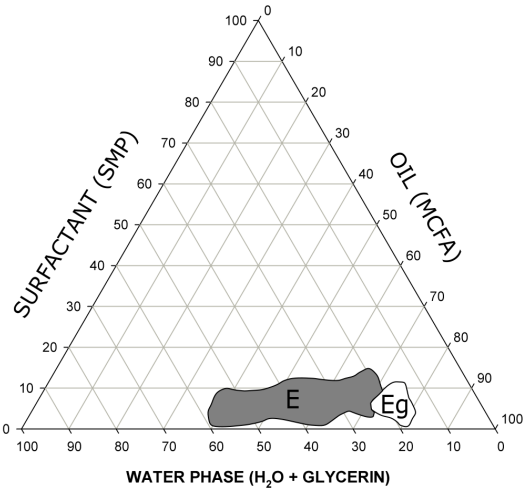

Figure 2.4: The **Eg** zone represents the transparent emulsion-gel phase domain whereas **E** zone represents the milky emulsion domain.

Table 2.4: Evaluated formulations, the highlighted lines are the formulations that lead to transparent emulsion gels.

Formulation	Oil (%)	SMP (%)	Water (%)	Glycerin (%)
1	40,0	2,0	19,3	38,7
3	75,0	10,0	5,0	10,0
4	40,0	8,0	17,3	34,7
5	66,7	13,3	6,7	13,3
6	60,0	2,0	12,7	25,3
7	80,0	2,7	5,8	11,5
15	63,1	6,1	10,3	20,5
16	80,0	4,0	5,3	10,7
17	54,2	10,8	11,6	23,4
18	40,5	4,5	18,3	36,7
19	60,0	10,0	25,0	5,0
20	51,5	4,1	14,8	29,6
21	71,5	5,6	7,6	15,3
22	69,0	8,1	7,6	15,3
23	51,5	7,1	13,8	27,6
24	64,9	9,7	8,5	16,9
25	61,5	4,1	11,7	22,7
26	71,5	4,4	8,0	16,1

2.4.3 Droplet size and electrokinetic potential analysis

It is worth noting that all the formulations have a viscosity too high to perform directly the scattering analysis, so it was necessary a dilution prior the measurement (see Sec. 2.3.2). The dilution of the formulations had a dramatic change on the internal structure, particularly, transparent lamellar phase become milky emulsions. So it is important to evaluate the droplet size and the ζ potential data only for comparison between formulations.

As reported in Table 2.5 the median diameters (D_{50}) of the formulations are between 0,28 and 9,15 μm with a PDI between 0,31 and 0,61. The PDI values indicate that the droplet size distribution are moderately polydisperse, but always $< 0{,}7$ (values greater than 0,7 indicate that the sample has a very broad size distribution and is probably not suitable for the DLS technique).

The magnitude of the zeta potential indicates the degree of electrostatic repulsion between adjacent, similarly charged particles in a dispersion. For particles that are small enough, a high zeta potential (e.g.$> \pm 30$ mV) will confer stability. When the potential is small (e.g.$< \pm 10$ mV), attractive forces may exceed this repulsion and the dispersion

Table 2.5: D50 with relative PDI and ζ values.

Formulation	**D50** (μm)	**PDI**	ζ (mV)
1	9,15	0,61	-51,0
3	0,28	0,48	-28,6
4	4,42	0,51	-36,2
5	0,47	0,54	-32,7
6	0,56	0,41	-47,6
7	2,61	0,39	-47,1
15	3,41	0,31	-44,2
16	3,91	0,55	-34,0
17	3,12	0,47	-37,5
18	5,23	0,46	-23,4
19	6,23	0,33	-41,2
20	4,48	0,45	-31,2
21	3,02	0,42	-55,6
22	1,35	0,34	-48,1
23	2,88	0,40	-57,1
24	0,67	0,55	-32,4
25	6,56	0,58	-21,8
26	0,48	0,36	-55,3

may break and flocculate [96, 97]. The formulations tested demonstrate to have a negative ζ potential between $\approx$ -20 and -60 mV therefore indicating a good stability against flocculation and agglomeration of droplets.

The D50 data show a glaring correlation between droplet size and SMP concentration as depicted in Fig. 2.5-a, in fact, increasing the concentration of surfactant the median diameter decreases as a consequence of the availability of amphiphilic molecules that can cover a lager area and thus a greater number of smaller droplets. Another noticeable relation showed in Fig. 2.5-b is the one between D50 and water phase concentration, increasing the concentration of water and glycerin also the droplet dimension increases, this is quite surprisingly because it would be expected a decrease in D50 in relation to a smaller oil concentration.

Although there is no unanimous opinion about the optimal droplet dimensions for a better oral absorption [98–100], it is generally accepted the idea that droplet dimensions $<$0,5 μm lead to a good compromise [101–103] between technological issues and absorption features. Thus, for the oral release and further characterization studies the two formulations presenting the lower D50 were selected: formulation n°3 and formulation n°26, therefore called F03 and F26.

2.4.4 Transmission electron microscopy

Although the two selected high HIPREs (F03 and F26) show the same clear and transparent appearance, they exhibit different internal structures. Representative TEM images of F03, depicted in Fig. 2.6 a-b, show the typical foam-like structure, often found in literature when approaching to HIPREs: densely packed oil droplets surrounded by a thin film of surfactant (SPM) and water phase. F3 has an internal phase volume fraction, Φ, of 0,75, that is just above the critical value of the most compact arrangement of uniform, undeformed spherical droplets of 0,74. In fact the droplet morphology is quite irregular and the dimensions have a high polydispersity.
The internal structure of F26, shown in Fig. 2.7 a-b, is quite different, although foam-like zones were found (data not shown), a bicontinuous lamellar-structured (L_α) zone was detected, indicating a liquid crystal organization of the oil phase synergistically with the other components of the formulation. It can be assumed that the capryc/caprylic blend composing the oil phase behave like an amphiphilic molecule and together with sucrose monopalmitate (see the molecular structures in Fig. 2.9) create a supramolecular organization as depicted in Fig. 2.8. It is a quite unexpected result, because in literature are present numerous articles reporting the capability of glycerol monooleate to form liquid crystals but no data are reported about MCFA and SMP liquid crystals.
TEM analysis performed on HIPREs formulations after the dilution (Fig. 2.6 c-d and 2.7 c-d) have demonstrated that during the dilution the initial typical structure of HIPREs is lost and replaced by a classical droplet emulsion structure, besides the observed droplet sizes are consistent with DLS measurements.

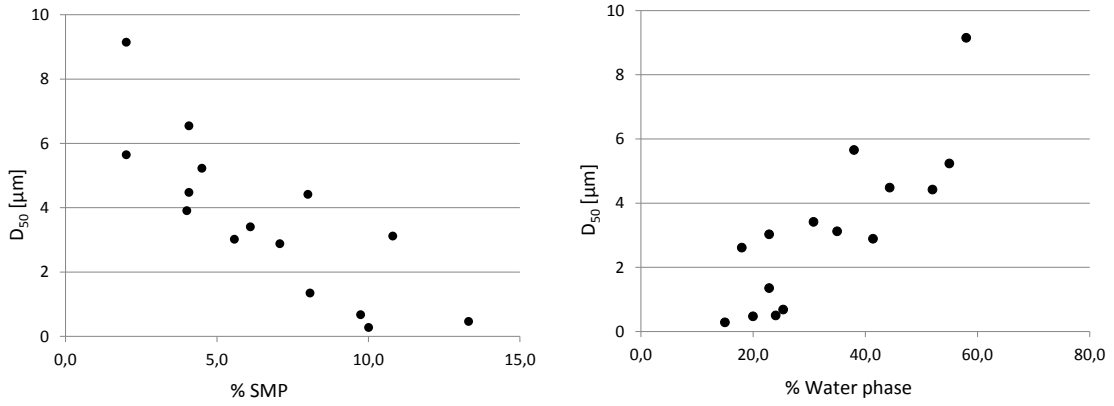

(a) *Relation between D50 and sucrose monopalmitate (SMP) concentration*

(b) *Relation between D50 and water phase concentration (H2O:glycerin/1:2)*

Figure 2.5: After water dilution of formulations, droplet dimension seems to be mainly related with concentrations of surfactantant (SMP) and water phase.

2.4.5 Rheology

Controlled-rate viscosity tests were carried out on the formulations at 25 ℃ and repeated at 55 ℃ to investigate if the physical state of SMP can affect the rheology. As reported in Table 2.6 and in Fig. 2.10 [2] at 25 ℃ viscosity has a wide range, from 0,2 to 35 KPa·s and is directly related with SMP concentration, in fact SMP is the only solid state component at 25 ℃ and it has thickening property. To validate the thickening capacity of SMP measures were repeated at higher temperature than the melting temperature of SMP (42-48 ℃), at 55 ℃ in fact the viscosity range is significantly lower, ranging from 0,02 to 0,35 KPa·s. Below its melting temperature SMP behave like a thickening agent, its alkyl chains are rigid and prevent fluid movement of the oil and water phases. Above its melting temperature SMP's alkyl chains lose rigidity and behave like a fluid, weakening the thickening ability, regardless of the relative quantity.

Thanks to a temporary collaboration with the University of Trieste[3] it was possible to perform some frequency sweep experiments. Frequency sweeps were recorded to study

[2]To provide a clean-cut comparison between formulations flow and viscosity curves were build performing controlled-rate tests and the maximum viscosity value was taken into account.

[3]Prof. Grassi, Chemical Engineering Department

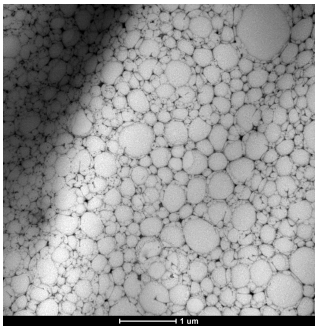

(a) *HIPREs F3*

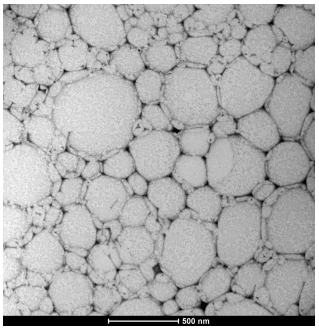

(b) *HIPREs F3*

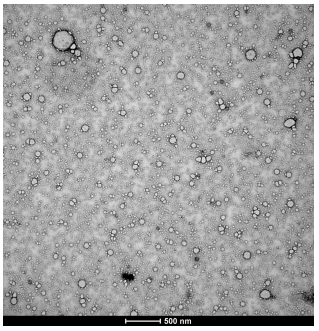

(c) *HIPREs F3 after water dilution*

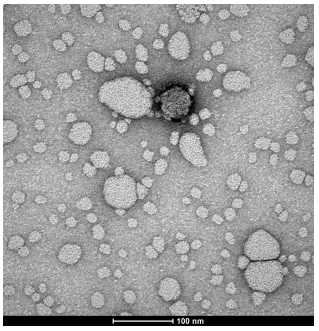

(d) *HIPREs F3 after water dilution*

Figure 2.6: TEM images of HIPREs F03, before (a, b) and after water dilution (c, d). The magnification is illustrated by the scale bars.

the emulsion gel strengths of the dispersions. In rheological terms, for a gel the storage (G') and the loss (G") modulus are frequency-independent and G'>G". Gels can usually be classified into two categories [104]: weak gels, where the moduli (G' and G") depend slightly on the frequency; and strong gels, where the moduli are relatively independent of frequency. Under increased deformation or continuous flow conditions, strong gels breaks into small gel regions rather than flow, while the weak gel network breaks down into smaller flow units and may flow homogeneously [104, 105]. Frequency sweep tests were carried out in the linear viscoelastic region to examine the frequency dependences of the storage and the loss moduli.

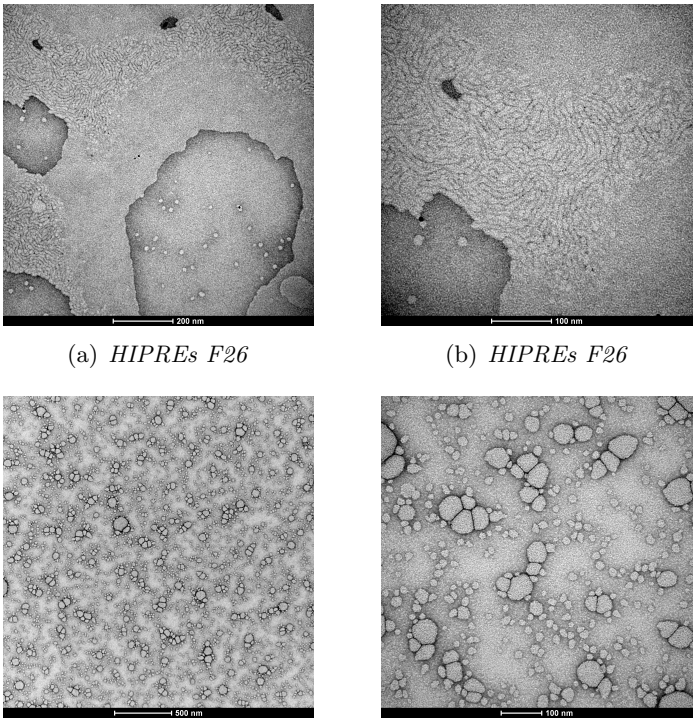

(a) *HIPREs F26*

(b) *HIPREs F26*

(c) *HIPREs F26 after water dilution*

(d) *HIPREs F26 after water dilution*

Figure 2.7: TEM images of HIPREs F26, before (a, b) and after water dilution (c, d). The magnification is illustrated by the scale bars.

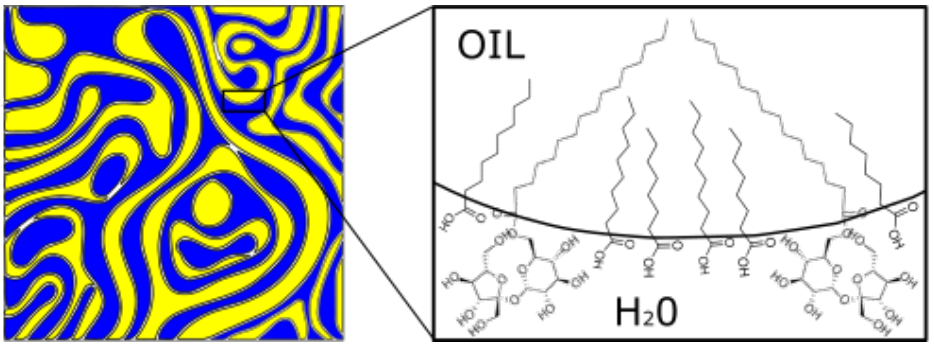

Figure 2.8: Possible disposition of sucrose monopalmitate (SMP) and medium chain fatty acid (MCFA) at the interface.

Table 2.6: Maximum viscosity values registered at 25 and 55°C.

Formulation	**Viscosity 25 °C** (KPa·s)	**Viscosity 55 °C** (KPa·s)
1	1,10	0,05
3	32,12	0,61
4	0,31	0,12
5	30,04	0,58
6	6,34	0,07
7	20,55	0,21
15	24,71	0,15
16	17,02	0,11
17	28,30	0,06
18	14,15	0,12
19	0,16	0,13
20	8,05	0,02
21	18,20	0,17
22	22,55	0,13
23	0,21	0,08
24	29,21	0,23
25	9,17	0,09
26	21,65	0,29

F03 was selected as formulation to be tested, in Fig. 2.11 G' and G" of the selected formulation is compared with G' and G" of the only water phase (AF). F03 display gel characteristics, because the storage moduli are higher than the loss moduli at all frequencies, while AF G' tend to reach G", indicating a solution-like behaviour. These results indicate that F03 gel-emulsion have more elastic behaviour (higher G' values) and better gel characteristics (lower slopes of the curves). The frequency dependence can be studied via the slopes of the logG' and logG" versus log f curves. The lower the slope, the stronger the gel structure. If only the slope is regarded, the moduli show a

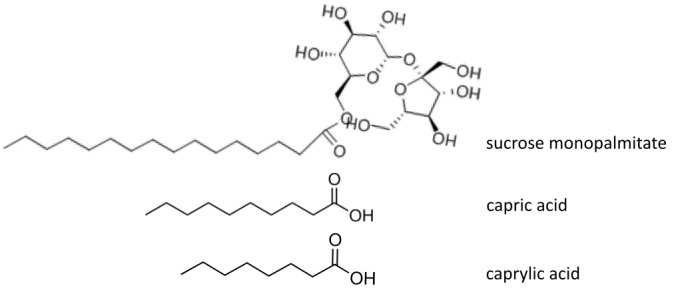

Figure 2.9: Molecular structures of the amphiphilic molecules involved.

slight dependence on the frequency, which indicates that F03 has a strong gel structure.

2.4.6 Differential scanning calorimetry (DSC)

Thermograms of all formulation components actives and final formulations were registered. Results show that no significant interactions between actives and formulation excipients were detected. Thermogram of SMP is reported in Fig. 2.12-a, it shows an endothermic fusion peak between 42 and 47 °C while the melting range reported in literature is between 47 and 54 °C. Thermograms of the formulations report a shift of the

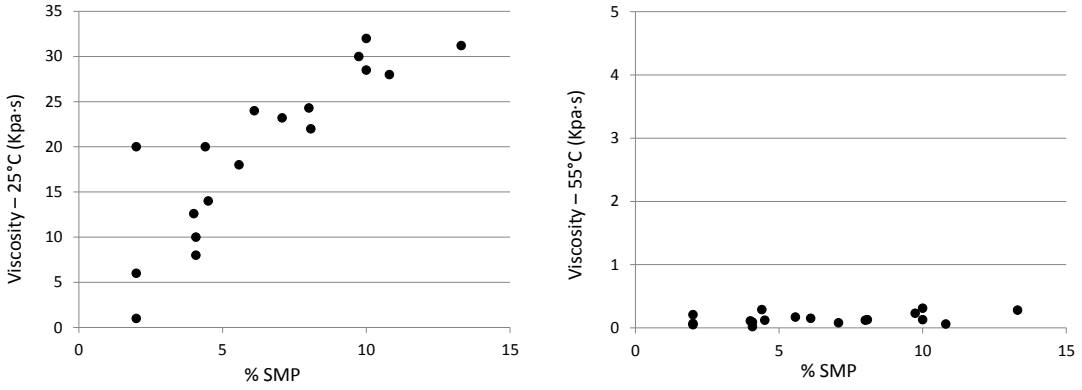

(a) (b)

Figure 2.10: Maximum viscosity values registered at 25 °C (a) and at 55 °C (b) related to SMP concentration.

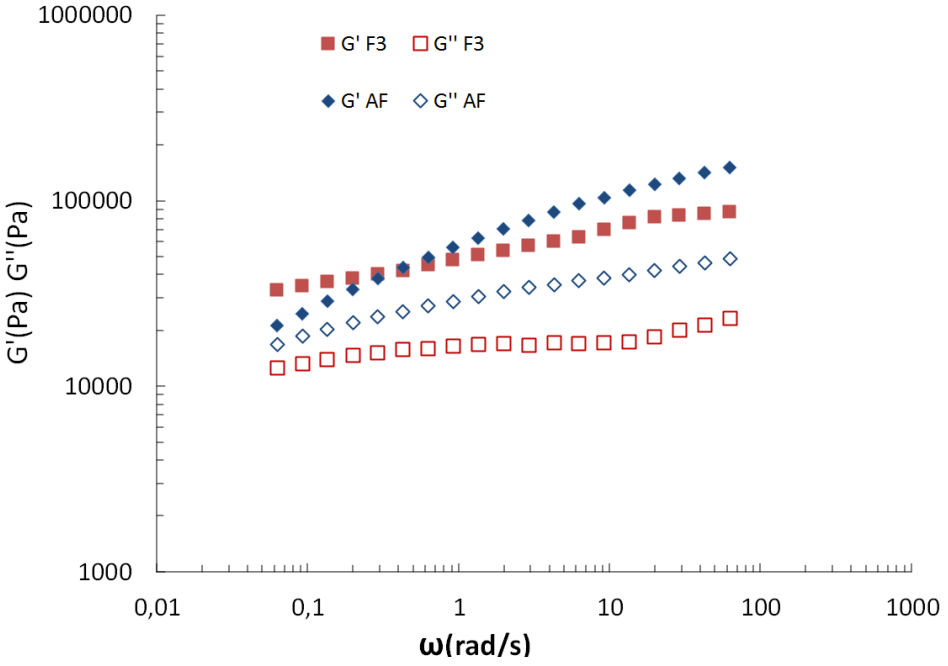

Figure 2.11: Storage (G') and loss (G") modulus of formulation n°3 (F03) and its water phase (AF).

SMP melting to lower temperatures in two different modality: emulsions show a single peak shifted to 39-40 ℃, F01 and F17 are reported as an example in Fig. 2.12-b, while HIPREs (F06, F26 and F23) show a double peak at respectively 37-38 ℃ and 39-40 ℃ (Fig. 2.12-c). In both cases the lowering of the melting endothermic peak is due to the increase in surface area exposed to heat treatment and because of an increase in SMP alkyl chain movement freedom. It is reasonable to conclude that the formation of lamellar structures affect the surfactant's tail degree of freedom, which is pronounced as an early endothermic event.

2.5 Stability studies

All the 18 formulations were subjected to stability test. During freeze-thaw cycles no physical variations were noticed, long term and accelerated stability results are reported in Tab. 2.7. For editorial reasons only two formulation are reported in this section, the full list of stability reports is available in appendix A. However, all the formulations were compliant to initial conditions during 6 months of accelerated stability (40 ℃ ±2 ℃ /

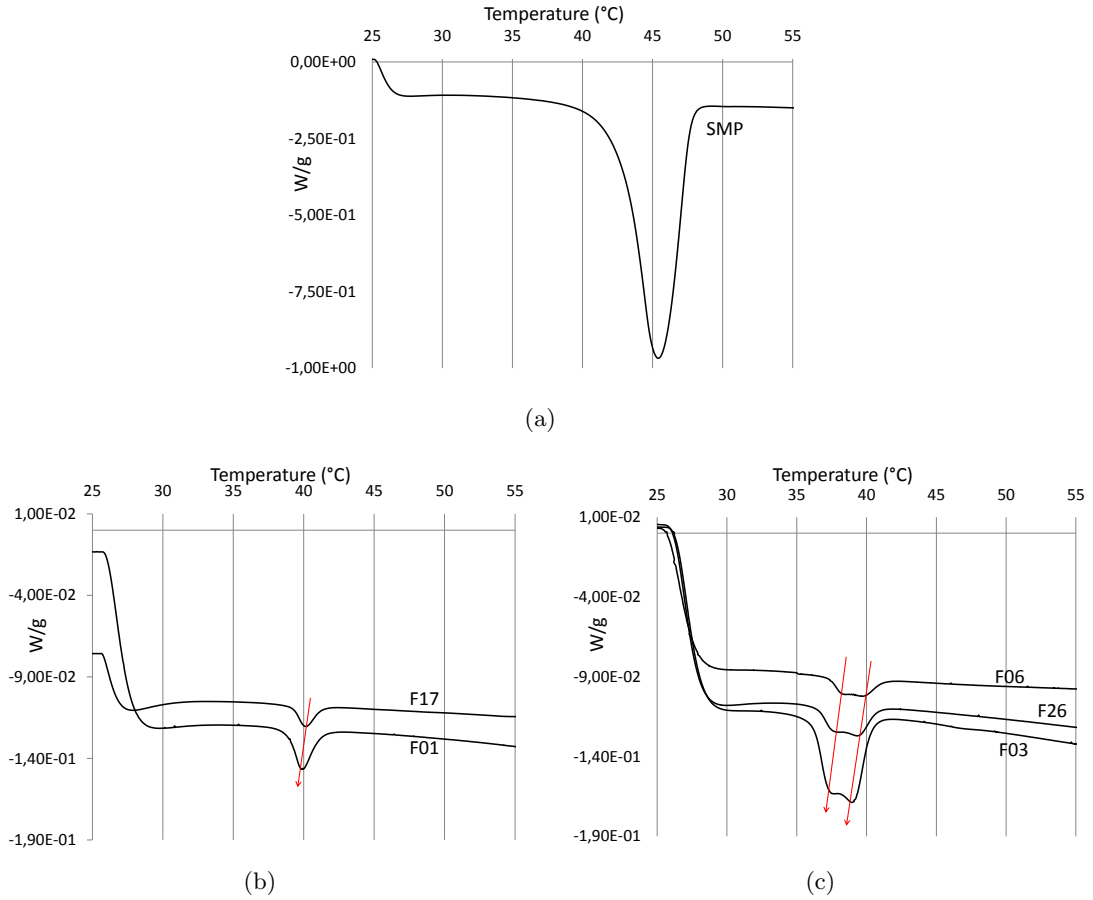

Figure 2.12: DSC thermograms of SMP (a), emulsions (b), and HIPREs (c).

75% ± 5% R.U.) and during 24 months of long term storage (25 °C ±2 °C / 60% ± 5% R.U.).

2.6 Discussion

In the present study innovative SEs-based formulations were investigated and characterized. The main purpose was to develop a formulation platform suitable both for food, cosmetic and medical devices industry able to deliver lipophilic molecules. An optimization with an experimental design allowed the systematic evaluation of the ratios between phases and surfactant, resulting in 18 experimental runs. Formulations were characterized by several methods, including dynamic light scattering. Results have highlighted the formulation ability to form emulsion having a droplet size up to 280 nm after dispersion in water. Classical rheology measurements showed the direct relation between sucrose monopalmitate and viscosity and thus the possibility to reach a wide range of consistency by simply varying its concentration while sweep test described the gel-like internal structure. It was found that the combination of SEs, water, glycerine and medium chain fatty acids (MCFA) is able to form both classical emulsions and transparent gel-emulsion, also referred as high internal phase ratio emulsions (HIPREs) exhibiting a liquid crystalline molecular organization as showed by differential scanning calorimetry analysis and transmission electron microscopy.

Table 2.7: Long term and accelerated stability report.

F01 - long term	**T0**	**T3**	**T6**	**T12**	**T18**	**T24**
Visual aspect	color: ivory	color: ivory	color: ivory	color: ivory	color: ivory	color: ivory
pH	7,23	7,12	7,45	6,98	7,31	7,35
Viscosity (KPa·s)	1,10	1,15	1,13	1,19	1,08	1,11
Centrifuge test	compliant	compliant	compliant	compliant	compliant	compliant
F01 - accelerated						
Visual aspect	color: ivory	color: ivory	color: ivory			
pH	7,23	6,83	7,44			
Viscosity (KPa·s)	1,10	1,38	1,53			
Centrifuge test	compliant	compliant	compliant			
F03 - long term	**T0**	**T3**	**T6**	**T12**	**T18**	**T24**
Visual aspect	color: transparent	color: transparent	color: transparent	color: transparent	color: transparent	color: transparent
pH	6,45	6,89	7,78	6,54	6,77	6,85
Viscosity (KPa·s)	32,12	31,43	32,76	33,15	29,88	29,61
Centrifuge test	compliant	compliant	compliant	compliant	compliant	compliant
F03 - accelerated						
Visual aspect	color: transparent	color: transparent	color: transparent			
pH	6,45	7,38	7,12			
Viscosity (KPa·s)	32,12	30,04	29,86			
Centrifuge test	compliant	compliant	compliant			

43

Chapter 3

Development of Oral Dosage Forms

Oral administration of drugs is the most convenient and, therefore, the most common route for active molecules administration. The formulations obtained with the method described in Sec. 2.3.1 do not completely satisfy the initially stated aims (see Sec. 1.1). The two main issues were:

- **unpleasant taste:** the high concentration of SEs produces an unpleasant bitter taste
- **difficulties in primary packaging:** the high viscosity of the selected formulations does not permit an easy and fast pouring from bulk to package.

To overcome those problems two alternative dosage forms were taken into account:

- **adsorbed-HIPREs**
- **medicated jellies**

HIPREs F03 was chosen as starting formulation because of its high oil phase ratio, capable to solubilize the highest amount of active molecules respect to other formulations. F03 was then used to prepare adsorbed-HIPREs and medicated jellies.

3.1 Introduction

3.1.1 Buccal absorption

Theoretically, drug absorption can occur throughout the entire alimentary canal. However, the mucosal surface area of each segment, coupled with the time the drug remains in contact with the mucosal surface, dictate the degree of absorption from any segment of the gastrointestinal tract. Very limited drug absorption takes place within the mouth after oral administration because the surface area is small and the residence time is very short. Nevertheless highly lipophilic molecules can be readily absorbed from the mouth when placed sublingually. Sublingual administration of the drug means placement of the drug under the tongue and drug reaches directly the blood stream through the ventral surface of the tongue and floor of the mouth. The drug solutes are rapidly absorbed into the reticulated vein which lies underneath the oral mucosa, and transported through the facial veins, internal jugular vein, and brachiocephalic vein and then drained in to systemic circulation. The main mechanism for the absorption of the drug in to oral mucosa is via passive diffusion into the lipoidal membrane [106]. The absorption of the drug through the sublingual route is 3 to 10 times greater than oral route and is only surpassed by hypodermic injection. For these formulations, the small volume of saliva is usually sufficient to result in disintegration/dissolution in the oral cavity. In terms of permeability, the sublingual area is more permeable than the buccal (cheek) area, which in turn is more permeable than the palatal (roof of the mouth) area. The differences in permeability are generally based on the relative thickness, blood supply, and degree of keratinization of these membranes. In addition to the differences in the permeability of the various mucous membranes, the extent of drug delivery is also affected by the physico-chemical properties of the drug to be delivered [107, 108].
Factors affecting the sublingual absorption are [109]:

- **Drug lipophilicity:** in order to achieve the passive permeation through the sublingual mucosae and obtain complete absorption the drug molecule must be lipophilic
- **Solubility in salivary secretion:** however to achieve sublingual absorption the drug should be also soluble in aqueous buccal fluids.
- **pH and pKa:** the mean pH of the saliva is 6,0, this pH favors the absorption of unionized drugs. Also, the absorption of the drugs through the oral mucosa occurs if the pKa is greater than 2 for an acid and less than 10 for a base.

- **Thickness of oral epithelium:** the thickness of sublingual epithelium is 100-200 μm which is thinner than buccal thickness, consequently the absorption of drugs is faster.
- **Oil/water partition coefficient:** compounds with favorable oil-to-water partition coefficients are readily absorbed through the oral mucosa. An oil-water partition coefficient range of 40-2000 is considered optimal for the drugs to achieve sublingual absorption.

3.1.2 Gastric and small intestine absorption

After oral administration, most drugs quickly pass the mouth and the esophagus and reach the stomach that is primarily design to digest food. Its small surface area indicates that nutrient absorption is limited, although some drug absorption can occur in the stomach depending on the extent of ionization and on the degree of lipid solubility. For most orally administered drugs, the major site for absorption is the small intestine. The small intestine is designed to absorb nutrients, as evidenced by their enormous surface area. Because of the large surface area, the small intestine is the primary site for absorption of lipid soluble drugs while water soluble molecules are not readily absorbed. This might appear counterintuitive because absorption of weak acids and weak bases appears to occur in the small intestines independent of the environmental pH and drug pKa. For weak acids and weak bases that are ionized in the small intestines, only the uncharged molecules passively diffuse across the intestinal membranes. The rapid absorption of the uncharged molecules drives the charged molecules into the uncharged form, which is then quickly absorbed. Consequently, for drugs that are absorbed after oral administration, the small intestine constitutes the major site for absorption [110].

3.2 Materials and Methods

3.2.1 Materials

All materials used were of food grade: citric acid, glicerin and gelatin (Acef S.p.a. - Fiorenzuola d'Arda, Italy); granular sorbitol (Faravelli S.p.a - Milano, Italy); sucralose and silicon dioxide (Giellepi S.p.A - Seregno, Italy).

Table 3.1: Excipients used in adsorbed-HIPREs and relative functions, quantities are related to 1 g of original HIPREs F03.

Excipient	**Quantity (g)**	**E number**	**Function**
Granular sorbitol	6,00	E420	reduce micellar dispersion time
Silicon dioxide	0,10	E551	anticaking agent
Citric acid	0,30	E330	taste modification
Flavor	0,05	-	taste modification
Sucralose	0,01	E955	sweetener

3.2.2 Adsorbed-HIPREs preparation

The manufacturing of adsorbed-HIPREs consists in mixing the previously described selected HIPREs (F03) with an adequate amount of a solid water-soluble carrier. F03 was mixed with the solid excipients listed in Table 3.1. The main carrier used is sorbitol, however other granular powder could have been used (maltitol, xylitol, sucrose, destrose, etc.). The essential features that the solid carrier must have are: high water solubility, to facilitate the dispersion, and optimal particle size to facilitate the flow of the bulk during manifacturing. The finished product is a free-flowing powder (see Fig. 3.1), easily manageable by industrial manufacturing equipment.
The classical self-emulsifying drug delivery system (SEDDS) definition imply a formulation composed of surfactant/s and oil (optional). SEDDS are able to create an emulsion by simply dispersion in aqueous environment. Often, to create a solid dosage form, SEDDS are adsorbed on a solid carrier to create "solid-SEDDS". The formulations described here contain also a certain percentage of water so it was chosen to refer to them as "adsorbed-HIPREs" but it is worth noting the great similarity with classical solid-SEDDS. In fact, as classical solid-SEDDS, also for the adsorbed-HIPREs the first purpose is to provide a solid formulation able to increase bioavailability of lipophilic molecules by generating an emulsion when in contact with water (including saliva and gastric fluid).

3.2.3 Jellies preparation

The manufacturing of jellies is carried out mixing the initial HIPREs (F03) with a dispersion of gelatin, previously prepared hydrating the gelatin in 75 °C water. The quantities of the used excipients are reported in Table 3.2. The finished products are chewable soft jellies (see Fig. 3.1).

Table 3.2: Excipients used in jelly preparation and relative function, quantities are related to 1 g of HIPREs F03.

Excipient	Quantity (g)	E number	Function
Water	0,90	-	rheological modification
Gelatin	0,10	E411	rheological modification
Citric acid	0,10	E330	taste modification
Flavor	0,05	-	taste modification
Sucralose	0,01	E955	sweetener

3.2.4 Droplet size and electrokinetic potential determination

To assess the capability of adsorbed-emulsions and jellies to recreate a fine emulsion once dispersed in aqueous environment, small quantities of samples ($\approx 0{,}2$ g) were mixed with magnetic stirrer in 50 ml of phosphate buffer and analyzed in triplicate with the same procedure and instruments described in Sec. 2.3.2.

3.2.5 Dissolution studies

Actives release from the formulations was measured using a dissolution test apparatus of reduced capacity (50 mL) to simulate the buccal dissolution volume. Actually, a relatively small volume of the dissolution medium was urgently needed to to represent the salivary volume in a typical adult [111, 112], then dissolution tests were performed in non-sink conditions.
Dissolution tests were performed using a paddle stirrer (Arc Quiet, ALC International - Cologno Monzese, Italy) at 50 rpm and phosphate buffer pH 6,8 [113] as dissolution

(a) (b)

Figure 3.1: Examples of the two finished products: medicated jelly (a) and adsorbed-emulsion (b).

medium. Temperature of the dissolution medium was kept at $37 \pm 0,5$ ℃with a thermostated bath. During the release studies 1 ml of dissolution medium sample was removed and filtered. Samples were filtered and analyzed by HPLC method, as described Sec. 3.2.6. The assays were performed simultaneously at least on 3 replicates for each formulation. Dissolution tests were performed on the original HIPREs (F03), on the modified formulations (adsorbed-HIPREs an jelly) and on the active molecules bulk-powder in order to assess the solubility enhancement.

3.2.6 Analytical methods

3.2.6.1 Ubidecarenon

Quantitative determination of ubidecarenon is performed with HPLC method, using a Shimadzu liquid chromatograph (Japan) equipped with a XDB-C8 column ($5\,\mu m, 150\,mm \times 4,6\,mm$, Agilent) and a LC-6A model pump, the detector was a SPD-6, both provided by Shimadzu. The chromatographic conditions were described by Nazzal et. al [114]:

- $20\mu l$ loop
- isocratic mobile phase composition (1 L):
  - 6,8 g sodium acetate trihydrate
  - 695 ml metanol
  - 275 ml n-exane
  - 150 ml anhydrous acetic acid
  - 150 ml n-propanol
- 1,5 ml/min flux rate of mobile phase
- 275 nm detection wavelength

With these chromatographic conditions, ubichinon retention time was 5,6 min while ubichinol retention time was approximately 4,2 min. A chromatogram example is reported in Fig. 3.2.

3.2.6.2 Resveratrol

Quantitative determination of resveratrol is performed with the same equipment used for ubidecarenon. Chromatographic conditions were the ones described by Careri et. al [115]:

- 20 μl loop
- isocratic mobile phase composition (1 L):
  - 693 ml water
  - 7 ml formic acid
  - 220 ml acetonitrile
  - 80 ml 2-propanol
- 0,5 ml/min flux rate of mobile phase
- 306 nm detection wavelength

With these chromatographic conditions, trans-resveratrol retention time was approximately 12,4 min, however the run was extended to evaluate also the cis-resveratrol peak at 21 min. A chromatogram example is reported in Fig. 3.3.

3.3 Results

3.3.1 Droplet size and electrokinetic potential determination

DLS measurements reported in Table 3.3 show that the HIPREs modification both in adsorbed-HIPREs and in jelly does not affect significantly the D_{50} and the ζ potential

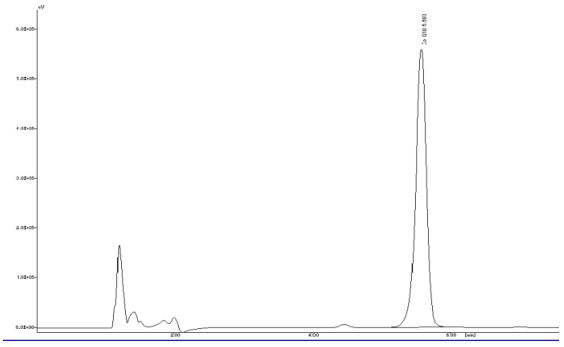

Figure 3.2: Example of a chromatogram of an ethanolic solution of ubidecarenon, obtained with the reported conditions.

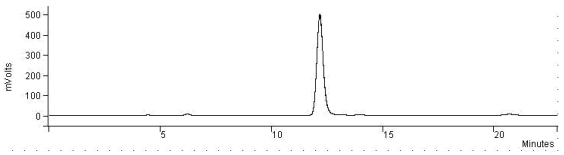

Figure 3.3: Example of a chromatogram of an ethanolic solution of resveratrol, obtained with the reported conditions.

after reconstitution in water, indicating the suitability of those dosage forms respect to the initial HIPREs.

Table 3.3: D50 with relative PDI and ζ values.

Formulation	**D50** (μm)	**PDI**	ζ (mV)
F03	0,28	0,48	-28,6
adsorbed-HIPREs	0,34	0,52	-33,6
jelly	0,39	0,55	-21,8

3.3.2 Dissolution studies

The dissolution of a solid in a solvent is a rather complex process determined by a multiplicity of physicochemical properties of solute and solvent. Indeed, it can be considered as a consecutive process driven by energy changes. The first step consists of the contact of the solvent with the solid surface (wetting), which leads to the production of a solid-liquid interface starting from solid-vapor one. The breakdown of molecular bonds of the solid (fusion) and passage of molecules to the solid-liquid interface (solvation) are the second and third steps, respectively. The final step implies the transfer of the solvated molecules from the interfacial region into the bulk solution (diffusion). Obviously, for performing each step, energy is required and the total energy required for solid dissolution is the sum of the energies relative to the four mentioned steps [116].
One of the main objectives of the study was to increase the bioavailability of lipophilic actives, generally poorly water soluble molecules and hence not suitable for oral delivery. Traditionally, dissolution testing has fulfilled two principal functions: as an instrument to control quality, dissolution is a sensitive, reproducible and straightforward test that can be used to effectively monitor batch-to-batch variability and ensure bioequivalence once bioavailability has been established [117]. In some circumstances, in-vitro dissolution tests can be used as a surrogate indicator of the likely in-vivo dissolution profile and, therefore, as a tool to predict the extent of absorption where dissolution is limiting [118]. The principal determinants of the dissolution rate of a poorly water-soluble compound, however, are the degree of wetting and extent of drug solubility in the intestinal contents. The use of simple aqueous media to assess the dissolution profile of poorly water-soluble drugs is often limited by the low intrinsic aqueous solubility of the drug (and, therefore, difficulty in maintaining *sink conditions*[1]). As suggested by various authors [113, 120, 121] it was therefore chosen to operate in non-sink conditions using a small dissolution volume and avoiding the use of surfactants in order to have a

[1] In the European Pharmacopeia [119], sink conditions are defined as a volume of dissolution medium that is at least three to ten times the saturation volume. It refers to a dissolution process according to Noyes-Whitney equation [59].

better discrimination of dissolution profiles between different formulations. Moreover, the addition of surfactants to the dissolution medium could affect the formation of the emulsion from the developed solid formulations after dispersion in water. Operating in non-sink conditions it was not possible to fit the experimental data to different order kinetic equations.
As stated before, dissolution tests were performed on the original HIPREs (F03), on the modified formulations (adsorbed-HIPREs and jelly) and on the active molecules bulk-powder in order to assess the solubility enhancement.

3.3.2.1 Ubidecarenon release

In Fig. 3.4 are depicted the release profiles of the formulations containing Ubidecarenon (CoQ_{10}), as expected bulk powder has no solubility in aqueous dissolution medium, in fact, CoQ_{10} is not detected. CoQ_{10} is slowly released from the jelly formulation, it reaches $208,93 \pm 48,21\,\mu g$ and thus enhance solubility until $4,17\,\mu g/ml$ corresponding to $20,06 \pm 7,34\,\%$ of the total CoQ_{10} in 120 min. The adsorbed-HIPREs reaches its maximum release of $241,81 \pm 37,22\,\mu g$ within the first 5 minutes with a final solubility of $4,84\,\mu g/ml$ corresponding to $35,03 \pm 6,51\,\%$ of the total CoQ_{10}. The HIPREs formulation has the best performance since it is capable to release $712,45 \pm 35,52\,\mu g$ with a final solubility of $14,25\,\mu g/ml$ corresponding to $65,31 \pm 5,96\,\%$ of the total CoQ_{10} contained in the formulation.

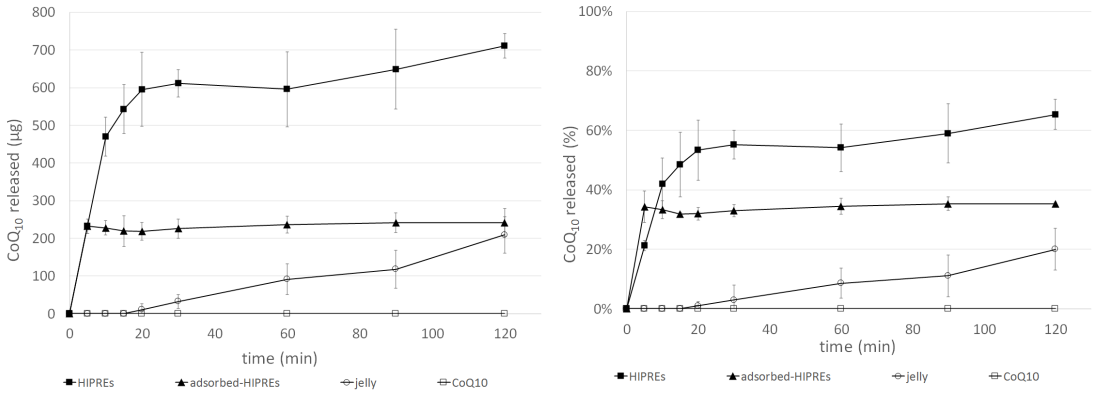

(a) Release curves expressed as quantity of CoQ_{10} released.

(b) Release curves expressed as percentage on the total amount of CoQ_{10}.

Figure 3.4: In-vitro release of ubidecarenon from the studied formulations. Error bars are calculated on three repetitions.

3.3.2.2 Resveratrol release

Resveratrol is released in greater quantities, the bulk powder reach a final value of $943,45 \pm 142,11\,\mu g$ with a final solubility of $18,87\,\mu g/ml$. The HIPREs formulation constantly release resveratrol until $1387,20 \pm 21,42\,\mu g$ with a final solubility of $27,74\,\mu g/ml$ corresponding to $68,37 \pm 7,55\,\%$ of the total resveratrol. The jelly formulation has a very similar profile, it reach $1619,46 \pm 40,78\,\mu g$ with a final solubility of $32,39\,\mu g/ml$ corresponding to $75,68 \pm 12,96\,\%$. The fastest and higher release values are registered by the absorbed-HIPREs, in 20 minutes it reach $1670,50 \pm 23,33\,\mu g$ with a final solubility of $33,4\,\mu g/ml$ corresponding to $99,87 \pm 12,32\,\%$ of the total resveratrol contained.

3.4 Discussion

After the formulation and characterization of a SEs-based delivery platform, oral dosage forms were formulated and their release performances were assessed. To increase bioavailability and compliance, and to overcome manufacturing issues, two dosage forms were evaluated, consisting in adsorbed-HIPREs and medicated jellies. HIPREs, labelled as F3 was chosen as formulation to be processed for the creation of the two solid dosage forms. Both of them were loaded with two model molecules, widely used in nutraceutical field: resveratrol and CoQ_{10}. The process which starting from F3 leads to adsorbed-HIPREs and medicated jellies does not affect the D_{50} of the droplets after water dilution, as showed by DLS measurements. Respect to bulk powder resveratrol release was increased two times by jelly formulation, and three times by adsorbed-HIPREs reaching a rapid onset. CoQ_{10} is practically water insoluble while the jelly formulation is able

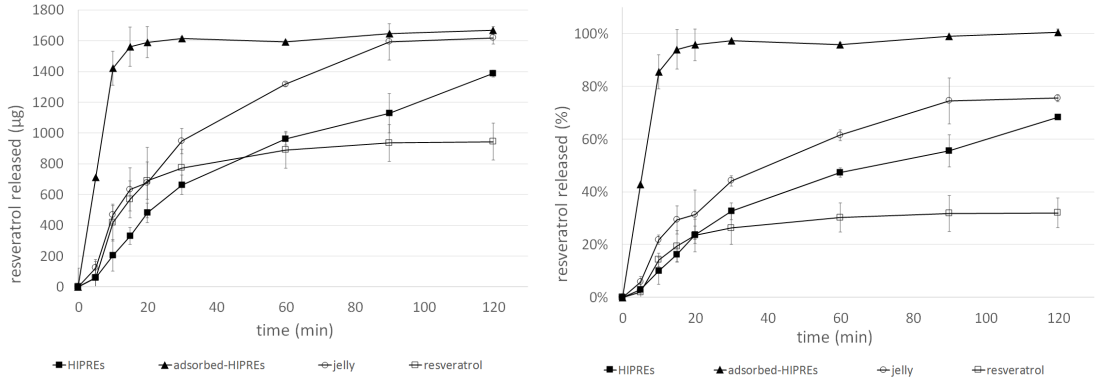

(a) Release curves expressed as quantity of resveratrol released.

(b) Release curves expressed as percentage on the total amount of resveratrol.

Figure 3.5: In-vitro release of resveratrol from the studied formulations. Error bars are calculated on three repetitions.

to release 20% of the total CoQ_{10}, as long as the adsorbed-HIPREs almost double this value. Surprisingly the initial formulation F3 releases up to 60% of the total CoQ_{10}.

Chapter 4

Development of Topical Dosage Forms

Some of the active molecules usually delivered by oral route in the food supplement field can be exploited in topical delivery to treat local skin disorders and to prevent skin aging and oxidative damage. Therefore it was evaluated the use of sucrose esters for the topical delivery of active molecules usually employed in food supplement.
The main purpose was to use a single formulation platform (based on sucrose esters) to develop different dosage forms (oral and topical) to reach every market chance, shortening the product development time and take a marketing advantage using food excipients as guarantee of eco-sustainability and bio-tolerability.
The aim of this part of the study is to use the previously developed formulation platform to create topical formulations. In particular, to produce formulations having good spreadability and compliance, the formulations F01 and F03 (see Sec. 2) will be mixed with different thickeners and solubilizers and their technological and release properties will be evaluated.

4.1 Introduction

4.1.1 Skin structure

Skin is the largest organ of our body, which acts as a protective barrier against the entry of foreign material and possible invasion of pathogens. The skin also prevents the loss of excessive endogenous material such as water [122]. In addition, the skin serves to reduce the damaging impact of solar UV radiation [123]. The structure of human skin is portrayed in Fig. 4.1. The skin is about 0,5 mm thick and is made up of two distinct layers,

the inner dermis and the overlaying epidermis. The dermis that forms the bulk of the skin (1–2 mm thick) is made up of connective tissue elements. Dermis is highly vascular and filled with pilosebaceous units, sweat glands, adipose cells, mast cells, and infiltrating leukocytes [124]. The epidermis is avascular in nature, consisting of several types of cell (corneocytes, melanocytes, Langerhans cells, and Merkel cells) and a variety of catabolic enzymes (esterases, phosphatases, proteases, nucleotidases, and lipases). The stratified epidermis is about 100-150 mm thick and comprises four distinct layers, namely the stratum basale, stratum spinosum, stratum granulosum, and stratum corneum. The stratum corneum is the outermost layer of skin that forms the main barrier for diffusion of the permeants through the skin. Stratum corneum consists of 18-21 layers of flat, roughly hexagonal cells called corneocytes that are constantly shed and renewed [124]. These keratin-rich dead cells, are interspersed within crystalline lamellar lipid matrix to assume a "bricks and mortar" arrangement. The extracellular lipid contributes 10% of the dry weight of this layer, while 90% is the intracellular keratin. The barrier function of the skin can be attributed to the lamellar lipids that are synthesized in the granular layer and subsequently organized into the extracellular lipid bilayer domains of the stratum corneum. The barrier function of the skin depends on the specific ratios of various lipids present, in particular, some studies reveal that relatively polar lipids play a critical role in maintaining the barrier integrity of the stratum corneum [124]. The epidermis is made up of keratinocytes at various stages of differentiation. Lipid catabolic enzymes, namely acid lipase, phospholipase, sphingomyelinase, and steroid sulfatase, are distributed throughout the epidermis, though mainly found in the stratum granulosum and stratum corneum [124]. The phospholipid content decreases while the sphingolipid and cholesterol content gradually increases as the cells differentiate during their migration to the surface.

Dermis and hypodermis

The dermis is rich in blood vessels, lymphatic vessels, and nerve endings. An extensive capillary network connects to the systemic circulation with substantial horizontal branching from the arterioles and venules in the papillary dermis. These in turn form plexus and supply capillaries to the hair follicles and the glands. The lymphatic vessels serve to drain the excess extracellular fluid and clear the antigenic materials. The dermis is filled with scattered fibroblasts, macrophages, leukocytes, and mast cells, in addition to the hair follicles, sebaceous glands, and sweat glands. On average, about 10 hair follicles, 15 sebaceous glands, 12 nerves, 100 sweat glands, 360 cm of nerves, and three blood vessels are present in one square centimeter of skin [125]. The hypodermis constitutes the deepest layer of the skin, and consists of the subcutaneous tissue filled with fat cells, fibroblasts, and macrophages.

4.1.2 Topical vs. Transdermal Delivery

4.1.2.1 Topical delivery

Topical drug delivery is the term used for localized treatment of dermatological condition where the medication is not targeted for systemic delivery [126]; examples include the treatment of dermatological diseases like eczema or psoriasis by topical application. Examples of drugs delivered topically include corticosteroids, antifungals, antivirals, antibiotics, antiseptics, local anesthetics, and antineoplastics. Topical agents that act by physical action would include protectives, adsorbents, emollients, and cleansing agents, whereas the astringents, irritants, rubefacients, and keratolytic agents are the ones which act by chemical means. Conventional topical drug delivery systems include semisolid dosage forms and liquid dosage forms. The semisolid dosage forms include ointments, creams, gels, or pastes, while the liquid dosage forms include emulsions, suspensions, and solutions [127]. Ointments usually contain less than 20% of water and more than 50% hydrocarbons, waxes, or polyols as vehicles. Ointments are used as carrier or delivery systems for active molecules but they also act as skin protective and emollient. Creams are bi-phase semisolid dosage forms usually containing more than 20% of water or volatile components and typically less than 50% of hydrocarbons, waxes, or polyols [126]. Gel are semisolid dosage form that contain a gelling agent to provide stiffness to the dispersion. Gels can be water based (hydrogels) or organic solvent based (oleogels). A paste can be defined as a semisolid dosage form, containing a large proportion of solids (20–50%) finely dispersed into a suitable vehicle. A lotion may be in the form of a solution or a suspension or an emulsion. Typically these formulations are intended to be applied to the intact skin, generally without any friction.

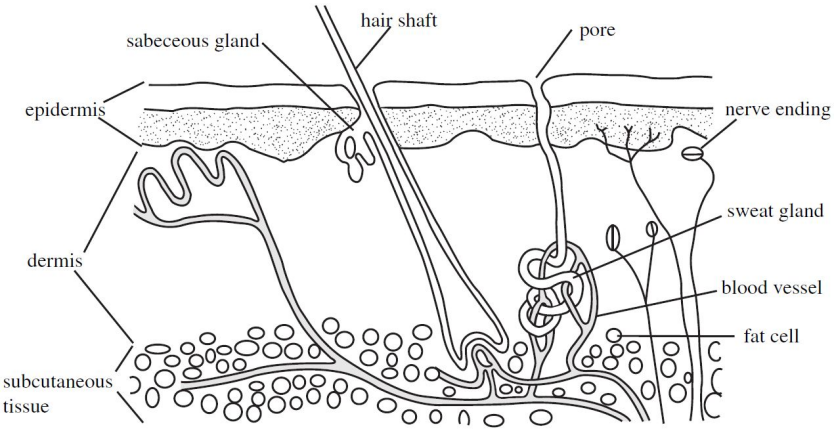

Figure 4.1: Anatomy of skin. Transverse section of skin showing different strata and the associated regions in the skin.

4.1.2.2 Transdermal delivery

Transdermal delivery is the term that is confined to a situation in which the drug diffuses through different layers of the skin reaching systemic circulation to elicit the therapeutic response [122]. An example would be the management of hypertension using a transdermal clonidine patch. In a broader sense transdermal delivery also includes local anesthetic patches in which the drug is intended to diffuse regionally in the skin to elicit the pharmacological action only in the treated area of the skin. Often, delivery of local anesthesia has been classified under topical drug delivery [128]. Transdermal drug delivery systems also termed as "patches" are self-contained discrete dosage forms designed to deliver a therapeutically effective amount of drug through intact skin. Most commercially available transdermal drug delivery systems are of three different types, namely reservoir systems, matrix systems with rate-controlling membrane, and matrix systems without rate-controlling membrane. The reservoir system is made up of three major components, namely the drug reservoir, the rate-controlling membrane, and the adhesive. The drug present in the reservoir, along with the other excipients, must permeate through the rate-controlling membrane before reaching the skin. The adhesive that holds the system placed on the skin can completely cover the drug release area or only the perimeter around the non-adhering drug release surface. In the matrix type, the drug may be embedded in an adhesive matrix. A rate controlling membrane may be present between the drug-loaded matrix and the adhesive or sometimes the matrix itself can control the rate of release of the actives from the system. Some drugs delivered successfully in transdermal drug delivery systems are scopolamine, nitroglycerine, nicotine, clonidine, fantanyl, estradiol, testosterone, lidocaine, and oxybutinin [129]. Recent additions to this list include lidocaine-tetracaine, selegiline, methyl phenidate, and rotigotine. However, the future focus is production of transdermal systems capable of delivering peptides and proteins including insulin, growth hormone, and vaccine across the skin.

4.1.3 Percutaneous Absorption Pathways

The lipid-rich and structurally complex intercellular region of stratum corneum plays an important role in the percutaneous absorption [130]. The stratum corneum is known to be selectively permeable and allows relatively lipophilic molecules to diffuse to the lower skin layers [122]. The transport of such molecules across the stratum corneum barrier is mainly by passive diffusion [131]. The permeation rate through the stratum corneum has been represented by a simple equation 4.1 [125]:

$$\frac{dm}{dt} = \frac{DC_0K}{h} \tag{4.1}$$

where dm is the amount of the diffusant passed through the membrane in time dt, C_0 is the drug concentration in the donor solution, K is the partition coefficient of the diffusant between the membrane and the solution, D is the diffusion coefficient of the diffusant in the membrane, and h is the membrane thickness. Considering the tortuous intercellular pathway between the corneocytes, the diffusional path length for the permeants is much longer than the thickness of the stratum corneum and is estimated to be $\sim 500\,\mu m$ [123]. The other potential routes of entry for the permeants from the skin surface to the subepidermal tissues are through the hair follicles with their associated sebaceous glands and via the sweat ducts or through the stratum corneum between these appendages [125]. These follicles passing from the skin surface through the epidermis and reaching the dermis or even the underlying subcutaneous region are the most important appendages of human skin.

4.2 Materials and Methods

4.2.1 Materials

Glycerin, Medium chain triglycerides (Delios®) were purchased by BASF Corp. (Ludwigshafen, Germany); glyceryl stearate (Cutina® MD) was purchased from Henkel Chimica S.p.A. (Lomazzo, Italy); ethoxydiglycol (Transcutol®) were a gift form Gattefosse (Saint-Priest, France); Polyethylene glycol 400 (PEG-400) was obtained by Croda (Mortara, Italy) and xanthan gum (XG) was purchased by ACEF (Fiorenzuola D'Arda, Italy).

4.2.2 Topical formulations preparation

Preparation methods and materials used for the old formulations F01 and F03, have been described in Sec. 2.3.1. In this section are described the preparation methods of the modified formulations for topical application. The detailed compositions are reported in Table 4.1 and summarized in Fig. 4.2.

Preparation methods

Where expected, glyceryl stearate is melted in oily phase before the emulsification (OPC01 and AF201). In formulations containing solubilizers (AF201 and APG01),

Table 4.1: Composition of the tested formulations.

	F01 %	**F03** %	**OPC01** %	**AF201** %	**APG01** %
Water	19,3	5,0	55,0	43,0	51,0
Glycerin	37,7	9,5	9,5	6,0	10,0
MCFA	40,5	75,0	20,0	10,0	20,0
Sucrose monopalmitate	2,0	10,0	3,0	2,5	3,0
Resveratrol	0,5	0,5	0,5	0,5	0,5
Glyceryl stearate	0	0	12	18,0	0
Ethoxydiglicol	0	0	0	20,0	0
Peg-400	0	0	0	0	15,0
Xanthan gum	0	0	0	0	0,5

resveratrol is solubilized in ethoxydiglycol HP or PEG-400 using a magnetic stirrer and the solution is then added to water phase before the emulsification. Where expected, xanthan gum is dispersed in half of the amount of water present in the formulation under gently stirring. The resulting thick gel was then mixed to the water phase before emulsification process (APG01).

Formulations containing glyceryl stearate: OPC01, AF201

To obtain the desired viscosity and spreadability glyceryl stearate is added to the formulation because of its ability to form a mesotropic structure in the oily phase. It also acts as a lubricant on the skin's surface, which gives the skin a soft and smooth appearance and it slows the loss of water from the skin by forming a barrier on the skin's surface.

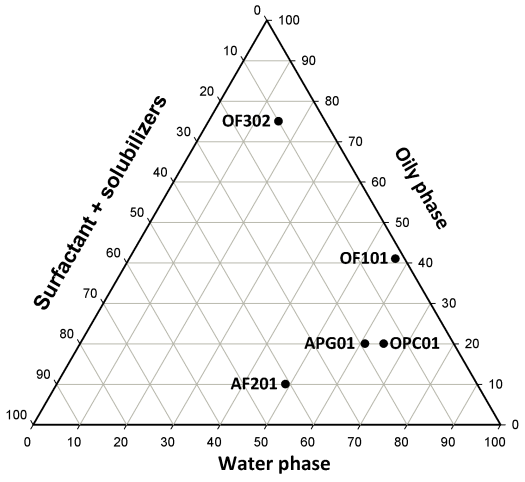

Figure 4.2: Composition of the studied formulations: *oily phase* is composed by MCFA, *water phase* is composed by water and glycerin, *surfactant+solubilizers* phase is composed by sucrose ester and ethoxydiglycol, peg-400, glyceril stearate and xanthan gum (where expected).

1. Water phase, composed by water, glycerine and surfactant (SMP), was gently stirred and heated at approximately 60 ℃ in water bath
2. Glyceryl stearate was melted in the oily phase (composed by MCFA) at approximately 60 ℃ in water bath. Immediately before the emulsification, resveratrol is added to this phase.
3. Under continuous stirring, oily phase was poured into water phase and the resulting emulsion/microemulsion was cooled at room temperature.

Formulations containig solubilizers: AF201, APG01
The two tested solubilizers, ethoxydiglicol and PEG-400 were used to solubilize resveratrol with magnetic stirrer and then added to the water phase previous emulsification with the oily phase as described above.

Formulations containing gelling agents: APG01
Xanthan gum was used as thickener of the water phase. It was hydrated in approximately half the water expected in the formulation. To speed up the hydration process water was heated at 70 ℃ and under gently stirring the polymer was added. The resulting thick gel was then mixed to the water phase before emulsification process, as described above.

4.2.3 Rheology

Flow and viscosity curves were acquired with the same instruments and in the same conditions described in Sec. 2.3.3.

4.2.4 Differential scanning calorimetry (DSC)

The thermal behavior of the formulation components was determined through DSC investigation using Mettler Toledo DSC 1, STAR^e System (Mettler Toledo GmbH Analytical, Giessen,Germany), weighing 8-13 mg of samples on a microbalance, in standard 40 μl aluminum pans, immediately sealed by a press. An empty pan was used as a reference. Samples were scanned starting from room temperature to 300 ℃ at a heating rate of 5 ℃/min. The melting temperatures of the components and the total heat transferred in any of the observed thermal processes was determined.

4.2.5 Microscopy

Optical microscopy

Placebo and verum formulations were analyzed with an optical microscope (Eclipse Ti-S, Nikon) equipped with a digital camera (Ds-FI1, Nikon) in order to investigate the formulations internal structure. Images were acquired and elaborated with an imaging software (Nis-Elements, Nikon), a 40x objective was used, resulting in a final magnification of 520x. Samples were spread on a microscope slide and covered. The optical microscope analysis was used to assess the presence of undissolved resveratrol in the formulations non-containing solubilizing agents and to verify the influence of the water/ethanol solution, used to simulate human sweat as receptor fluid, on the internal structure of the formulations: samples were analyzed before and after the release studies and the pictures were compared.

Transmission electron microscopy

Samples were spread on the observation grid and treated with an uranile acetate 1% solution for two minutes, then allowed to get dry and analyzed with an electron transmission microscope (Tecnai 12, FEI).

4.2.6 In-vitro release studies

According to FDA guidance SUPAC-SS (May 1997) *"In vitro release is one of several standard methods which can be used to characterize performance characteristics of a finished topical dosage form, release is theoretically proportional to the square root of time when the formulation in question is in control of the release process because the release is from a receding boundary. In vitro release method for topical dosage forms is based on an open chamber diffusion cell system such as a Franz cell system, fitted usually with a synthetic membrane. The test product is placed on the upper side of the membrane in the open donor chamber of the diffusion cell and a sampling fluid is placed on the other side of the membrane in a receptor cell. Diffusion of drug from the topical product to and across the membrane is monitored by assay of sequentially collected samples of the receptor fluid ... Aliquots removed from the receptor phase are analyzed for drug content by high pressure liquid chromatography (HPLC). A plot of the amount of drug released per unit area ($\mu g/cm^2$) against the square root of time yields a straight line, the slope of which represents the release rate. This release rate measure is formulation-specific and can be also used to monitor product quality" [132].*

In order to investigate the release of resveratrol from the formulations a modified Franz cell has been used. The apparatus (Fig. 4.3) is composed by a lower plate (c) containing the sample in a reservoir (d) and a upper plate (a) which function is to clamp the polymeric membrane (b) and allow exchanges between the donor chamber and reception chamber.

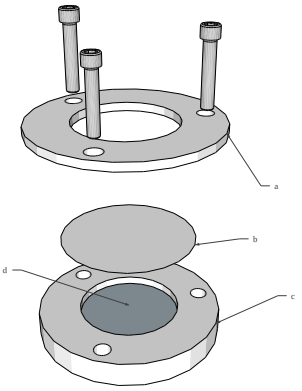

Figure 4.3: Modified Franz cell: once assembled is submerged in a thermostated vessel containing the receptor medium.

The clean pre-weighed sample holder was completely filled with the sample serving as the donor phase. The excess sample was removed from the surface using the edge of a spatula to obtain an even and smooth surface area. This was weighed again to determine the exact amount of sample employed in the experiment (usually around 2 g). A 45 mm cellulose acetate membrane (Visking Tubing, London, UK), soaked in dissolution medium for 20 h, was positioned on the surface of the samples[1]. Once assembled, the cell is placed in a dissolution test apparatus (Sotax A7 smart - Sotax), see Fig. 4.4. Vessels containing 900 of the receptor medium (kept at 33±0,5 ℃) were left under continuous stirring at 100 rpm. Samples of 1 ml were withdrawn and replaced with fresh medium. Samples were directly analyzed by HPLC method, as described in Sec. 3.2.6. The assay was performed simultaneously on 3 replicates for each formulation.

With topical dosage forms containing sparingly soluble drugs, the use of a hydro-alcoholic medium as a receptor phase is essential to increase drug solubility for detection and to maintain sink conditions[2]. When employing a hydro-alcoholic medium as a receptor phase, a challenge arises from the possibility of back diffusion of alcohol through the synthetic membrane and alteration of the integrity of the cream preparation. Suitable studies can detect or refute this occurrence, for example, in our case the microscopic

[1] About the membrane FDA suggests:*"Appropriate inert and commercially available synthetic membranes such as polysulfone, cellulose acetate/nitrate mixed ester, or Polytetrafluoroethylene 70 μm membrane of appropriate size to fit the diffusion cell diameter" [132].*

[2] Appropriate receptor medium such as aqueous buffer for water soluble drugs or a hydro-alcoholic medium for sparingly water soluble drugs or another medium with proper justification.[132]

Table 4.2: Composition of the receptor medium used: simulated human sweat + alcohol.

	% (p/p)
H_2O	89,4776
$Ethanol$	10
$CaCl_2$	0,0022
$NaCl$	0,2920
$MgSO_4$	0,0240
KH_2PO_4	0,2042

examination of the cream before and after the in-vitro release experiment showed no difference. Thus, the concentration of ethanol had a negligible effect on cream integrity. A hydro-alcoholic solution, described in Table 4.2 was used as receptor medium, salts composition simulate the sweat stratus normally covering the skin, the alcohol percentage was used to increase resveratrol solubility as described in Table 4.3.

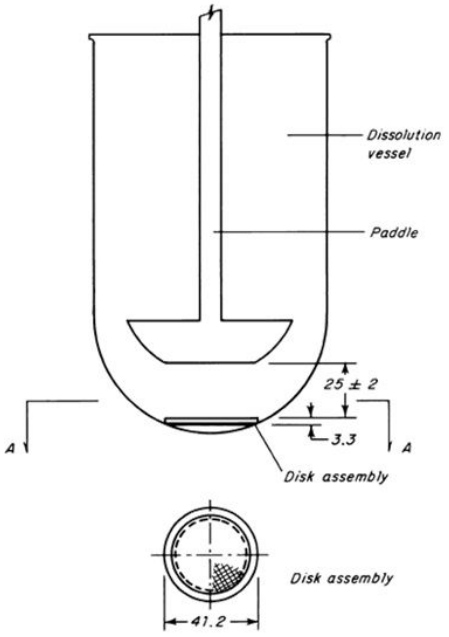

Figure 4.4: Schematic representation of the vessel used as receptor chamber, the "disk assembly" is represented by 4.3. Reproduced from [133]

Table 4.3: Solubility of resveratrol in different medium.

Medium	**Solubility [mg/ml]**
Water	0,0300
Phosphate buffer	0,0570
SHS (simulated human sweat)	0,0006
SHS + 10% ethanol	0,0820

4.2.7 In-vitro simulated absorption

To evaluate the in-vitro absorption the procedure for the release test described in Section 4.2.6 was used, but in this case the membrane was formed of two different coupled membranes, according to Realdon et al. [134–137]: the cellulose acetate membrane (Visking) soaked in release medium for 24 h as previously described was bonded with a cellulose mixed ester membrane (Millipore HAWP09000 type, 45 mm diameter) soaked by immersion for 24 h in isopropyl miristate [138, 139], then wiped between two disks of filterpaper. The membranes were made to adhere by using a rubber roller. The coupled membrane was placed with the cellulose membrane in contact with the cream sample. The resulting artificial membrane was composed of two layers:

- a hydrophilic barrier, simulating the stratum corneum
- a lipid barrier, simulating the hydrophobic compounds filling the stratum corneum and the underlying derma.

4.2.8 Analysis of release data

When operating with "infinite dose" conditions the release process across an artificial membrane occurs similar to the skin permeation except for the steady-state period, that can be described with Fick's first law [140]:

$$\frac{dQ}{dt} = K_p(C_D - C_R) \tag{4.2}$$

where Q (μg/cm^2) is the cumulative amount permeated through a unit of membrane surface, K_P (cm h^{-1}) is the permeability coefficient, and C_D and C_R (μm /cm^3) are the substance concentrations in the donor and receptor chambers. Generally, an artificial membrane, compared with the skin, does not represent such significant barrier. Therefore, the lag times are usually very small and can be neglected. If the release rates are very high at the beginning of the experiment, the apparent steady-state period is very short and the application of the Fick's first law is limited. The further drug release profile from topical formulations can be described using several kinetic models:

- **Zero-order model**
  It takes place at a constant rate independent of the existing concentration or initial concentration, generally it can be applied to dosage forms that do not disaggregate

and release the drug slowly, it can be represented by the equation:

$$Q_0 - Q_t = K_0 t \tag{4.3}$$

where Q_t is the amount of drug dissolved in time t, Q_0 is the initial amount of drug in the solution and K_0 is the zero order release constant expressed in units of concentration/ time. To study the release kinetics, data obtained from in vitro drug release studies were plotted as cumulative amount of drug released versus time.

- **Higuchi's model** [141]
  This model is based on the hypotheses that (1) initial drug concentration in the matrix is much higher than drug solubility; (2) drug diffusion takes place only in one dimension (edge effect must be negligible); (3) drug particles are much smaller than system thickness; (4) matrix swelling and dissolution are negligible; (5) drug diffusivity is constant; and (6) perfect sink conditions are always attained in the release environment.
  $$\frac{Q}{C_0} = 2\sqrt{\frac{D_v t}{\pi}} \tag{4.4}$$
  where D_v is the diffusion coefficient within the vehicle (cm^2/s). By plotting the cumulative released amount, normalized with initial concentration (Q/C_0) against the square root of time, the slope of linear regression (K_H) is determined as follows, so that D_v value can be calculated:
  $$K_H = 2\sqrt{\frac{D_v}{\pi}} \tag{4.5}$$
  The data obtained were plotted as cumulative percentage drug release versus square root of time

- **First order model**
  Drug release is proportional to drug concentration in the donor compartment. Release rate increases linearly with increase in drug concentration and can be expressed by the equation:
  $$logC = logC_0 - \frac{K_t}{2,303} \tag{4.6}$$
  where C_0 is the initial concentration of drug, k is the first order rate constant, and t is the time. The data obtained are plotted as log cumulative of drug remaining vs. time which would yield a straight line with a slope of -K/2,303.

4.3 Results

In order to develop topic formulations having good spreadability and compliance, formulation platforms F01 and F03 were mixed with water and different thickeners to obtain hydrophilic creams. The two selected thickeners are: glyceryl stearate and xanthan gum. In particular glyceryl stearate was selected due to its ability to form a mesotropic structure in the oily phase and to act a lubricant on the skin's surface, which gives the skin a soft and smooth appearance. It is also able to reduce the loss of water from the skin by forming a barrier on the skin's surface. Xanthan gum was selected in order to produce a cream with soft appearance and light feeling and thus a good compliance. In order to investigate the effect of the presence of a solubilizer on resveratrol availability and to increase the amount of the active in solution, a solubilizer was introduced in the formulation. In particular, the solubilizers were selected on the basis of resveratrol solubility. Among the different solubilizers tested, ethoxydiglycol and PEG 400 are those that provide to the greater solubilization (Fig. 4.5).

4.3.1 Thermal analysis

Differential scanning calorimetry (DSC) has been widely used for studying the thermal behaviors of multi-component emulsions and microemulsions, which give an insight into the states of water and microstructure transition. DSC curves are showed in Fig. 4.6. The DSC thermogram of pure resveratrol showed an endothermic peak at 265 ℃, corresponding to the melting point of the active. The SEs used (SMP) has an endothermic peak at 52 ℃that can not be observed in the original formulations F01 and F03. In the

Figure 4.5: Solubility of resveratrol in different oils (o) and solubilizers (s).

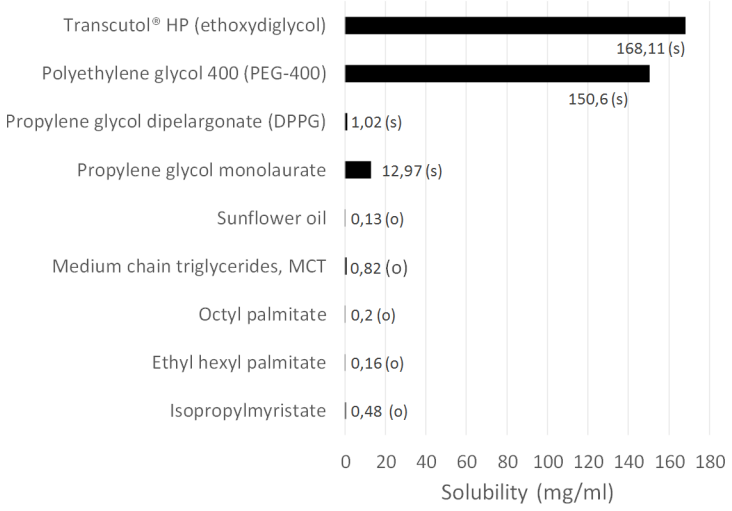

other formulations the presence of glyceryl stearate (melting point 58-59,℃) or xanthan gum (melting point ≈150,℃) produce interactions altering the melting points of the formulation components. The endothermic peaks in the range of approximately 50-100 ℃ corresponding to the melting of SMP and the others excipients listed in the graphs. OPC01 show also a peak at approximately 100 ℃ corresponding to the evaporation of bulk water, which was confirmed by the partial weight loss of the samples over the predefined temperature ranges, detected on the TGA thermograms (data not shown).

4.3.2 Rheology

The main purpose of rheological studies carried out on formulations was to understand the influence of thickeners and solubilizers introduced in the initial formulations F01 and F03. Flow and viscosity curves were build performing controlled-rate tests: shear rate[3]

[3]Is the rate of change of deformation through an element of a fluid due to an imposed deformation of stress.

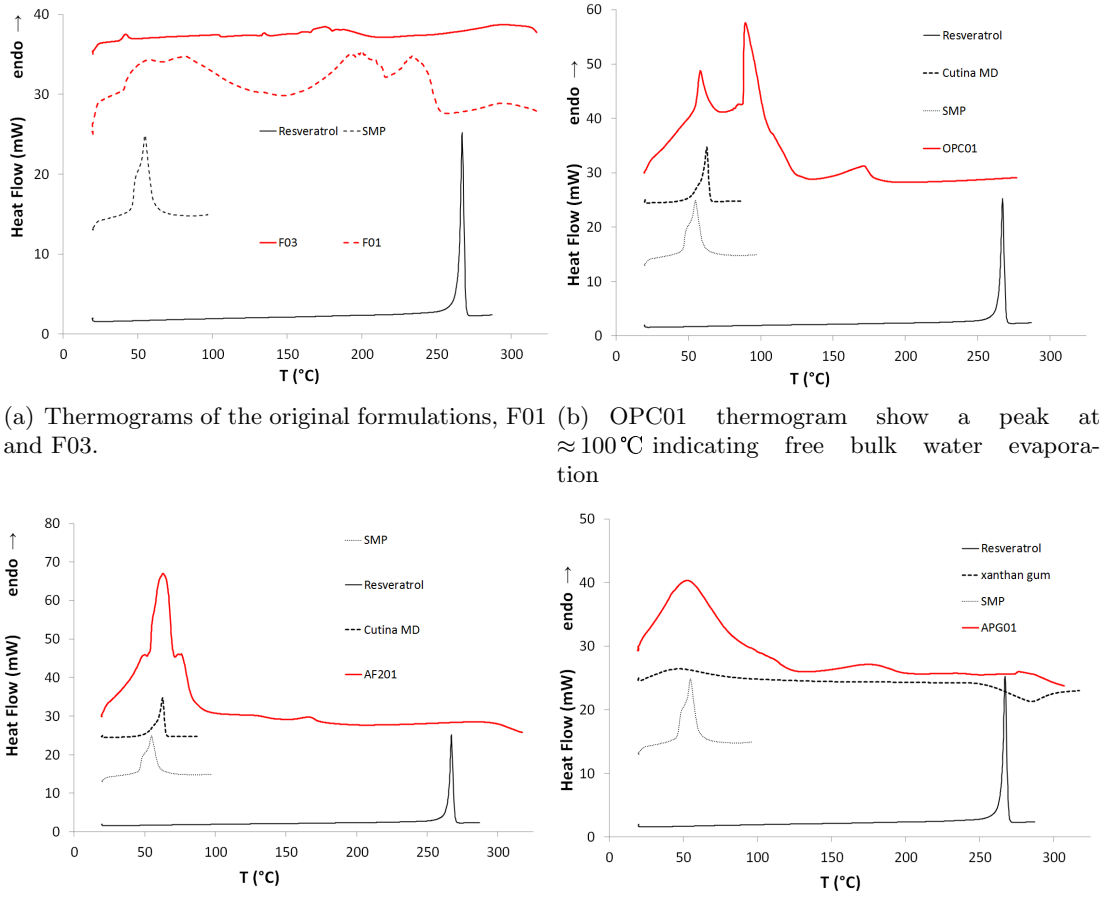

(a) Thermograms of the original formulations, F01 and F03.

(b) OPC01 thermogram show a peak at ≈ 100 ℃ indicating free bulk water evaporation

(c) AF201 thermogram

(d) APG01 thermogram

Figure 4.6: DSC curves of the formulations, compared to the pure raw materials.

was imposed and shear stress[4] registered in order to evaluate the thixotropic and/or pseudoplastic behavior.

Pseudoplasticity: some materials do not have a yield stress[5], nevertheless they behave non-linear, these are considered pseudoplastic. They flow instantaneously upon application of stress but also display shear thinning behavior.

Thixotropy: for many fluid materials, viscosity is mostly independent of time, and is only a function of the shear rate and the temperature. For structured fluids viscosity does not reach a steady value for some time upon application of stress, or shear rate. Steady state is dependent on the stabilization of internal structures that can be broken down by shearing, and require time to rebuild. A steady state plateau in viscosity is reached if an equilibrium has been established between structure breakdown and rebuilding. Upon ceasing the shear rate which caused the breakdown, the material reforms its internal network, and the viscosity recovers. Thixotropic materials present different behavior: in most cases when the shear rate is decreased the shear stress presents a hysteresis loop. The area within the hysteresis loop represents the energy consumed in structure breakdown.

An intuitive way to compare viscosity of the formulations is to consider the shear stress or viscosity maximum values, as reported in Table 4.4.

Hence formulations can be sorted in three viscosity levels:

1. *High viscosity* - F03
2. *Medium viscosity* - AF201 and OPC01
3. *Low viscosity* - F01 and APG01

[4]Shear stress is the force per unit area imposed on a element of fluid.
[5]Yield stress is the minimum shear stress required to initiate flow in a fluid.

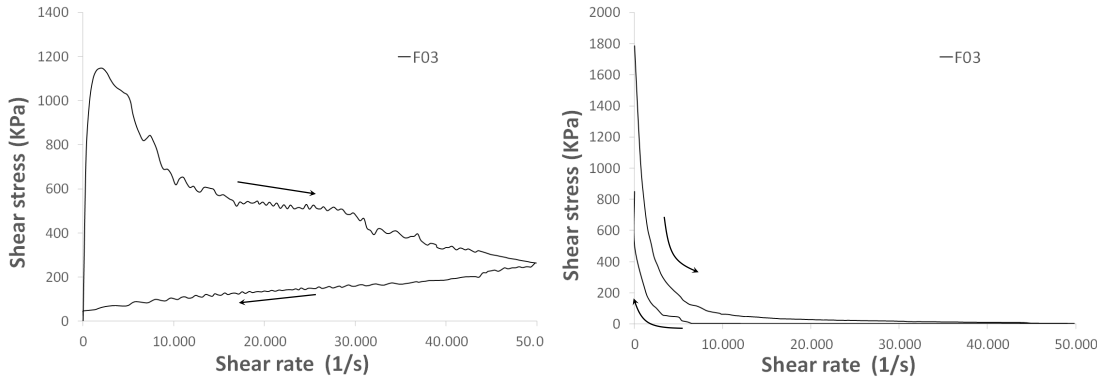

(a) F03 flow curve

(b) F03 viscosity curve

Figure 4.7: F03 rheology.

Table 4.4: Maximum viscosity and shear stress values obtained.

	Shear stress $\tau\ [Pa]$	**Viscosity** $\eta\ [Pa \cdot s]$
F03	$1,17 \times 10^6$	$1,79 \times 10^6$
AF201	$5,14 \times 10^5$	$5,05 \times 10^5$
OPC01	$1,74 \times 10^5$	$1,72 \times 10^5$
F01	$6,29 \times 10^4$	$1,57 \times 10^3$
APG01	$1,38 \times 10^4$	$2,19 \times 10^3$

A more accurate analysis that underline rheological behavior of formulation F03, is reported in Fig. 4.7, in particular Fig. 4.7(a) shows a broad thixotropic loop suggesting a time-dependent change in viscosity. The quick loss of viscosity describes how formulation's internal structure is almost immediately lost, then there is a shear-thinning behavior until the shear-rate begin to decrease. During the decreasing shear rate phase viscosity is only gained when shear rate is near zero. It's worth noting that in F03 there aren't thickening agents, thus the high viscosity level is due to the micro structure created by the high amount of oil droplets and by the presence of surfactant. As reported by the microscopical analysis (section 4.3.3) the main internal structure is a micro-drops domain, it's likely that in absence of a external force (as shear rate) the micro-drops pack together, resulting in a high viscosity semi-solid. In presence of low shear rate the drops slip one on the other and decreasing dramatically shear stress and viscosity. Once the initial packed-structure is lost the only way to gain the starting viscosity is to remove the external force, allowing the micro drops to pack again.

Formulations AF201 and OPC01 show very similar rehological behaviour, both are included in the *medium viscosity* category and have a very similar flow and viscosity profile as shown in Fig. 4.8. After an initial decrease, shear stress remain stable for the

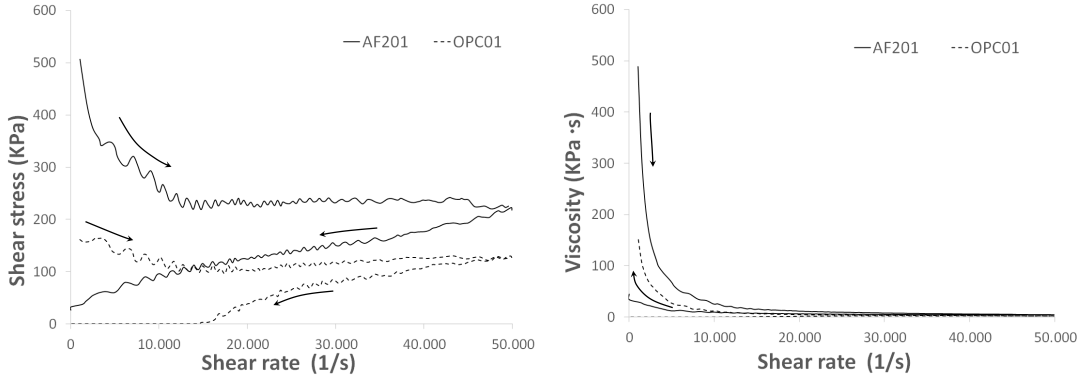

(a) AF201 and OPC01 flow curve

(b) AF201 and OPC01 viscosity curves

Figure 4.8: AF201 and OPC01 rheology.

entire growing phase and slowly reduce while returning to the initial state, creating an hysteresis loop (Fig. 4.8(a)). As in the previous case, an internal micro-structure producing a viscous formulation is present. However, in this case, the hysteresis loop is small due to the presence of glyceryl stearate able to form a lamellar micro-structure. Consequently in this case viscosity is given both from sucrose ester and glyceryl stearate.

Formulations APG01 and F01 are the least viscous of the tested formulations, both exhibit a rheological behavior more similar to a newtonian fluid in respect to the previous formulations, as depicted in 4.9. The concentration of sucrose ester is probably not sufficient to form the gel-emulsion structure found in F03, and not even the xanthan gum concentration is high enough to behave like a pseudoplastic or thixotropic fluid.

4.3.3 Microscopy

Verum formulations were first evaluated with an optical microscope (see section 4.2.5), results are depicted in Fig. 4.10. Resveratrol crystals are clearly visible in those formulations not containing solubilizers: OPC01, F01 and F03; whilst they cannot be recognized in formulations containing ethoxydiglycol and PEG-400, respectively AF201 and APG01. Analysis of formulations without resveratrol confirmed the hypothesis that in formulations not containing solubilizers resveratrol is also present in solid form, since none of the analyzed formulations showed crystals, as depicted in Fig. 4.11.
Despite the different compositions AF201 and F03 show a very similar structure when evaluated through optical microscopy, with a dense pattern in which is difficult to discern oily phase from water phase. However when evaluated through transmission electron microscopy (see Fig. 4.12) AF201 and F03 display a different appearance, AF201 has

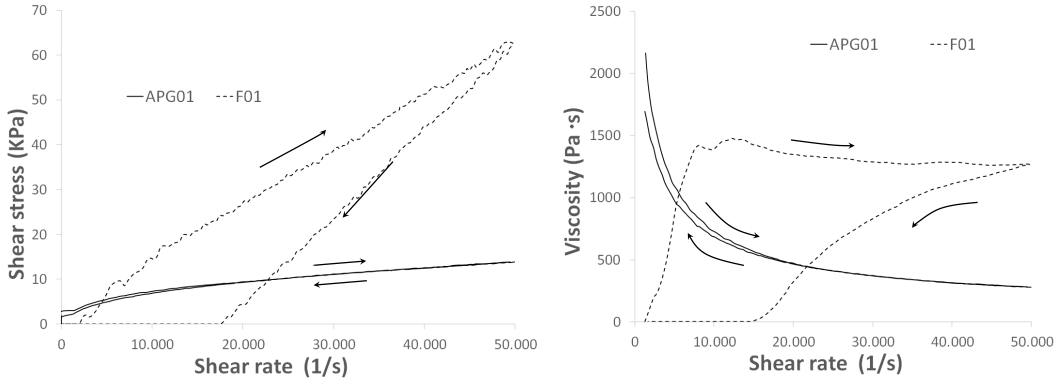

(a) APG01 and F01 flow curve

(b) APG01 and F01 viscosity curves

Figure 4.9: APG01 and F01 rheology.

a *flakes* structure with layers standing one on the other (probably created by the interactions of ethoxydiglycol and glyceryl stearate whereas F03 has a more predictable structure showing a packed droplets pattern, typical of emulsions, where the oily phase is represented by the white part of the image and the water phase is the black outline. For formulations APG01, OPC01 and F01 there are also significant differences between what pointed out by the optical microscopy analysis and what showed by the electron transmission electron microscopy: optical microscopy show a very similar appearance, typical emulsion structure where can be recognized with spherical shaped drops representing oily phase surrounded by water phase, drops width seem to be similar. Electron microscopy highlights great differences between those formulations, APG01 has a filamentary structure, probably due to the presence of xanthan gum polymeric chains; OPC01 show a *flake* pattern, similar to AF201, probably because of the glyceryl stearate creating a lamellar structure; F01 has a drops pattern similar to F03 but the presence of a higher water phase and a lower surfactant concentration lead to larger oil drops.

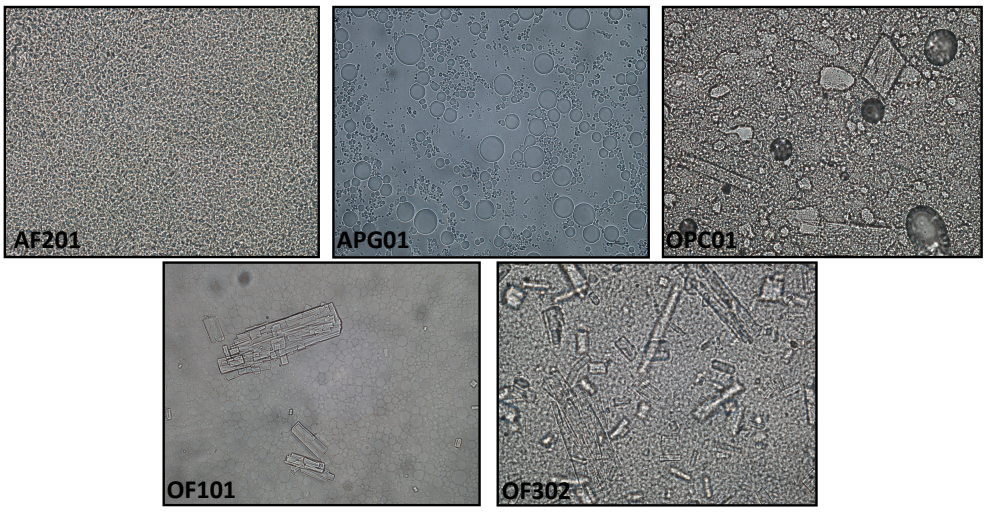

Figure 4.10: Optical microscopy images of verum formulations show how resveratrol is non entirely dissolved in formulations not containing solubilizers as OPC01, F01 and F03. Final magnification is 520 x.

4.3.4 In-vitro release and absorption

The various resveratrol formulations were tested using the previously mentioned synthetic membranes using a solution of simulated human sweat and ethanol as the receptor medium. To provide a complete evaluation of release and absorption phenomena the cumulative amounts of resveratrol released and permeated over a period of 24 h were expressed as $\mu g/cm^2$ and as percentage and were plotted against the time.

4.3.4.1 Release

Release profiles are reported in Fig. 4.13. Formulations containing solubilizers have the greater release values, indeed APG01 (containing PEG-400) reach $1020{,}34 \pm 1{,}84\,\mu g/\mathrm{cm}^2$, corresponding to 96% of the resveratrol content, and AF201 (containing ethoxydiglycol) reach $969{,}11 \pm 8{,}18\,\mu g/\mathrm{cm}^2$ (corresponding to 96% of the total resveratrol amount). One of the possible explanations for such behavior was offered by optical microscopical analysis (see Sec. 4.3.3). In formulations containing solubilizers resveratrol is free to diffuse through the membrane, without the dissolution limiting step affecting formulations containing dispersed resveratrol.
F01 and F03 show similar release profiles reaching respectively $657{,}87 \pm 0{,}14$ and $527{,}16 \pm 4{,}84\,\mu g/\mathrm{cm}^2$ (corresponding to approximately 50% of the total amount of resveratrol).

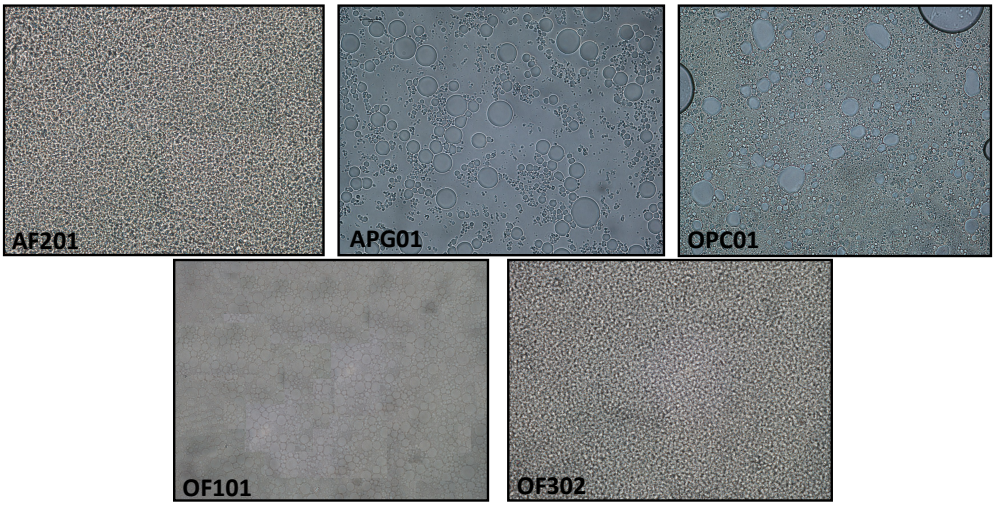

Figure 4.11: Optical microscopy images of placebo formulations. Magnification 520 x.

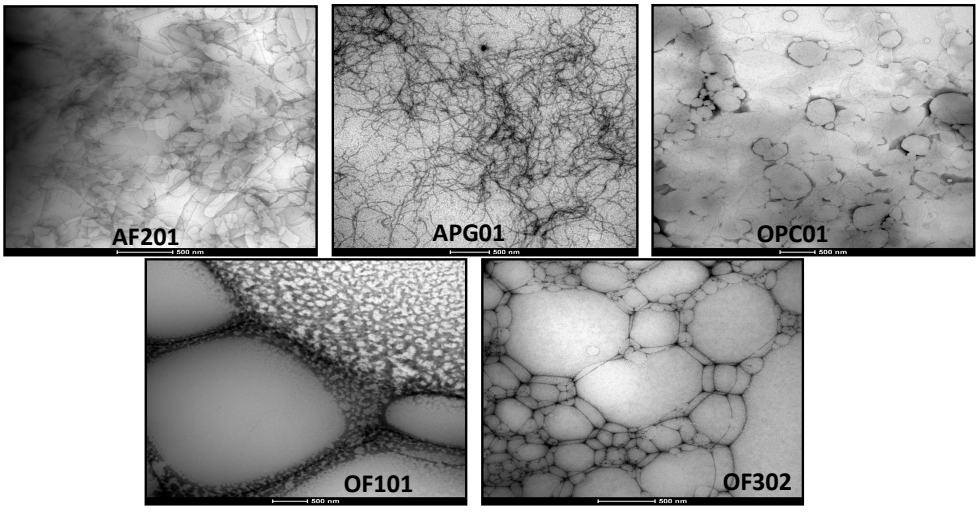

Figure 4.12: Transmission electron microscopy highlights differences between formulations that cannot be evaluated with optical microscopy.

F01 show a slightly higher release value respect to F03, probably due to its lower viscosity which leads to a higher diffusion rate of the resveratrol particles through the formulation.
OPC01 release the lower amount of resveratrol, $290{,}93 \pm 2{,}88\,\mu g/\mathrm{cm}^2$ (about 25% of the total amount). Despite its viscosity is comparable to AF201 viscosity, the amount of resveratrol released is considerably lower, this is probably due to the combined effect of the presence of glyceryl stearate, and to the absence of ethoxydiglycol. Glyceryl stearate indeed acts as a thickening agent and emulsifier arranging at the water/oil interface and slowing the diffusion of resveratrol from oil to water and thus its dissolution rate, at the same time ethoxydiglycol plays a key role as solubilizer an its absence prevents a fast and complete release of resveratrol.

4.3.4.2 Absorption

Absorption profiles are reported in Fig. 4.14. AF201 is the formulation that provides the higher absorption, reaching $933{,}45 \pm 92{,}06\,\mu g/\mathrm{cm}^2$ after 24 hours (corresponding to 79% of the total resveratrol contained), APG01 values are much lower reaching $644{,}69 \pm 4{,}70\,\mu g/\mathrm{cm}^2$ (equal to 61%). The absorption differences between AF201 and APG01, not observed in release studies, are probably due to the different lipophilicity of the solubilizers used: ethoxydiglycol, used in AF201, is a mild lipophilic substance since it has a log P of 0,9 while PEG-400 (polyethylene glycol), used in APG01, is strongly hydrophilic considering its Log P of -4,8. The higher lipophilicity of ethoxydiglycol provide a higher resveratrol permeation rate through the isopropyl myristate soaked membrane, acting as an effective permeation enhancer.

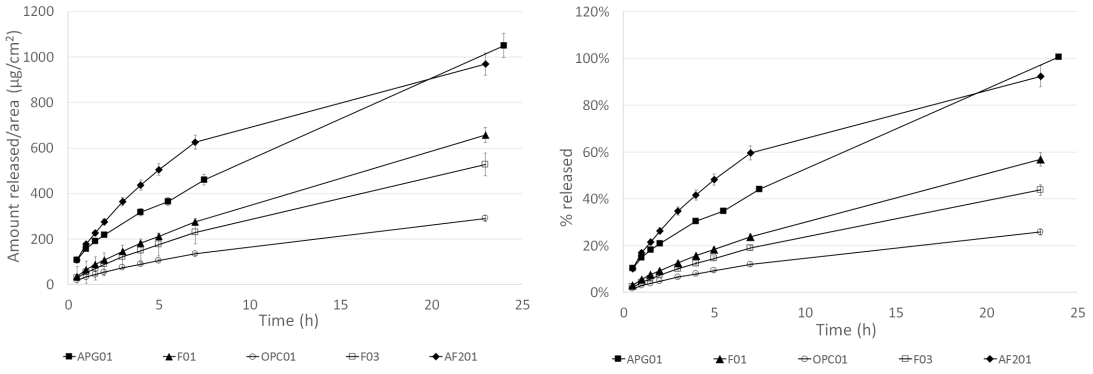

(a) Release curves expressed as $\mu g/cm^2$.

(b) Release curves expressed as percentage of the total amount of resveratrol.

Figure 4.13: In-vitro release of resveratrol from the five studied formulations, release data are expressed against time to evaluate zero order model. Error bars are calculated on three repetitions.

F01, F03 and OPC01 absorption profiles are similar to those seen in the release studies: F01 reach $436{,}21 \pm 31{,}73\,\mu g/\mathrm{cm}^2$ after 24 hours (equal to 39%), F03 allow to permeate $369{,}38 \pm 12{,}26\,\mu g/\mathrm{cm}^2$ (equal to 36%) and OPC01 not exceed $248 \pm 12{,}67\,\mu g/\mathrm{cm}^2$ (equal to 21%).

4.3.4.3 Kinetics

The release profiles were also evaluated by fitting the experimental data to different order kinetic equations. Data linear regression analysis was performed using zero-order, first-order and Higuchi equations (Fig. 4.13-4.16). The Pearson correlation coefficient values (r) and the relative release and absorption rates are listed in Table 4.5 and 4.6.
Quite surprisingly the majority of the formulations showed release and permeation profiles following first-order kinetic, in fact, the release and the permeation of resveratrol from AF201, F01 and F03 is concentration-dependent and it follow the Noyes-Whitney's equation [59] that can be re-arranged as $\frac{dM_t}{dt} = k(M_0 - M_t)$ where M_0 is resveratrol amount at $t = 0$ and consequently $M_0 - M_t$ represents the resveratrol amount that has to be released yet and decreases with time. As the concentration of resveratrol in the formulations decreases, also the release rate proportionally decrease generating a burst effect in the first hours, this means that the rate-limiting step of the overall process is not diffusion through the slab or the membrane crossing but dissolution in the receptor medium.
Only formulation AF201 shows a zero-order release kinetic both in release and absorption simulation. Release and absorption rates are constant during time and follow the general equation $\frac{dM_t}{dt} = k$, the formulation behave like a ordinary reservoir system, where

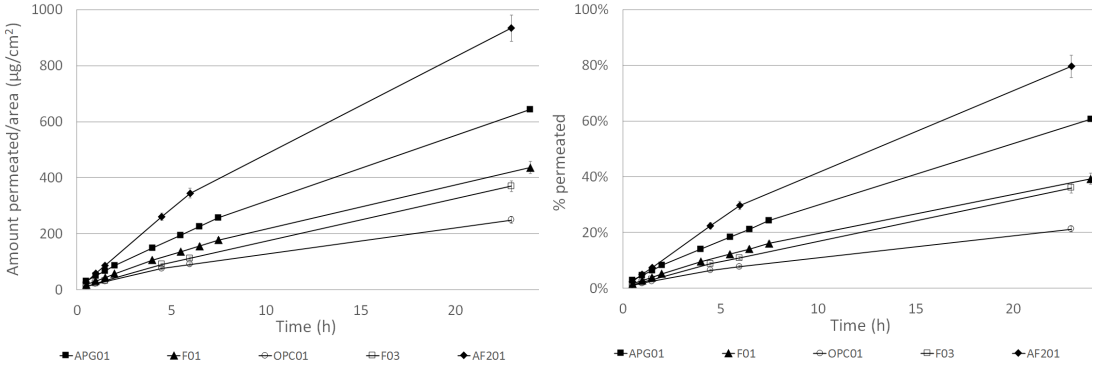

(a) Absorption curves expressed as $\mu g/cm^2$.

(b) Absorption curves expressed as percentage of the total amount of resveratrol.

Figure 4.14: In-vitro absorption of resveratrol from the five studied formulations, absorption data are expressed against time to evaluate zero order model. Error bars are calculated on three repetitions.

Table 4.5: Correlation coefficients (r^2) and relative release rates (K) of the three mathematical models taken into account, applied to release profiles.

Release	Zero order		Higuchi		First order	
	r^2	K_0 (s^{-1})	r^2	$K_{H(s^{-1/2})}$	r^2	K_1 (s^{-1})
AF201	0,8712	35,622	0,9798	215,65	0,9993	0,2577
APG01	0,9923	38,923	0,9781	222,89	0,9697	0,3102
F01	0,9874	25,856	0,9857	153,17	0,9997	0,0822
F03	0,9827	21,527	0,9896	123,31	0,9967	0,0557
OPC01	0,9740	11,637	0,9946	67,130	0,9856	0,0280

the rate-limiting step is the membrane crossing that occur at constant rate, determining a constant rate release, independent of resveratrol concentration.
OPC01 follow the first-order kinetic in absorption studies (as described above) but fits better with the Higuchi equation in release experiments. In this case release rate is inversely proportional to square root of time: $\frac{dM_t}{dt} = \frac{k}{\sqrt{t}}$. According to Fick's law, the prevailing process in this case is the diffusion of resveratrol through the slab: as the receptor medium spread through the formulation dissolving the resveratrol a receding boundary is created. Since only dissolved molecules can diffuse through the membrane and the interface between solid resveratrol and dissolved resveratrol moves like a front toward the inside, the diffusion pathway length increases with time.

4.4 Discussion

Topical dosage forms loaded with resveratrol were successfully developed starting from F10 and F03. Glyceryl stearate and xanthan gum were tested to obtain desired rheological features, ethoxydiglycol and polyethylene glycol 400 were used to solubilize

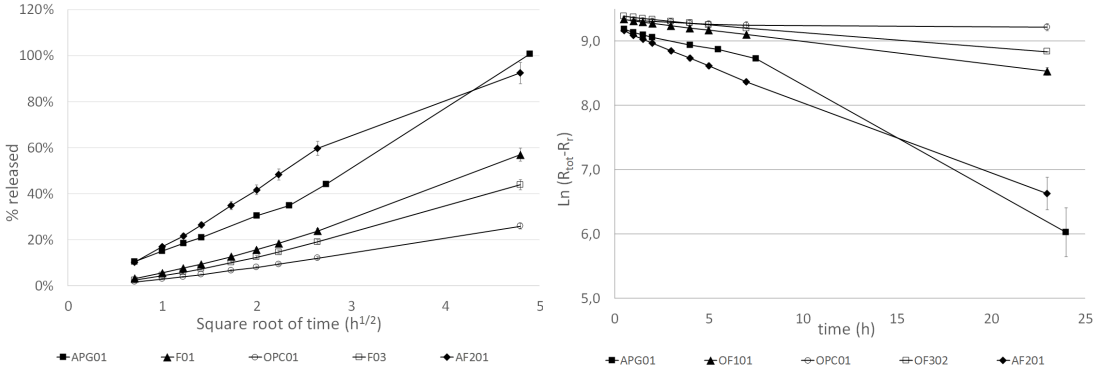

(a) Release curves are expressed as percentage of the total amount of resveratrol vs. square root of time to evaluate Higuchi model.

(b) Release curves are expressed as ln of the difference between total resveratrol (R_{tot}) and released resveratrol (R_r) to evaluate first order model.

Figure 4.15

Table 4.6: Correlation coefficients (r^2) and relative release rates (K) of the three mathematical models taken into account, applied to absorption profiles.

Absorption	**Zero order**		**Higuchi**		**First order**	
	r^2	$K_{0\ (s^{-1})}$	r^2	$K_{H(s^{-1/2})}$	r^2	$K_{1\ (s^{-1})}$
AF201	0,9860	39,588	0,9901	226,09	0,9984	0,0702
APG01	0,9987	25,872	0,9728	146,50	0,9912	0,0386
F01	0,9884	17,616	0,9789	100,27	0,9985	0,0204
F03	0,9978	15,738	0,9729	88,563	0,9999	0,0193
OPC01	0,9878	10,302	0,9896	58,760	0,9933	0,0099

resveratrol. Optical and TEM microscope analysis have highlighted how solubilizers and thickeners influence the physical state of resveratrol and the whole internal structure. By modulating rheology and physical state of the active molecule we were able to control its release and absorption. When fast release is required the use of solubilizers is recommended, e.g. formulation AF201 is capable to release 100% of its resveratrol content during 24 hours with a relevant burst effect, typical of first-order release kinetics. When a slower and constant release rate is required a zero-order kinetic is recommended (e.g. formulation APG01). When the use of irritating excipients must be avoided and an emollient effect is desirable (e.g. the application on psoriasis wounded skin) a formulation like F01 and F03 can be a brilliant solution.

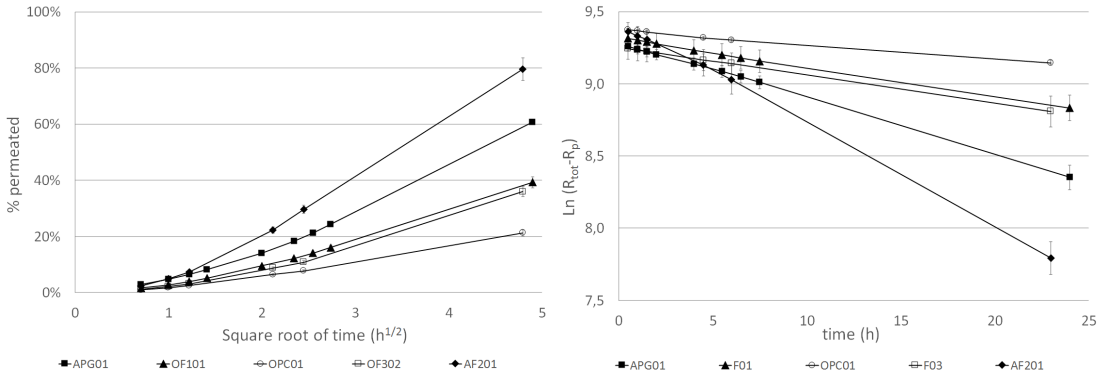

(a) Absorption curves are expressed as percentage of the total amount of resveratrol vs. square root of time to evaluate Higuchi model.

(b) Absorption curves are expressed as ln of the difference between total resveratrol (R_{tot}) and permeated resveratrol (R_P) to evaluate first order model.

Figure 4.16

Chapter 5

General Conclusions

This study investigated the association of commonly used medium chain fatty acids with sucrose monopalmitate, water and glycerin to form both classical emulsions and transparent gel-emulsions for the delivery of lipophilic active molecules. Although in the last 15 years several studies about the use of sucrose esters in food industry have been reported, none of them mentioned their capability to form gel-emulsions (also called high internal phase ratio emulsions, HIPREs). The physical and mechanical properties and the internal structure of the new formulations was assessed by several analytical techniques such as DSC, TEM, DLS and rheology measurements. All the emulsion formulated have proved to be stable at the ICH conditions tested, in particular HIPREs showed great stability features, surely useful in food supplements and cosmetics applications.

Two oral dosage forms were developed starting from one of the previously described HIPREs: adsorbed-HIPREs and medicated jellies. Resveratrol and ubidecarenon were selected as model molecules to evaluate the release performances. For both actives it was registered a significant increase in solubility using HIPREs, adsorbed-HIPREs and medicated jellies respect to bulk powder. In particular resveratrol showed to be especially suitable for this kind of formulations since its complete solubility when formulated in the adsorbed-HIPREs dosage form.

Also topical application of resveratrol was investigated, two HIPREs formulations were selected and modified by adding ethoxydiglycol and PEG-400 as solubilizers and glyceryl stearate and xanthan gum as thickeners. The obtained formulations were characterized with the techniques described above and in addition in-vitro release and absorption tests were performed. Release and absorption data were fitted with three mathematical models, showing close relations between the release profiles and the excipients chosen. It was proven that the physical state of the active molecule and the lipophilicity of the solubilizer are the main factor affecting the release, indeed when resveratrol is dissolved

in ethoxydiglycol, it is released and adsorbed in higher amount respect to other formulations tested.

One of the main focuses of this study was to establish the factors that influence the formation and stability of lipid-based formulations produced using sucrose monopalmitate as surfactant and medium chain fatty acids as oil phase. The information obtained from this study should facilitate the rational design and fabrication of lipid-based delivery systems for lipophilic food and cosmetic actives. The initial aim to produce a formulation platform capable to delivery lipophilic active molecules by oral and topical administration was achieved. Once chosen the administration route and the active molecule, an affordable and effective formulation can be provided and adapted to nutraceutical, cosmetic and pharmaceutical industry as well.

Appendix A

Stability reports

Table A.1: Long term and accelerated stability report.

F04 - long term	**T0**	**T3**	**T6**	**T12**	**T18**	**T24**
Visual aspect	color: ivory	color: ivory	color: ivory	color: ivory	color: ivory	color: ivory
pH	7,98	7,87	7,43	6,21	6,96	6,83
Viscosity (KPa·s)	0,31	0,87	0,55	0,47	0,83	0,96
Centrifuge test	compliant	compliant	compliant	compliant	compliant	compliant
F04 - accelerated						
Visual aspect	color: ivory	color: ivory	color: ivory			
pH	7,98	6,74	7,25			
Viscosity (KPa·s)	0,31	0,51	0,98			
Centrifuge test	compliant	compliant	compliant			
F05 - long term	**T0**	**T3**	**T6**	**T12**	**T18**	**T24**
Visual aspect	color: ivory	color: ivory	color: ivory	color: ivory	color: ivory	color: ivory
pH	6,63	6,86	7,14	6,98	7,33	7,11
Viscosity (KPa·s)	30,04	30,85	30,46	30,12	29,65	29,87
Centrifuge test	compliant	compliant	compliant	compliant	compliant	compliant
F05 - accelerated						
Visual aspect	color: ivory	color: ivory	color: ivory			
pH	6,45	6,88	7,19			
Viscosity (KPa·s)	30,04	30,89	29,22			
Centrifuge test	compliant	compliant	compliant			

Table A.2: Long term and accelerated stability report.

F06 - long term	**T0**	**T3**	**T6**	**T12**	**T18**	**T24**
Visual aspect	color: transparent	color: transparent	color: transparent	color: transparent	color: transparent	color: transparent
pH	7,56	7,33	7,32	6,76	7,39	7,12
Viscosity (KPa·s)	6,34	6,44	6,56	6,82	6,19	6,47
Centrifuge test	compliant	compliant	compliant	compliant	compliant	compliant
F06 - accelerated						
Visual aspect	color: transparent	color: transparent	color: transparent			
pH	7,56	6,97	6,65			
Viscosity (KPa·s)	6,34	6,16	6,02			
Centrifuge test	compliant	compliant	compliant			
F07 - long term	**T0**	**T3**	**T6**	**T12**	**T18**	**T24**
Visual aspect	color: ivory	color: ivory	color: ivory	color: ivory	color: ivory	color: ivory
pH	7,59	7,15	7,42	7,51	6,21	6,99
Viscosity (KPa·s)	20,55	21,78	20,46	20,53	20,20	19,54
Centrifuge test	compliant	compliant	compliant	compliant	compliant	compliant
F07 - accelerated						
Visual aspect	color: ivory	color: ivory	color: ivory			
pH	7,59	7,12	7,09			
Viscosity (KPa·s)	20,55	19,04	18,43			
Centrifuge test	compliant	compliant	compliant			

Table A.3: Long term and accelerated stability report.

F15 - long term	**T0**	**T3**	**T6**	**T12**	**T18**	**T24**
Visual aspect	color: ivory	color: ivory	color: ivory	color: ivory	color: ivory	color: ivory
pH	7,01	7,49	7,45	6,83	6,59	6,88
Viscosity (KPa·s)	24,71	24,82	22,01	23,58	23,63	25,54
Centrifuge test	compliant	compliant	compliant	compliant	compliant	compliant
F15 - accelerated						
Visual aspect	color: ivory	color: ivory	color: ivory			
pH	7,01	6,94	7,16			
Viscosity (KPa·s)	24,71	21,46	22,11			
Centrifuge test	compliant	compliant	compliant			

F16 - long term	**T0**	**T3**	**T6**	**T12**	**T18**	**T24**
Visual aspect	color: ivory	color: ivory	color: ivory	color: ivory	color: ivory	color: ivory
pH	6,54	6,46	7,32	6,91	7,37	7,14
Viscosity (KPa·s)	17,02	17,45	16,36	16,88	17,43	18,17
Centrifuge test	compliant	compliant	compliant	compliant	compliant	compliant
F16 - accelerated						
Visual aspect	color: ivory	color: ivory	color: ivory			
pH	6,54	6,31	7,15			
Viscosity (KPa·s)	17,02	16,15	15,78			
Centrifuge test	compliant	compliant	compliant			

Table A.4: Long term and accelerated stability report.

F17 - long term	**T0**	**T3**	**T6**	**T12**	**T18**	**T24**
Visual aspect	color: ivory	color: ivory	color: ivory	color: ivory	color: ivory	color: ivory
pH	7,45	7,31	7,83	7,14	6,76	6,38
Viscosity (KPa·s)	28,30	24,27	25,32	23,93	23,41	25,11
Centrifuge test	compliant	compliant	compliant	compliant	compliant	compliant
F17 - accelerated						
Visual aspect	color: ivory	color: ivory	color: ivory			
pH	7,45	7,24	7,76			
Viscosity (KPa·s)	28,30	21,46	22,11			
Centrifuge test	compliant	compliant	compliant			
F18 - long term	**T0**	**T3**	**T6**	**T12**	**T18**	**T24**
Visual aspect	color: ivory	color: ivory	color: ivory	color: ivory	color: ivory	color: ivory
pH	6,89	6,16	7,43	7,16	7,94	7,52
Viscosity (KPa·s)	14,15	13,76	15,66	14,76	14,90	12,25
Centrifuge test	compliant	compliant	compliant	compliant	compliant	compliant
F18 - accelerated						
Visual aspect	color: ivory	color: ivory	color: ivory			
pH	6,89	6,55	7,16			
Viscosity (KPa·s)	14,15	13,44	12,18			
Centrifuge test	compliant	compliant	compliant			

Table A.5: Long term and accelerated stability report.

F19 - long term	**T0**	**T3**	**T6**	**T12**	**T18**	**T24**
Visual aspect	color: ivory	color: ivory	color: ivory	color: ivory	color: ivory	color: ivory
pH	7,88	7,93	7,21	7,43	7,19	7,98
Viscosity (KPa·s)	0,16	0,11	0,44	0,77	0,41	0,08
Centrifuge test	compliant	compliant	compliant	compliant	compliant	compliant
F19 - accelerated						
Visual aspect	color: ivory	color: ivory	color: ivory			
pH	7,88	7,24	7,76			
Viscosity (KPa·s)	0,16	0,13	0,07			
Centrifuge test	compliant	compliant	compliant			

F20 - long term	**T0**	**T3**	**T6**	**T12**	**T18**	**T24**
Visual aspect	color: ivory	color: ivory	color: ivory	color: ivory	color: ivory	color: ivory
pH	6,54	6,16	7,43	7,16	7,94	7,52
Viscosity (KPa·s)	8,05	8,11	8,51	7,73	7,70	7,56
Centrifuge test	compliant	compliant	compliant	compliant	compliant	compliant
F20 - accelerated						
Visual aspect	color: ivory	color: ivory	color: ivory			
pH	6,77	6,52	6,44			
Viscosity (KPa·s)	8,05	8,41	8,32			
Centrifuge test	compliant	compliant	compliant			

88

Table A.6: Long term and accelerated stability report.

F21 - long term	**T0**	**T3**	**T6**	**T12**	**T18**	**T24**
Visual aspect	color: ivory	color: ivory	color: ivory	color: ivory	color: ivory	color: ivory
pH	8,61	8,27	7,86	7,16	7,45	7,88
Viscosity (KPa·s)	18,20	17,13	17,54	17,22	16,37	16,21
Centrifuge test	compliant	compliant	compliant	compliant	compliant	compliant
F21 - accelerated						
Visual aspect	color: ivory	color: ivory	color: ivory			
pH	8,61	7,76	8,22			
Viscosity (KPa·s)	18,20	18,16	18,55			
Centrifuge test	compliant	compliant	compliant			

F22 - long term	**T0**	**T3**	**T6**	**T12**	**T18**	**T24**
Visual aspect	color: ivory	color: ivory	color: ivory	color: ivory	color: ivory	color: ivory
pH	6,15	6,16	7,43	7,08	7,02	6,32
Viscosity (KPa·s)	22,55	22,66	22,43	21,03	20,79	20,49
Centrifuge test	compliant	compliant	compliant	compliant	compliant	compliant
F22 - accelerated						
Visual aspect	color: ivory	color: ivory	color: ivory			
pH	6,15	6,08	6,58			
Viscosity (KPa·s)	22,55	22,95	19,47			
Centrifuge test	compliant	compliant	compliant			

Table A.7: Long term and accelerated stability report.

F23 - long term	**T0**	**T3**	**T6**	**T12**	**T18**	**T24**
Visual aspect	color: ivory	color: ivory	color: ivory	color: ivory	color: ivory	color: ivory
pH	6,55	6,39	7,12	7,01	6,75	6,82
Viscosity (KPa·s)	0,21	0,44	0,63	0,28	0,56	0,18
Centrifuge test	compliant	compliant	compliant	compliant	compliant	compliant
F23 - accelerated						
Visual aspect	color: ivory	color: ivory	color: ivory			
pH	6,55	6,98	6,78			
Viscosity (KPa·s)	0,21	0,12	0,15			
Centrifuge test	compliant	compliant	compliant			

F24 - long term	**T0**	**T3**	**T6**	**T12**	**T18**	**T24**
Visual aspect	color: ivory	color: ivory	color: ivory	color: ivory	color: ivory	color: ivory
pH	7,86	7,31	7,54	7,77	7,16	7,15
Viscosity (KPa·s)	29,21	26,13	25,47	23,76	22,45	22,32
Centrifuge test	compliant	compliant	compliant	compliant	compliant	compliant
F24 - accelerated						
Visual aspect	color: ivory	color: ivory	color: ivory			
pH	7,86	7,11	7,16			
Viscosity (KPa·s)	29,21	23,95	22,15			
Centrifuge test	compliant	compliant	compliant			

Table A.8: Long term and accelerated stability report.

F25 - long term	**T0**	**T3**	**T6**	**T12**	**T18**	**T24**
Visual aspect	color: ivory	color: ivory	color: ivory	color: ivory	color: ivory	color: ivory
pH	6,16	6,85	7,03	7,51	6,87	6,95
Viscosity (KPa·s)	9,17	9,43	9,14	9,21	9,84	9,12
Centrifuge test	compliant	compliant	compliant	compliant	compliant	compliant
F25 - accelerated						
Visual aspect	color: ivory	color: ivory	color: ivory			
pH	6,16	6,74	6,98			
Viscosity (KPa·s)	9,17	9,84	9,21			
Centrifuge test	compliant	compliant	compliant			

F26 - long term	**T0**	**T3**	**T6**	**T12**	**T18**	**T24**
Visual aspect	color: transparent	color: transparent	color: transparent	color: transparent	color: transparent	color: transparent
pH	6,82	6,19	6,77	6,14	6,22	6,04
Viscosity (KPa·s)	21,65	26,13	25,47	23,76	22,45	22,32
Centrifuge test	compliant	compliant	compliant	compliant	compliant	compliant
F26 - accelerated						
Visual aspect	color: transparent	color: transparent	color: transparent			
pH	6,82	6, 64	6,36			
Viscosity (KPa·s)	21,65	20,08	19,57			
Centrifuge test	compliant	compliant	compliant			

91

Bibliography

[1] Angela Szuts and Piroska Szab-Revsz. Sucrose esters as natural surfactants in drug delivery systems: a mini-review. *International Journal of Pharmaceutics*, 433(1 - 2):1 – 9, 2012. ISSN 0378-5173. doi: http://dx.doi.org/10.1016/j.ijpharm.2012.04.076. URL http://www.sciencedirect.com/science/article/pii/S037851731200422X.

[2] Angela Szuts, Peter Lung, Rita Ambrus, Lara, Kiss, Maria A. Deli, and Piroska Szaba-Ravasz. Applicability of sucrose laurate as surfactant in solid dispersions prepared by melt technology. *International Journal of Pharmaceutics*, 410 (1 - 2):107 – 110, 2011. ISSN 0378-5173. doi: http://dx.doi.org/10.1016/j.ijpharm.2011.03.033. URL http://www.sciencedirect.com/science/article/pii/S037851731100250X.

[3] Casimir C. Akoh. Emulsification properties of polyesters and sucrose ester blends i: Carbohydrate fatty acid polyesters. *Journal of the American Oil Chemists Society*, 69(1):9–13, 1992. ISSN 0003-021X. doi: 10.1007/BF02635868. URL http://dx.doi.org/10.1007/BF02635868.

[4] Victoria Klang, Nadejda Matsko, Karoline Raupach, Nivine El-Hagin, and Claudia Valenta. Development of sucrose stearate-based nanoemulsions and optimisation through gamma-cyclodextrin. *European Journal of Pharmaceutics and Biopharmaceutics*, 79(1):58 – 67, 2011. ISSN 0939-6411. doi: http://dx.doi.org/10.1016/j.ejpb.2011.01.010. URL http://www.sciencedirect.com/science/article/pii/S0939641111000178. New facets of nanopharmaceutics.

[5] Augusta Obikili, Michel Deyme, Denis Wouessidjewe, and Dominique Duchene. Improvement of aqueous solubility and dissolution kinetics of canrenone by solid dispersion in sucroester. *Drug Development and Industrial Pharmacy*, 14(6):791–803, 1988. doi: 10.3109/03639048809151901. URL http://www.tandfonline.com/doi/abs/10.3109/03639048809151901.

[6] P.C. Lerk and H. Sucker. Application of sucrose laurate, a new pharmaceutical excipient, in peroral formulations of cyclosporin a. *International Journal of Pharmaceutics*, 92(1 - 3):197 – 202, 1993. ISSN 0378-5173. doi: http://dx.doi.org/10.1016/0378-5173(93)90280-S. URL `http://www.sciencedirect.com/science/article/pii/037851739390280S`.

[7] P.C. Lerk and H. Sucker. Application of sucrose laurate in topical preparations of cyclosporin a. *International Journal of Pharmaceutics*, 92(1–3):203 – 210, 1993. ISSN 0378-5173. doi: http://dx.doi.org/10.1016/0378-5173(93)90281-J. URL `http://www.sciencedirect.com/science/article/pii/037851739390281J`.

[8] An Vermeire, Christian De Muynck, Geert Vandenbossche, and Eechaute. Sucrose laurate gels as a percutaneous delivery system for oestradiol in rabbits. *Journal of Pharmacy and Pharmacology*, 48(5):463–467, 1996. ISSN 2042-7158. doi: 10.1111/j.2042-7158.1996.tb05955.x. URL `http://dx.doi.org/10.1111/j.2042-7158.1996.tb05955.x`.

[9] Hilda A. Ayala-Bravo, David Quintanar-Guerrero, Aarti Naik, YogeshvarN. Kalia, JoséM. Cornejo-Bravo, and Adriana Ganem-Quintanar. Effects of sucrose oleate and sucrose laureate on in vivo human stratum corneum permeability. *Pharmaceutical Research*, 20(8):1267–1273, 2003. ISSN 0724-8741. doi: 10.1023/A:1025013401471. URL `http://dx.doi.org/10.1023/A%3A1025013401471`.

[10] Hirokazu Okamoto, Takashi Sakai, and Kazumi Danjo. Effect of sucrose fatty acid esters on transdermal permeation of lidocaine and ketoprofen. *Biological and Pharmaceutical Bulletin*, 28(9):1689–1694, 2005. doi: 10.1248/bpb.28.1689.

[11] G. Csóka, S. Marton, R. Zelko, N. Otomo, and I. Antal. Application of sucrose fatty acid esters in transdermal therapeutic systems. *European Journal of Pharmaceutics and Biopharmaceutics*, 65(2):233 – 237, 2007. ISSN 0939-6411. doi: http://dx.doi.org/10.1016/j.ejpb.2006.07.009. URL `http://www.sciencedirect.com/science/article/pii/S0939641106001937`.

[12] E. Csizmazia, G. Erős, O. Berkesi, S. Berkó, P. Szabó-Révész, and E. Csányi. Pénétration enhancer effect of sucrose laurate and transcutol on ibuprofen. *Journal of Drug Delivery Science and Technology*, 21(5):411 – 415, 2011. ISSN 1773-2247. doi: http://dx.doi.org/10.1016/S1773-2247(11)50066-8. URL `http://www.sciencedirect.com/science/article/pii/S1773224711500668`.

[13] J.W. Daniel, C.J. Marshall, H.F. Jones, and D.J. Snodin. The metabolism of beef tallow sucrose esters in rat and man. *Food and Cosmetics Toxicology*, 17(1):19 – 21, 1979. ISSN 0015-6264. doi: http://dx.doi.org/10.

1016/0015-6264(79)90153-6. URL http://www.sciencedirect.com/science/article/pii/0015626479901536.

[14] T. Shigeoka, O. Izawa, K. Kitazawa, F. Yamauchi, and T. Murata. Studies on the metabolic fate of sucrose esters in rats. *Food and Chemical Toxicology*, 22(6):409 – 414, 1984. ISSN 0278-6915. doi: http://dx.doi.org/10.1016/0278-6915(84)90321-1. URL http://www.sciencedirect.com/science/article/pii/0278691584903211.

[15] P.E. Noker, T.-H. Lin, D.L. Hill, and T. Shigeoka. Metabolism of 14c-labelled sucrose esters of stearic acid in rats. *Food and Chemical Toxicology*, 35(6):589 – 595, 1997. ISSN 0278-6915. doi: http://dx.doi.org/10.1016/S0278-6915(97)00012-4. URL http://www.sciencedirect.com/science/article/pii/S0278691597000124.

[16] K. Takeda and M. Flood. Chronic toxicity and carcinogenicity of sucrose fatty acid esters in fischer 344/ducrj rats. *Regulatory Toxicology and Pharmacology*, 35(2):157 – 164, 2002. ISSN 0273-2300. doi: http://dx.doi.org/10.1006/rtph.2001.1502. URL http://www.sciencedirect.com/science/article/pii/S0273230001915028.

[17] Jacob N. Israelachvili and D.John Mitchell. A model for the packing of lipids in bilayer membranes. *Biochimica et Biophysica Acta (BBA) - Biomembranes*, 389(1):13 – 19, 1975. ISSN 0005-2736. doi: http://dx.doi.org/10.1016/0005-2736(75)90381-8. URL http://www.sciencedirect.com/science/article/pii/0005273675903818.

[18] Jacob N. Israelachvili, D.John Mitchell, and Barry W. Ninham. Theory of self-assembly of lipid bilayers and vesicles. *Biochimica et Biophysica Acta (BBA) - Biomembranes*, 470(2):185 – 201, 1977. ISSN 0005-2736. doi: http://dx.doi.org/10.1016/0005-2736(77)90099-2. URL http://www.sciencedirect.com/science/article/pii/0005273677900992.

[19] J. Th. G. Overbeek. The first rideal lecture. microemulsions, a field at the border between lyophobic and lyophilic colloids. *Faraday Discuss. Chem. Soc.*, 65: 7–19, 1978. doi: 10.1039/DC9786500007. URL http://dx.doi.org/10.1039/DC9786500007.

[20] G.W.J. Lee and Th.F. Tadros. Formation and stability of emulsions produced by dilution of emulsifiable concentrates. part ii. the influence of surfactant concentration on the stability of oil-in-water emulsions. *Colloids and Surfaces*, 5(2):117 – 127, 1982. ISSN 0166-6622. doi: http://dx.doi.org/10.1016/0166-6622(82)80067-X. URL http://www.sciencedirect.com/science/article/pii/016666228280067X.

[21] Hironobu Kunieda and Kozo Shinoda. Solution behavior and hydrophile-lipophile balance temperature in the aerosol ot-isooctane-brine system: Correlation between microemulsions and ultralow interfacial tensions. *Journal of Colloid and Interface Science*, 75(2):601 – 606, 1980. ISSN 0021-9797. doi: http://dx.doi.org/10.1016/0021-9797(80)90482-8. URL `http://www.sciencedirect.com/science/article/pii/0021979780904828`.

[22] M. Kahlweit, R. Strey, D. Haase, H. Kunieda, T. Schmeling, B. Faulhaber, M. Borkovec, H.-F. Eicke, G. Busse, F. Eggers, Th. Funck, H. Richmann, L. Magid, O. Söderman, P. Stilbs, J. Winkler, A. Dittrich, and W. Jahn. How to study microemulsions. *Journal of Colloid and Interface Science*, 118(2):436 – 453, 1987. ISSN 0021-9797. doi: http://dx.doi.org/10.1016/0021-9797(87)90480-2. URL `http://www.sciencedirect.com/science/article/pii/0021979787904802`.

[23] P. A. Winsor. Hydrotropy, solubilisation and related emulsification processes. *Trans. Faraday Soc.*, 44:376–398, 1948. doi: 10.1039/TF9484400376. URL `http://dx.doi.org/10.1039/TF9484400376`.

[24] Wilder D. Bancroft. The theory of emulsification, v. *The Journal of Physical Chemistry*, 17(6):501–519, 1912. doi: 10.1021/j150141a002. URL `http://dx.doi.org/10.1021/j150141a002`.

[25] G. H. A. Clowes. Protoplasmic equilibrium. *The Journal of Physical Chemistry*, 20(5):407–451, 1915. doi: 10.1021/j150167a004. URL `http://dx.doi.org/10.1021/j150167a004`.

[26] Terence Cosgrove. *Colloid science: principles, methods and applications*. John Wiley & Sons, 2010.

[27] Paul Becher. Microemulsions and related systems: Formulation, solvency, and physical properties (surfactant science series, vol. 30). m. bourrel and r. s. schechter. marcel dekker, inc., new york and basel, 1988. pp. nil + 483. *Journal of Dispersion Science and Technology*, 11(4):431–432, 1990. doi: 10.1080/01932699008943264. URL `http://dx.doi.org/10.1080/01932699008943264`.

[28] K.J Lissant. The geometry of high-internal-phase-ratio emulsions. *Journal of Colloid and Interface Science*, 22(5):462 – 468, 1966. ISSN 0021-9797. doi: http://dx.doi.org/10.1016/0021-9797(66)90091-9. URL `http://www.sciencedirect.com/science/article/pii/0021979766900919`.

[29] K.J Lissant, B.W Peace, S.H Wu, and K.G Mayhan. Proceedings of the 47th national colloid symposium acs division of colloid and surface chemistry structure of high-internal-phase-ratio emulsions. *Journal of Colloid and Interface*

Science, 47(2):416 – 423, 1974. ISSN 0021-9797. doi: http://dx.doi.org/10.1016/0021-9797(74)90273-2. URL `http://www.sciencedirect.com/science/article/pii/0021979774902732`.

[30] H. Kunieda, C. Solans, N. Shida, and J.L. Parra. The formation of gel-emulsions in a water/nonionic surfactant/oil system. *Colloids and Surfaces*, 24(2–3):225 – 237, 1987. ISSN 0166-6622. doi: http://dx.doi.org/10.1016/0166-6622(87)80352-9. URL `http://www.sciencedirect.com/science/article/pii/0166662287803529`.

[31] C. Solans, J.G. Dominguez, J.L. Parra, J. Heuser, and S.E. Friberg. Gelled emulsions with a high water content. *Colloid and Polymer Science*, 266(6):570–574, 1988. ISSN 0303-402X. doi: 10.1007/BF01420770. URL `http://dx.doi.org/10.1007/BF01420770`.

[32] Bernard P Binks. *Modern aspects of emulsion science*. Royal Society of Chemistry, 1998.

[33] C Solans, R Pons, S Zhu, HT Davis, DF Evans, K Nakamura, and H Kunieda. Studies on macro-and microstructures of highly concentrated water-in-oil emulsions (gel emulsions). *Langmuir*, 9(6):1479–1482, 1993.

[34] Hironobu Kunieda, Md Hemayet Uddin, Makiko Horii, Haruhiko Furukawa, and Asao Harashima. Effect of hydrophilic-and hydrophobic-chain lengths on the phase behavior of ab-type silicone surfactants in water. *The Journal of Physical Chemistry B*, 105(23):5419–5426, 2001.

[35] Susana Vilchez, Lourdes A Perez-Carrillo, Jonathan Miras, Conxita Solans, and Jordi Esquena. Oil-in-alcohol highly concentrated emulsions as templates for the preparation of macroporous materials. *Langmuir*, 28(20):7614–7621, 2012.

[36] HM Princen. Rheology of foams and highly concentrated emulsions: I. elastic properties and yield stress of a cylindrical model system. *Journal of Colloid and interface science*, 91(1):160–175, 1983.

[37] HM Princen and AD Kiss. Rheology of foams and highly concentrated emulsions: Iii. static shear modulus. *Journal of Colloid and Interface Science*, 112(2):427–437, 1986.

[38] Ramon Pons, Pilar Erra, Concepcion Solans, Jean Claude Ravey, and Marie Jose Stebe. Viscoelastic properties of gel-emulsions: their relationship with structure and equilibrium properties. *The Journal of Physical Chemistry*, 97(47):12320–12324, 1993.

[39] Kazuyo Ozawa, Conxita Solans, and Hironobu Kunieda. Spontaneous formation of highly concentrated oil-in-water emulsions. *Journal of colloid and interface science*, 188(2):275–281, 1997.

[40] Gordon JT Tiddy. Surfactant-water liquid crystal phases. *Physics reports*, 57(1): 1–46, 1980.

[41] Thomas Kaasgaard and Calum J. Drummond. Ordered 2-d and 3-d nanostructured amphiphile self-assembly materials stable in excess solvent. *Phys. Chem. Chem. Phys.*, 8:4957–4975, 2006. doi: 10.1039/B609510K. URL `http://dx.doi.org/10.1039/B609510K`.

[42] Jaymin C Shah, Yogesh Sadhale, and Dakshina Murthy Chilukuri. Cubic phase gels as drug delivery systems. *Advanced drug delivery reviews*, 47(2):229–250, 2001.

[43] Kiran Kumar, Manish H Shah, Anant Ketkar, KR Mahadik, and Anant Paradkar. Effect of drug solubility and different excipients on floating behaviour and release from glyceryl monooleate matrices. *International journal of pharmaceutics*, 272 (1):151–160, 2004.

[44] Shui-Mei Khoo, Benjamin Boyd, Darryl Whittaker, Gregory Davey, Calum Drummond, Annette Murphy, and Russell Tait. Compositions and methods for delivery of biologically active agents, September 1 2004. US Patent App. 10/569,948.

[45] Tri-Hung Nguyen, Tracey Hanley, Christopher J.H. Porter, and Ben J. Boyd. Nanostructured liquid crystalline particles provide long duration sustained-release effect for a poorly water soluble drug after oral administration. *Journal of Controlled Release*, 153(2):180 – 186, 2011. ISSN 0168-3659. doi: http://dx.doi.org/10.1016/j.jconrel.2011.03.033. URL `http://www.sciencedirect.com/science/article/pii/S0168365911002173`.

[46] Calum J Drummond and Celesta Fong. Surfactant self-assembly objects as novel drug delivery vehicles. *Current opinion in colloid & interface science*, 4(6):449–456, 1999.

[47] Wye-Khay Fong, Tracey Hanley, and Ben J Boyd. Stimuli responsive liquid crystals provide 'on-demand'drug delivery in vitro and in vivo. *Journal of Controlled Release*, 135(3):218–226, 2009.

[48] James Swarbrick and JamesR. Siverly. The influence of liquid crystalline phases on drug percutaneous absorption. ii. permeation studies through excised human skin. *Pharmaceutical Research*, 9(12):1550–1555, 1992. ISSN 0724-8741. doi: 10.1023/A:1015852022343. URL `http://dx.doi.org/10.1023/A%3A1015852022343`.

[49] Christopher A Lipinski. Lead-and drug-like compounds: the rule-of-five revolution. *Drug Discovery Today: Technologies*, 1(4):337–341, 2004.

[50] Bhupinder Singh, Shantanu Bandopadhyay, Rishi Kapil, Ramandeep Singh, and Om Parkash Katare. Self-emulsifying drug delivery systems (sedds): formulation development, characterization, and applications. *Critical Reviews™ in Therapeutic Drug Carrier Systems*, 26(5), 2009.

[51] Colin W Pouton. Lipid formulations for oral administration of drugs: non-emulsifying, self-emulsifying and 'self-microemulsifying'drug delivery systems. *European Journal of Pharmaceutical Sciences*, 11:S93–S98, 2000.

[52] Colin W Pouton and Christopher JH Porter. Formulation of lipid-based delivery systems for oral administration: materials, methods and strategies. *Advanced Drug Delivery Reviews*, 60(6):625–637, 2008.

[53] Kanchan Kohli, Sunny Chopra, Deepika Dhar, Saurabh Arora, and Roop K Khar. Self-emulsifying drug delivery systems: an approach to enhance oral bioavailability. *Drug Discovery Today*, 15(21):958–965, 2010.

[54] Colin W Pouton. Formulation of poorly water-soluble drugs for oral administration: physicochemical and physiological issues and the lipid formulation classification system. *European Journal of Pharmaceutical Sciences*, 29(3):278–287, 2006.

[55] M.A. Thevenin, J.L. Grossiord, and M.C. Poelman. Sucrose esters/cosurfactant microemulsion systems for transdermal delivery: Assessment of bicontinuous structures. *International Journal of Pharmaceutics*, 137(2):177 – 186, 1996. ISSN 0378-5173. doi: http://dx.doi.org/10.1016/0378-5173(96)04518-8. URL `http://www.sciencedirect.com/science/article/pii/0378517396045188`.

[56] N. Garti, V. Clement, M. Leser, A. Aserin, and M. Fanun. Sucrose ester microemulsions. *Journal of Molecular Liquids*, 80(2 - 3):253 – 296, 1999. ISSN 0167-7322. doi: http://dx.doi.org/10.1016/S0167-7322(99)80010-5. URL `http://www.sciencedirect.com/science/article/pii/S0167732299800105`.

[57] N. Garti, V. Clement, M. Leser, A. Aserin, and M. Fanun. Sucrose ester microemulsions. *Journal of Molecular Liquids*, 80(2-3):253 – 296, 1999. ISSN 0167-7322. doi: http://dx.doi.org/10.1016/S0167-7322(99)80010-5. URL `http://www.sciencedirect.com/science/article/pii/S0167732299800105`.

[58] S. Ezrahi, E. Tuval, A. Aserin, and N. Garti. The effect of structural variation of alcohols on water solubilization in nonionic microemulsions: 1. from linear to

branched amphiphiles—general considerations. *Journal of Colloid and Interface Science*, 291(1):263 – 272, 2005. ISSN 0021-9797. doi: http://dx.doi.org/10.1016/j.jcis.2005.04.097. URL `http://www.sciencedirect.com/science/article/pii/S0021979705004911`.

[59] Arthur A Noyes and Willis R Whitney. The rate of solution of solid substances in their own solutions. *Journal of the American Chemical Society*, 19(12):930–934, 1897.

[60] Pirjo Mattila and Jorma Kumpulainen. Coenzymes q 9 and q 10: Contents in foods and dietary intake. *Journal of Food Composition and Analysis*, 14(4):409–417, 2001.

[61] R.W. Purchas, J.R. Busboom, and B.H.P. Wilkinson. Changes in the forms of iron and in concentrations of taurine, carnosine, coenzyme q10, and creatine in beef longissimus muscle with cooking and simulated stomach and duodenal digestion. *Meat Science*, 74(3):443 – 449, 2006. ISSN 0309-1740. doi: http://dx.doi.org/10.1016/j.meatsci.2006.03.015. URL `http://www.sciencedirect.com/science/article/pii/S030917400600088X`.

[62] Hemmi N Bhagavan and Raj K Chopra. Plasma coenzyme q10 response to oral ingestion of coenzyme q10 formulations. *Mitochondrion*, 7:S78–S88, 2007.

[63] Xuyi Gao, Katsunori Nishimura, Fumitoshi Hirayama, H Arima, K Uekama, G Schmid, K Terao, D Nakata, and H Fukumi. Enhanced dissolution and oral bioavailability of coenzyme q10 in dogs obtained by inclusion complexation with γ-cyclodextrin. *Asian J. Pharm. Sci*, 1(2):95–102, 2006.

[64] Keiji Terao, Daisuke Nakata, Hiroshi Fukumi, Gerhard Schmid, Hidetoshi Arima, Fumitoshi Hirayama, and Kaneto Uekama. Enhancement of oral bioavailability of coenzyme q 10 by complexation with γ-cyclodextrin in healthy adults. *Nutrition Research*, 26(10):503–508, 2006.

[65] F. Carli, E.E. Chiellini, B. Bellich, S. Macchiavelli, and G. Cadelli. Ubidecarenone nanoemulsified composite systems. *International Journal of Pharmaceutics*, 291(1–2):113 – 118, 2005. ISSN 0378-5173. doi: http://dx.doi.org/10.1016/j.ijpharm.2004.07.048. URL `http://www.sciencedirect.com/science/article/pii/S0378517304006593`. Proceedings of the 5th Central European Symposium on Pharmaceutical Technology and BiotechnologyProceedings of the 5th Central European Symposium on Pharmaceutical Technology and Biotechnology.

[66] TR Kommuru, B Gurley, MA Khan, and IK Reddy. Self-emulsifying drug delivery systems (sedds) of coenzyme q 10: formulation development and bioavailability assessment. *International journal of pharmaceutics*, 212(2):233–246, 2001.

[67] Shuqin Xia, Shiying Xu, and Xiaoming Zhang. Optimization in the preparation of coenzyme q10 nanoliposomes. *Journal of agricultural and food chemistry*, 54(17): 6358–6366, 2006.

[68] Bret C Vastano, Yong Chen, Nanqun Zhu, Chi-Tang Ho, Zhengyi Zhou, and Robert T Rosen. Isolation and identification of stilbenes in two varieties of polygonum c uspidatum. *Journal of agricultural and food chemistry*, 48(2):253–256, 2000.

[69] Samarjit Das and Dipak K Das. Resveratrol: a therapeutic promise for cardiovascular diseases. *Recent Patents on Cardiovascular Drug Discovery*, 2(2):133–138, 2007.

[70] Li-Man Hung, Ming-Jai Su, and Jan-Kan Chen. Resveratrol protects myocardial ischemia-reperfusion injury through both no-dependent and no-independent mechanisms. *Free Radical Biology and Medicine*, 36(6):774–781, 2004.

[71] Meishiang Jang, Lining Cai, George O Udeani, Karla V Slowing, Cathy F Thomas, Christopher WW Beecher, Harry HS Fong, Norman R Farnsworth, A Douglas Kinghorn, Rajendra G Mehta, et al. Cancer chemopreventive activity of resveratrol, a natural product derived from grapes. *Science*, 275(5297):218–220, 1997.

[72] Konrad T Howitz, Kevin J Bitterman, Haim Y Cohen, Dudley W Lamming, Siva Lavu, Jason G Wood, Robert E Zipkin, Phuong Chung, Anne Kisielewski, Li-Li Zhang, et al. Small molecule activators of sirtuins extend saccharomyces cerevisiae lifespan. *Nature*, 425(6954):191–196, 2003.

[73] Dario R. Valenzano, Eva Terzibasi, Tyrone Genade, Antonino Cattaneo, Luciano Domenici, and Alessandro Cellerino. Resveratrol prolongs lifespan and retards the onset of age-related markers in a short-lived vertebrate. *Current Biology*, 16(3):296 – 300, 2006. ISSN 0960-9822. doi: http://dx.doi.org/10.1016/j.cub.2005.12.038. URL `http://www.sciencedirect.com/science/article/pii/S0960982206010207`.

[74] Joseph A Baur and David A Sinclair. Therapeutic potential of resveratrol: the in vivo evidence. *Nature reviews Drug discovery*, 5(6):493–506, 2006.

[75] Robert E King, Kyle D Kent, and Joshua A Bomser. Resveratrol reduces oxidation and proliferation of human retinal pigment epithelial cells via extracellular signal-regulated kinase inhibition. *Chemico-biological interactions*, 151(2):143–149, 2005.

[76] Leonid Buryanovskyy, Yue Fu, Molly Boyd, Yuliang Ma, Tze-chen Hsieh, Joseph M Wu, and Zhongtao Zhang. Crystal structure of quinone reductase 2 in complex with resveratrol. *Biochemistry*, 43(36):11417–11426, 2004.

[77] Andrea Lisa Holme and Shazib Pervaiz. Resveratrol in cell fate decisions. *Journal of bioenergetics and biomembranes*, 39(1):59–63, 2007.

[78] Ludovic Le Corre, Pierre Fustier, Nasséra Chalabi, Yves-Jean Bignon, and Dominique Bernard-Gallon. Effects of resveratrol on the expression of a panel of genes interacting with the {BRCA1} oncosuppressor in human breast cell lines. *Clinica Chimica Acta*, 344(1–2):115 – 121, 2004. ISSN 0009-8981. doi: http://dx.doi.org/10.1016/j.cccn.2004.02.024. URL `http://www.sciencedirect.com/science/article/pii/S0009898104000919`.

[79] Vaqar Mustafa Adhami, Farrukh Afaq, and Nihal Ahmad. Suppression of ultraviolet b exposure-mediated activation of nf-kb in normal human keratinocytes by resveratrol. *Neoplasia*, 5(1):74 – 82, 2003. ISSN 1476-5586. doi: http://dx.doi.org/10.1016/S1476-5586(03)80019-2. URL `http://www.sciencedirect.com/science/article/pii/S1476558603800192`.

[80] S. Reagan-Shaw, F. Afaq, M. H. Aziz, and N. Ahmad. Modulations of critical cell cycle regulatory events during chemoprevention of ultraviolet B-mediated responses by resveratrol in SKH-1 hairless mouse skin. *Oncogene*, 23(30):5151–5160, Jul 2004.

[81] M. H. Aziz, S. Reagan-Shaw, J. Wu, B. J. Longley, and N. Ahmad. Chemoprevention of skin cancer by grape constituent resveratrol: relevance to human disease? *FASEB J.*, 19(9):1193–1195, Jul 2005.

[82] H. C. Polonini, L. L. Lima, K. M. Goncalves, A. M. do Carmo, A. D. da Silva, and N. R. Raposo. Photoprotective activity of resveratrol analogues. *Bioorg. Med. Chem.*, 21(4):964–968, Feb 2013.

[83] Y. Wu, L. L. Jia, Y. N. Zheng, X. G. Xu, Y. J. Luo, B. Wang, J. Z. Chen, X. H. Gao, H. D. Chen, M. Matsui, and Y. H. Li. Resveratrol protects human skin from damage due to repetitive ultraviolet irradiation. *J Eur Acad Dermatol Venereol*, 27(3):345–350, Mar 2013.

[84] D. Buonocore, A. Lazzeretti, P. Tocabens, V. Nobile, E. Cestone, G. Santin, M. G. Bottone, and F. Marzatico. Resveratrol-procyanidin blend: nutraceutical and antiaging efficacy evaluated in a placebocontrolled, double-blind study. *Clin Cosmet Investig Dermatol*, 5:159–165, 2012.

[85] S. Bastianetto, Y. Dumont, A. Duranton, F. Vercauteren, L. Breton, and R. Quirion. Protective action of resveratrol in human skin: possible involvement of specific receptor binding sites. *PLoS ONE*, 5(9):e12935, 2010.

[86] G. Fabbrocini, S. Staibano, G. De Rosa, V. Battimiello, N. Fardella, G. Ilardi, M. I. La Rotonda, A. Longobardi, M. Mazzella, M. Siano, F. Pastore, V. De Vita, M. L. Vecchione, and F. Ayala. Resveratrol-containing gel for the treatment of acne vulgaris: a single-blind, vehicle-controlled, pilot study. *Am J Clin Dermatol*, 12(2):133–141, Apr 2011.

[87] G.A. Lewis, D. Mathieu, and R. Phan-Tan-Luu. *Pharmaceutical Experimental Design*. Drugs and the Pharmaceutical Sciences. CRC Press, 1998. ISBN 9780824746889. URL `https://books.google.it/books?id=jqFZOyBtS98C`.

[88] R Cela, R Phan-Tan-Luu, and M Claeys-Bruno. Screening strategies. In *Comprehensive Chemometrics*, volume 1, page 251. Elsevier Amsterdam, 2009.

[89] R. Tauler and S.D. Brown. *Comprehensive Chemometrics: Chemical and Biochemical Data Analysis*. Elsevier Science, 2009. ISBN 9780444527011. URL `https://books.google.it/books?id=KQYKYcSHCG8C`.

[90] J.A. Cornell. *Experiments with Mixtures: Designs, Models, and the Analysis of Mixture Data*. Wiley Series in Probability and Statistics. Wiley, 2011. ISBN 9781118150498. URL `https://books.google.it/books?id=piWpe3yEAjYC`.

[91] L Sagalowicz, ME Leser, HJ Watzke, and M Michel. Monoglyceride self-assembly structures as delivery vehicles. *Trends in Food Science & Technology*, 17(5):204–214, 2006.

[92] Costas Demetzos. Differential scanning calorimetry (dsc): a tool to study the thermal behavior of lipid bilayers and liposomal stability. *Journal of liposome research*, 18(3):159–173, 2008.

[93] N. Becerra, C. Toro, A.L. Zanocco, E. Lemp, and G. Günther. Characterization of micelles formed by sucrose 6-o-monoesters. *Colloids and Surfaces A: Physicochemical and Engineering Aspects*, 327(1-3):134 – 139, 2008. ISSN 0927-7757. doi: http://dx.doi.org/10.1016/j.colsurfa.2008.06.012. URL `http://www.sciencedirect.com/science/article/pii/S092777570800410X`.

[94] Gorgias Garofalakis, Brent S. Murray, and Douglas B. Sarney. Surface activity and critical aggregation concentration of pure sugar esters with different sugar headgroups. *Journal of Colloid and Interface Science*, 229(2):391 – 398, 2000. ISSN 0021-9797. doi: http://dx.doi.org/10.1006/jcis.2000.7035. URL `http://www.sciencedirect.com/science/article/pii/S0021979700970358`.

[95] BP Binks, PDI Fletcher, and L Tian. Influence of nanoparticle addition to winsor surfactant microemulsion systems. *Colloids and Surfaces A: Physicochemical and Engineering Aspects*, 363(1):8–15, 2010.

[96] Richard W áO'Brien et al. Electroacoustic studies of moderately concentrated colloidal suspensions. *Faraday Discussions of the Chemical Society*, 90:301–312, 1990.

[97] Dorian Hanaor, Marco Michelazzi, Cristina Leonelli, and Charles C. Sorrell. The effects of carboxylic acids on the aqueous dispersion and electrophoretic deposition of zro2. *Journal of the European Ceramic Society*, 32(1):235 – 244, 2012. ISSN 0955-2219. doi: http://dx.doi.org/10.1016/j.jeurceramsoc.2011.08.015. URL `http://www.sciencedirect.com/science/article/pii/S0955221911004171`.

[98] Min-Jeong Park, Prabagar Balakrishnan, and Su-Geun Yang. Polymeric nanocapsules with {SEDDS} oil-core for the controlled and enhanced oral absorption of cyclosporine. *International Journal of Pharmaceutics*, 441(1–2):757 – 764, 2013. ISSN 0378-5173. doi: http://dx.doi.org/10.1016/j.ijpharm.2012.10.018. URL `http://www.sciencedirect.com/science/article/pii/S0378517312009581`.

[99] Fei Li, Shuangshuang Song, Yingxin Guo, Qianqian Zhao, Xuemei Zhang, Weisan Pan, and Xinggang Yang. Preparation and pharmacokinetics evaluation of oral self-emulsifying system for poorly water-soluble drug lornoxicam. *Drug Delivery*, 22(4):487–498, 2015. doi: 10.3109/10717544.2014.885615. URL `http://dx.doi.org/10.3109/10717544.2014.885615`. PMID: 24524289.

[100] Martine Armand, Bérengère Pasquier, Marc André, Patrick Borel, Michèle Senft, Jacques Peyrot, Jacques Salducci, Henri Portugal, Véronique Jaussan, and Denis Lairon. Digestion and absorption of 2 fat emulsions with different droplet sizes in the human digestive tract. *The American journal of clinical nutrition*, 70(6): 1096–1106, 1999.

[101] Robert A. Myers and Valentino J. Stella. Systemic bioavailability of penclomedine (nsc-338720) from oil-in-water emulsions administered intraduodenally to rats. *International Journal of Pharmaceutics*, 78(1):217 – 226, 1992. ISSN 0378-5173. doi: http://dx.doi.org/10.1016/0378-5173(92)90374-B. URL `http://www.sciencedirect.com/science/article/pii/037851739290374B`.

[102] Tugrul T Kararli, Thomas E Needham, Marty Griffin, Grant Schoenhard, Leonard J Ferro, and Lisa Alcorn. Oral delivery of a renin inhibitor compound using emulsion formulations. *Pharmaceutical research*, 9(7):888–893, 1992.

[103] M. Jayne Lawrence and Gareth D. Rees. Microemulsion-based media as novel drug delivery systems. *Advanced Drug Delivery Reviews*, 64(0):175 – 193, 2012. ISSN 0169-409X. doi: http://dx.doi.org/10.1016/j.addr.2012.09.018. URL `http://www.sciencedirect.com/science/article/pii/S0169409X12002785`.

[104] Romano Lapasin. *Rheology of industrial polysaccharides: theory and applications*. Springer Science & Business Media, 2012.

[105] Irma Rosalina and Mrinal Bhattacharya. Dynamic rheological measurements and analysis of starch gels. *Carbohydrate Polymers*, 48(2):191–202, 2002.

[106] Robert P Walton. Absorption of drugs through the oral mucosa. ii. *Experimental Biology and Medicine*, 32(9):1486–1488, 1935.

[107] Yuji Kurosaki, Toshihito Takatori, Hidekatsu Nishimura, Taiji Nakayama, and Toshikiro Kimura. Regional variation in oral mucosal drug absorption: permeability and degree of keratinization in hamster oral cavity. *Pharmaceutical research*, 8(10):1297–1301, 1991.

[108] M David Richman, C David Fox, and Ralph F Shangraw. Preparation and stability of glyceryl trinitrate sublingual tablets prepared by direct compression. *Journal of pharmaceutical sciences*, 54(3):447–451, 1965.

[109] Neha Narang and Jyoti Sharma. Sublingual mucosa as a route for systemic drug delivery. *Int J Pharm Pharm Sci*, 3(Suppl 2):18–22, 2011.

[110] Lester Sultatos. Drug absorption from the gastrointestinal tract. In S.J. Enna and David B. Bylund, editors, *xPharm: The Comprehensive Pharmacology Reference*, pages 1 – 2. Elsevier, New York, 2007. ISBN 978-0-08-055232-3. doi: http://dx.doi.org/10.1016/B978-008055232-3.60021-2. URL `http://www.sciencedirect.com/science/article/pii/B9780080552323600212`.

[111] Heba A. Hazzah, Ragwa M. Farid, Maha M.A. Nasra, Magda A. EL-Massik, and Ossama Y. Abdallah. Lyophilized sponges loaded with curcumin solid lipid nanoparticles for buccal delivery: Development and characterization. *International Journal of Pharmaceutics*, 492(1–2):248 – 257, 2015. ISSN 0378-5173. doi: http://dx.doi.org/10.1016/j.ijpharm.2015.06.022. URL `http://www.sciencedirect.com/science/article/pii/S0378517315005426`.

[112] Joshua S. Boateng and Isaac Ayensu. Preparation and characterization of laminated thiolated chitosan-based freeze-dried wafers for potential buccal delivery of macromolecules. *Drug Development and Industrial Pharmacy*, 40(5):611–618, 2014. doi: 10.3109/03639045.2014.884126. URL `http://www.tandfonline.com/doi/abs/10.3109/03639045.2014.884126`. PMID: 24506457.

[113] Peng Liu, Odile De Wulf, Johanna Laru, Teemu Heikkilä, Bert van Veen, Juha Kiesvaara, Jouni Hirvonen, Leena Peltonen, and Timo Laaksonen. Dissolution studies of poorly soluble drug nanosuspensions in non-sink conditions. *AAPS PharmSciTech*, 14(2):748–756, 2013.

[114] Sami Nazzal, Necip Guven, Indra K. Reddy, and Mansoor A. Khan. Preparation and characterization of coenzyme q10 eudragit solid dispersion. *Drug Development and Industrial Pharmacy*, 28(1):49–57, 2002. doi: 10.1081/DDC-120001485. URL `http://informahealthcare.com/doi/abs/10.1081/DDC-120001485`. PMID: 11858524.

[115] Maria Careri, Claudio Corradini, Lisa Elviri, Isabella Nicoletti, and Ingrid Zagnoni. Direct hplc analysis of quercetin and trans-resveratrol in red wine, grape, and winemaking byproducts. *Journal of Agricultural and Food Chemistry*, 51(18): 5226–5231, 2003. doi: 10.1021/jf034149g. URL `http://dx.doi.org/10.1021/jf034149g`. PMID: 12926863.

[116] Romano Colombo Mario Grassi, Gabriele Lapasin. *Understanding drug release and absorption mechanisms: a physical and mathematical approach*. CRC Press, 2006.

[117] Christopher JH Porter and William N Charman. In vitro assessment of oral lipid based formulations. *Advanced Drug Delivery Reviews*, 50:S127–S147, 2001.

[118] Jennifer B Dressman, Gordon L Amidon, Christos Reppas, and Vinod P Shah. Dissolution testing as a prognostic tool for oral drug absorption: immediate release dosage forms. *Pharmaceutical research*, 15(1):11–22, 1998.

[119] European Directorate for the Quality of Medicines, European Pharmacopoeia Commission, et al. *European pharmacopoeia*. Council of Europe, 2009.

[120] Martin Siewert, Jennifer Dressman, Cynthia K Brown, Vinod P Shah, Jean-Marc Aiache, Nobuo Aoyagi, Dennis Bashaw, Cynthia Brown, William Brown, Diane Burgess, et al. Fip/aaps guidelines to dissolution/in vitro release testing of novel-/special dosage forms. *AAPS PharmSciTech*, 4(1):43–52, 2003.

[121] Delia L Bernik, Diana Zubiri, María Eugenia Monge, and R Martín Negri. New kinetic model of drug release from swollen gels under non-sink conditions. *Colloids and Surfaces A: Physicochemical and Engineering Aspects*, 273(1):165–173, 2006.

[122] Marc B. Brown, Gary P. Martin, Stuart A. Jones, and Franklin K. Akomeah. Dermal and transdermal drug delivery systems: Current and future prospects. *Drug Delivery*, 13(3):175–187, 2006. doi: 10.1080/10717540500455975.

URL http://informahealthcare.com/doi/abs/10.1080/10717540500455975. PMID: 16556569.

[123] Jonathan Hadgraft. Skin deep. *European Journal of Pharmaceutics and Biopharmaceutics*, 58(2):291 – 299, 2004. ISSN 0939-6411. doi: http://dx.doi.org/10.1016/j.ejpb.2004.03.002. URL http://www.sciencedirect.com/science/article/pii/S093964110400044X. The International Association of Pharmaceutical Technology (APV).

[124] Gopinathan K Menon. New insights into skin structure: scratching the surface. *Advanced Drug Delivery Reviews*, 54, Supplement:S3 – S17, 2002. ISSN 0169-409X. doi: http://dx.doi.org/10.1016/S0169-409X(02)00121-7. URL http://www.sciencedirect.com/science/article/pii/S0169409X02001217. Human skin: the Medium of Touch.

[125] Barry B.W. *Dermatological Formulations: Percutaneous Absorption*, volume 18. Marcel Dekker New York, 1983.

[126] David W. Osborne. Review of changes in topical drug product classification. *Pharmaceutical Technology*, 32(10), 2008. URL http://www.pharmtech.com/review-changes-topical-drug-product-classification.

[127] Lucinda Buhse, Richard Kolinski, Benjamin Westenberger, Anna Wokovich, John Spencer, Chi Wan Chen, Saleh Turujman, Mamta Gautam-Basak, Gil Jong Kang, Arthur Kibbe, Brian Heintzelman, and Eric Wolfgang. Topical drug classification. *International Journal of Pharmaceutics*, 295(1–2):101 – 112, 2005. ISSN 0378-5173. doi: http://dx.doi.org/10.1016/j.ijpharm.2005.01.032. URL http://www.sciencedirect.com/science/article/pii/S037851730500102X.

[128] Anna M. Wokovich, Suneela Prodduturi, William H. Doub, Ajaz S. Hussain, and Lucinda F. Buhse. Transdermal drug delivery system (tdds) adhesion as a critical safety, efficacy and quality attribute. *European Journal of Pharmaceutics and Biopharmaceutics*, 64(1):1 – 8, 2006. ISSN 0939-6411. doi: http://dx.doi.org/10.1016/j.ejpb.2006.03.009. URL http://www.sciencedirect.com/science/article/pii/S0939641106000804.

[129] Robert Langer. Transdermal drug delivery: past progress, current status, and future prospects. *Advanced Drug Delivery Reviews*, 56(5):557 – 558, 2004. ISSN 0169-409X. doi: http://dx.doi.org/10.1016/j.addr.2003.10.021. URL http://www.sciencedirect.com/science/article/pii/S0169409X03002357. Breaking the Skin Barrier.

[130] P M Elias and D S Friend. The permeability barrier in mammalian epidermis. *The Journal of Cell Biology*, 65(1):180–191, 1975. doi: 10.1083/jcb.65.1.180. URL `http://jcb.rupress.org/content/65/1/180.abstract`.

[131] R. J. Scheuplein and I. H. Blank. Permeability of the skin. *Physiological Reviews*, 51(4):702–747, 1971.

[132] U.S. Department of Health, Food Human Services, Center for Drug Evaluation Drug Administration, and Research (CDER); SUPAC-SS; CMC 7. Guidance for Industry: Nonsterile Semisolid Dosage Forms, May 1997.

[133] United States Pharmacopeial Convention. Committee of Revision. The united states pharmacopeia. In *The United States Pharmacopeia, USP 32-NF 27*. United States Pharmacopeial Convention, Incorporated, 2007.

[134] N. Realdon, E. Ragazzi, and M. Dal Zotto. Kinetics of release and simulated absorption of methyl nicotinate from different ointment formulations: in vitro-in vivo correlations. *Die Pharmazie*, 51(2):113–116, 1996.

[135] N Realdon, Eug Ragazzi, and M Dal Zotto. Influence of ointment formulation on skin erythema induced by nicotinate esters. *Die Pharmazie*, 50(9):603–606, 1995.

[136] N Realdon, A Tagliaboschi, F Perin, and E Ragazzi. The "bubble point" for validation of drug release or simulated absorption tests for ointments. *Die Pharmazie-An International Journal of Pharmaceutical Sciences*, 60(12):910–916, 2005.

[137] Enrico Ragazzi, Nicola Realdon, and Marisa Dal Zotto. *Galenica pratica: formulazione e tecnologia*. Libreria internazionale Cortina, 2006.

[138] Jonathan Hadgraft and Geoffrey Ridout. Development of model membranes for percutaneous absorption measurements. i. isopropyl myristate. *International Journal of Pharmaceutics*, 39(1):149 – 156, 1987. ISSN 0378-5173. doi: http://dx.doi.org/10.1016/0378-5173(87)90210-9. URL `http://www.sciencedirect.com/science/article/pii/0378517387902109`.

[139] Jonathan Hadgraft and Geoffrey Ridout. Development of model membranes for percutaneous absorption measurements. ii. dipalmitoyl phosphatidylcholine, linoleic acid and tetradecane. *International journal of pharmaceutics*, 42(1):97–104, 1988.

[140] Douglas HK Lee et al. *Handbook of physiology: a critical, comprehensive presentation and physiological knowledge and concepts: section 9, reactions to environmental agents*. American Physiological Society, 1977.

[141] T Higuchi. Mechanism of sustained-action medication. theoretical analysis of rate of release of solid drugs dispersed in solid matrices. *Journal of pharmaceutical sciences*, 52(12):1145–1149, 1963.